



Design and Fabrication of Biomorphic Scaffolds for Tissue Regrowth by 3D Printing

A Major Qualifying Project Report
Submitted to the Faculty of
WORCESTER POLYTECHNIC INSTITUTE
In partial fulfillment of the requirements for the
Degree of Bachelor of Science

Authored By:

Kellie Chadwick

Kali Manning

Johan Skende

Sarah Walker

Handwritten signatures of the authors: Kellie Chadwick, Kali Manning, Johan Skende, and Sarah J. Walker. Each signature is written in black ink and is positioned to the right of the author's name.

Date Approved: April 25, 2013

Approved by:

Professor Domhnull Granquist-Fraser, Ph.D.

Professor Sakthikumar Ambady, Ph.D.

Abstract

Tissue engineering has shown a need for three-dimensional (3D) tissue scaffolds for cell growth as an improvement over slab scaffolds. We present a novel scaffold design and manufacturing process, utilizing biomorphic scaffold shapes based on computational models and defined by optimal surface area to volume ratios. Using these models and a low-cost 3D printer, we developed fractal-based biocompatible 3D tissue scaffolds that supported cell proliferation.

Authorship

This report was equally prepared by all team members: Kellie Chadwick, Kali Manning, Johan Skende, and Sarah Walker.

Acknowledgements

The authors of this study would like to thank the following individuals:

- Domhnall Granquist-Fraser and Sakthikumar Ambady for their advice and support throughout the duration of this project.
- Lisa Wall, Hans Snyder, Victoria Huntress and Harold Hovagimian for their assistance in the laboratory.
- MakerBot Inc., Glycosan, Sigma Aldrich, and Akrylix for their technical expertise and support.

Table of Contents

Abstract	I
Authorship	II
Acknowledgements	III
Table of Contents	IV
Table of Figures	VI
Table of Tables	VII
Chapter 1. Introduction	1
Chapter 2. Literature Review	2
2.1 Biomorphic Fractal Geometry	2
2.2 MakerBot Thing-O-Matic.....	6
2.3 Material Properties and Selection	7
2.4 Sterilization Techniques	9
2.5 Fibroblast Physiology	11
2.6 Review of Three-Dimensional Tissue Engineering	12
2.6.1. Tissue Engineering Approaches	13
2.6.2. Hydrogels	13
2.6.3. Fibrous Scaffolds.....	14
2.6.4. Amorphous Foam Scaffolds.....	14
2.6.5. Three-Dimensional Tissue Engineering Scaffold Fabrication Methods.....	14
2.6.6. Rapid Prototyping.....	15
2.7 Previous Publications and Approaches.....	15
Chapter 3. Project Strategy	18
3.1 Initial Client Statement	18
3.2 Objectives and Constraints.....	19
3.2.1. Quantitative Analysis of Objectives.....	19
3.3 Revised Client Statement	21
3.4 Project Approach.....	21
Chapter 4. Alternative Designs	23
4.1 Needs Analysis.....	23
4.2 Functions and Specifications	24
4.3 Design Alternatives.....	25
4.3.1. Fabrication Alternatives	25
4.3.2. Geometric Alternatives.....	28
4.4 Feasibility Study.....	31
4.5 Experimental Methods	32
4.5.1. NIH/3T3 Cell Culture Protocol.....	32
4.5.2. Hydrogel Protocols and Preliminary Data.....	33
4.5.3. Material Degradation Study.....	48
4.5.4. 3D Printer Protocols and Preliminary Data	48
Chapter 5. Final Design and Validation	52
5.1 Conceptual Final Design	52
5.1.1. Fabrication Method Selection.....	52

5.1.2.	Fractal Classification and Generation.....	55
5.1.3.	Fractal Selection	58
5.2	3D Printing of Fractal Molds	61
5.3	Surface Area to Volume Ratio Calculations	61
5.4	Hydrogel Protocol	63
5.5	Cell Maintenance Protocol.....	65
5.6	Hydrogel Transfer and Washing	65
5.7	Cell Imaging	66
5.8	Cell Fixation and Sectioning Protocol	66
5.9	Cell Staining Protocols.....	67
Chapter 6.	Design Verification	68
6.1	Cell Images Over Time.....	68
6.2	Cell Viability / Histology Results.....	69
6.3	Confocal Microscopy Results	72
Chapter 7.	Discussion.....	73
7.1	Review of Raw Data.....	73
7.2	Limitations	74
7.3	Manufacturability.....	75
7.4	Political, Ethical, and Sociological Ramifications	75
Chapter 8.	Conclusions and Recommendations.....	78
8.1	Objectives.....	78
8.2	Future Improvements and Recommendations	78
8.3	Future Printer Selection	79
8.4	Impact.....	81
Glossary		82
References		83
Appendix A: Gantt Chart		85
Appendix B: Glycosan Biosystems Inc. Extracel Protocol.....		93
Appendix C: Matlab Code		95
Appendix D: Fractal Mold Images.....		96
Appendix E: BrdU Protocol		98
Appendix F: Leica CM3050 Cryostat Microtome SOP		99
Appendix G: H&E Protocol		105
Appendix H: Sigma Aldrich HyStem-C Protocol.....		106
Appendix I: Sigma Aldrich HyStem-HP Protocol.....		108
Appendix J: Final Experiment Protocol		111
Appendix K: Glycosan Hydrogel Digestion Protocol.....		112
Appendix L: MatLab Code Usage License		113

Table of Figures

Figure 1: Computer-Generated 3D Fractal Tree (Chandra & Rani, 2009).....	4
Figure 2: Variation in Xenophyophore Morphologies (Levin, 1994).....	5
Figure 3: Objectives Tree	20
Figure 4: Schematic of Printed Biomaterial Tissue Scaffold	26
Figure 5: Schematic of Hydrogel Mold.....	27
Figure 6: Sacrificial Lattice Schematic	27
Figure 7: Embedded Cells Schematic	28
Figure 8: Tree Fractal (Chandra & Rani, 2009)	29
Figure 9: Coral (Anonymous, 2012)	29
Figure 10: Variation in Xenophyophore Morphologies (Levin, 1994).....	30
Figure 11: Nerves (National Institute of Health).....	30
Figure 12: The base mesh for the fractal molds. Also used as the control.	50
Figure 13: Flow Chart of Fractal Generation and Classification Program in MatLab. See Appendix C for code.....	56
Figure 14: Function Selection Screen.....	57
Figure 15: Fractal Classification Window.....	57
Figure 16: Menger Sponge Fractal Cross-Section.....	59
Figure 17: An Iterated Function System Fractal Modeling a Fern	60
Figure 18: A Bifurcating Fractal Tree.....	60
Figure 19: Three-Dimensional Sierpinski Triangle Fractal Shape.....	61
Figure 20: Setup of Scaffold Rinsing on Day 4 of Culture	66
Figure 21: H&E staining of fern section	70
Figure 22: Actin (<i>left</i>) and DAPI (<i>right</i>) staining of tube-like formations in cluster section (40X top and bottom, 20X middle)	71
Figure 23: Actin (<i>left</i>) and DAPI (<i>right</i>) of cell clusters in control section (32X).....	71
Figure 24: Actin (<i>left</i>) and DAPI (<i>right</i>) of cells in control section (20X).....	72
Figure 25: Actin and DAPI stain at 63X and 1.8 zoom of tube-like formation in cluster section.....	72

Table of Tables

Table 1: Properties of PolyLactic Acid (MatBase, 2009)	8
Table 2: Properties of Water Soluble Polyvinyl Alcohol	8
Table 3: Natural and Synthetic Polymeric Materials (Ng <i>et al.</i> , 2012)	9
Table 4: Pairwise Comparison Chart.....	21
Table 5: Needs Analysis	24
Table 6: Complete Media Protocol	32
Table 7: Published data on Gelation time (Extracel™ and Extracel™-HP Gelation Time Variation, Glycosan Biosystems Inc., 2011)	34
Table 8: Gelation Study 1 without Media.....	34
Table 9: Gelation Study 1 with Media	35
Table 10: Gelation Study 2.....	35
Table 11: Gelation Study 1 without Media Results	35
Table 12: Gelation Study 1 with Media Results.....	35
Table 13: Gelation Study 2 Results.....	36
Table 14: Glycosil : Gelin-S (Extracel™ and Extracel™-HP Gelation Time Variation, Glycosan Biosystems Inc., 2011).....	36
Table 15: Thickness study	37
Table 16: Thickness Study 1 Results	37
Table 17: Volume of Extracel™ Hydrogel Components.....	40
Table 18: Thickness Study 2 Results	40
Table 19: 3D Density 96-well plate Arrangement.....	43
Table 20: 3D Density Experiment Staining.....	44
Table 21: 3D Cell Dispersion	46
Table 22: Staining of 3D Cell Dispersion.....	47
Table 23: Functions/Means Matrix.....	52
Table 24: Matrix of Design Constraints	53
Table 25: Pairwise Comparison Chart of Design Functions	53
Table 26: Function/Means Matrix.....	54
Table 27: Weighted Design Matrix	55
Table 28: Surface Area and Volumes for Fractal Molds and Hydrogel.....	62
Table 29: Surface Area, Volume, and SA:V Ratio for all hydrogel scaffolds.....	63
Table 30: Volume of Gel and Cell Density Components of Scaffolds	64
Table 31: Final volumes of gel components and cell suspension.....	65
Table 32: Microscopy Images of Hydrogels from Days 5, 10, and 16	68
Table 33: Affordable 3D Printer Specifications and Prices.....	80

Chapter 1. Introduction

Three-dimensional (3D) biodegradable scaffolds can support effective tissue regeneration and delivery of therapeutic molecules. One of the challenges in 3D tissue culture is the inability of nutrients to diffuse deep into a scaffold, resulting in cell death at the inner core (Rajagopalan & Robb, 2006). Nutrient availability can be optimized by incorporating biologically inspired geometries into tissue scaffold design, improving scaffold function and cell growth. To achieve this goal, we improved scaffold material and geometries using a commercially available, affordable 3D printer, the MakerBot Thing-O-Matic. We created fractal shaped 3D tissue scaffolds with greater surface area to volume ratios than current slab structures, to achieve optimal geometry and ensure the greatest availability of growth media to the cells in each tissue scaffold (Rajagopalan & Robb, 2006). We also developed a novel technique to fabricate 3D fractal tissue scaffolds and grow cells *in vitro*.

There are many technologies in the current market place that aim to reduce the presence of a necrotic core in 3D cultures. One such method is the rapid casting of scaffolds using carbohydrate glass encapsulated in an ECM-cell mixture (Miller *et al.*, 2012). The lattice dissolves in media, leaving behind the patterned vasculature within. Using this method, cells that are exposed to media within and around the scaffold remain viable with minimal necrosis within these 3D scaffolds (Miller *et al.*, 2012). This is an important proof-of-concept that combines complex geometric patterns with vasculature by utilizing rapid 3D printing. A second approach is the creation of a sacrificial lattice to allow for efficient media perfusion within the 3D tissue scaffold (Lee *et al.*, 2010). However, this approach limits perfusion to the X and Y directions, making it less than ideal for true 3D cell culture. Both of these existing approaches limit the types of complex 3D geometries that can be used. We propose that the use of biomorphic geometries can improve the efficiency of nutrient supply within 3D scaffolds as they already do in nature. Our design approach aims to develop 3D biocompatible tissue scaffolds using a commercially available and inexpensive desktop 3D printer.

Chapter 2. Literature Review

This project explores strategies and fabrication methods for designing an optimal 3D tissue scaffold based on biomorphic fractal patterns using a 3D printer with a thermoplastic extrusion tip. In this chapter, we review, evaluate, and summarize background literature relevant to biomorphic fractal design, mathematical modeling of fractal systems, 3D printer specifications, biomaterial properties, biocompatible sterilization techniques, cell culture, current bioscaffold fabrication research, and pertinent current and past research in the field of Biomedical Engineering.

2.1 Biomorphic Fractal Geometry

A frontier in modern tissue engineering research is to utilize design cues from nature to optimize cell growth in tissue scaffolds by maximizing nutrient availability. In nature, many organisms increase their survivability by optimizing their surface area to volume ratios such that maximum nutrient transfer is achieved with the environment. This enables survival in suboptimal conditions; thus, over millions of years, many such organisms have evolved highly optimized shapes and structures to achieve this goal. Engineering using biomorphic design cues from such organisms provides a research shortcut to achieving better, more efficient nutrient delivery to cells cultured on manufactured tissue scaffolds.

A number of universal design concepts must be considered when designing the optimal biomorphic tissue scaffold. Within practical limitations, the largest surface area possible per unit volume must be achieved, so the largest number of cells can adhere to the scaffold and receive adequate nutrition (Rajagopalan & Robb, 2006). Most importantly, pore size in the bioscaffold must be optimized for the cell type being cultured. According to Rajagopalan and Robb (2006), the best experimentally determined pore sizes are 5 μm for vascularization, 5-15 μm for fibroblasts, 20 μm for hepatocytes, 100-350 μm for bone, and 500 μm for fibrovascularization. These pores must be interconnected with curved cross sections, while maintaining the rigidity required to grow the target cell type and the flexibility required for cell proliferation and locomotion (Rajagopalan & Robb, 2006). Achieving the optimal combination of these parameters for the target cell type is essential to producing a successful tissue scaffold, regardless of the geometry being utilized.

Two major pathways exist for the biomorphic design of tissue scaffolds – mosaic and fractal. Mosaic structures utilize pores with curved cross-sections, tessellated to create a 3D repeating structure with sufficient structural integrity (Rajagopalan & Robb, 2006). In prior research, such structures have shown promise in providing cultured cells with sufficient nutrients; however, the required micro-geometry requires submicron printing accuracy and reproducibility that 3D printers within our price range cannot currently achieve. Fractal structures utilize geometry that is common in nature, from tree roots and branches to DNA. The use of fractal geometry enables tissue scaffolds to utilize the natural self-organization of cells and the optimal shape on which cells may grow. Additionally, such geometry is feasible from printers within our desired price range (<\$2,500) because even inaccuracies and imperfections in the reproduction of each fractal can be considered fractal in nature. Thus, even these imperfections can potentially contribute to optimal nutrient delivery and cell growth.

The fractal nature of a biological structure can be quantified through fractal dimension (D) and lacunarity (L). Fractal dimension is computed by counting border pixels as a function of sampling region (Smith *et al.*, 1996). Lacunarity is computed by measuring the variation inside a fractal structure (Smith *et al.*, 1996). Together, these metrics can be used to quantify the relative fractal nature of a system. Furthermore, they can be used to compare natural fractals to computer generated ones, making it easier to select the shapes that best replicate natural fractals. These two metrics allow for accurate determination and classification of fractal structure in biological systems, and may be used to develop mathematical analogs that can be digitized and used to create new tissue scaffolds.

Fractal structures appear throughout nature, in clouds, rivers, blood vessel structure, lightning, DNA, trees, and more – that’s just a small sample. Fractal geometry, when found in nature, generally represents one of the most optimal shapes for the task for which it is being utilized by an organism (Smith *et al.*, 1996). Some of the natural fractals that will be explored for the design and modeling of tissue bioscaffolds are: trees, coral, axons, blood vessels, and a class of organisms known as Xenophyophores.

Blood vessels and neural axons are among the most studied natural fractal geometries. Tissues are innervated and vascularized in a fractal pattern – that is, the macro arrangement and branching structures of these vessels resemble each other at different

levels of zoom. This phenomenon is known as self-similarity. For example, a Purkinje neuron has a fractal dimension $D = 1.89$, while a mathematically generated Koch Snowflake fractal has a fractal dimension $D = 1.26$ (Smith *et al.*, 1996). This indicates that some natural structures, such as neurons, exhibit greater fractal character than some artificially generated fractals. Many natural fractal structures contain two or more fractals integrated into one. In these cases, a simple calculation of fractal dimension will not accurately represent the fractal character of the system. However, if both fractal dimension and lacunarity are calculated, they can be used together to uniquely classify any natural fractal (Smith *et al.*, 1996). However, such classification is beyond the scope of this project and will not be pursued further.

Most parts of a tree – roots, branches, and leaves – utilize self-similar fractal structures to optimize nutrient transfer. Chandra and Rani (2006) demonstrated that the self-similar portions of plants, such as the branches or roots, could be modeled using the set of Noble numbers as a function of the golden mean. Using this method, they developed the following mathematical model for the generation of 3D trees, with a variety of customizable factors:

$$x_n = \lambda f(x_{n-1}) + (1 - \lambda)x_{n-1}, x = 1, 2, \dots$$

Using this equation with different scaling factors, images such as the one in Figure 1 were generated.

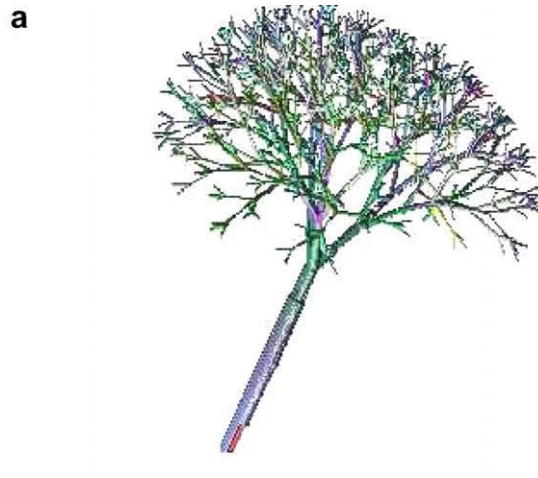


Figure 1: Computer-Generated 3D Fractal Tree (Chandra & Rani, 2009).

Xenophyophores are interesting and almost entirely unique organisms which have evolved for millions of years, optimizing their surface area to volume ratios to survive in harsh environments at the bottom of the ocean. Their uniqueness is attributable to the fact that they are single celled organisms, yet they grow to relatively large sizes – up to 25 cm across. Figure 2 illustrates some of the different Xenophyophore morphologies that have been discovered living on the ocean floor in some of the deepest parts of the world's oceans. In general, these organisms utilize complex systems of folds, sometimes in fractal patterns, to maximize their surface area to volume ratios. However, some Xenophyophores, such as items b and g in Figure 2, use complex networks of tubes and craters that can be utilized to optimize nutrient transfer when designing tissue scaffolds (Levin, 1994). Xenophyophore morphology may be replicated or adapted in tissue bioscaffolds to optimize the surface area to volume ratio enough for cells to adhere, differentiate, and proliferate as desired.

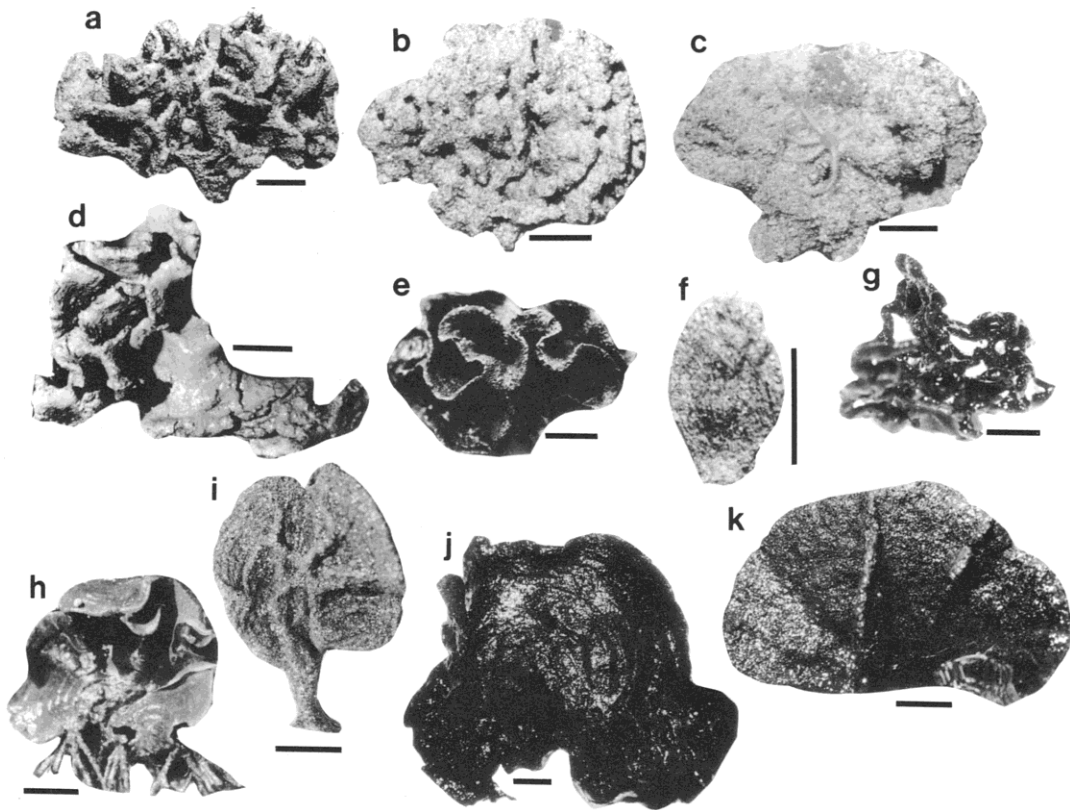


Figure 2: Variation in Xenophyophore Morphologies (Levin, 1994)

2.2 MakerBot Thing-O-Matic

We will be using a MakerBot Thing-O-Matic 3D Printer (TOM) for production of our tissue scaffold molds. The TOM was one of the first open-source personal 3D printers and has a large support community as well as significant continuing manufacturer support. It achieves 3D thermoplastic extrusion through a technique called fuse deposition modeling, which will be explained further below. Though it is now several generations behind in technology, it was originally available for purchase for \$1,275.00; it accurately represents an affordable 3D printer as it is significantly less expensive than the professional 3D printing options.

The TOM that we will be using for this project has a single StepStruder Mk6+ extruder, though dual extrusion is available as an optional, experimental modification. The materials that are officially supported and available for purchase are acrylonitrile butadiene styrene (ABS), polylactic acid (PLA), and water-soluble polyvinyl alcohol (PVA). The StepStruder Mk6+ is a thermal extrusion tip that operates at a maximum temperature of 230°C and uses a five-axis stepper motor to extrude plastic filament. Filament sizes between 1.75 mm and 3.00 mm may be used with this upgraded Mk6+ extruder, though non-standard sizes require calibration to achieve acceptable print quality. The motors in the TOM enable 2 µm positioning resolution in the lateral (X/Y) direction at a filament feed rate of at least 500 cm/min, and 5 µm positioning resolution in the vertical (Z) direction at a filament feed rate of at least 100 cm/min.

The chosen thermoplastic can be extruded onto the heated build platform (HBP) included with this TOM, covered in aluminum, glass, Kapton (polyimide) tape, or blue painter's tape. The maximum safe operating temperature of the HBP is 130°C. Using the default build platform and stepper motors, the maximum print size is 100 mm x 100 mm x 100 mm. The TOM can print files using the ReplicatorG software in conjunction with Skeinforge. ReplicatorG accepts the .STL file format and, using Skeinforge and the calibrated printer settings, generates a .GCODE file that contains the full set of commands used to produce each print. .STL files can be created using a number of computer-aided design (CAD) programs, including Dassault Systèmes SolidWorks (MakerBot Industries, 2012).

2.3 Material Properties and Selection

Material selection is an important part of tissue scaffold design. While there are many factors in selecting the appropriate material, it is necessary for the material to meet certain criteria. Biomaterials can promote or hinder cell attachment, proliferation, organization, and differentiation. The optimal biomaterial for this project will have controlled degradation in a biological environment without releasing toxic substances. It should also provide for nutrient and waste transport, have cell-recognizable surface chemistries, and promote signal transduction pathways (Naderi *et al.*, 2011). Porosity and connectivity determine which cell line is best suited for each application based on pore size and cell migration rates. It must also be possible to sterilize the chosen material in a manner that will not damage it or change its degradation rate.

Primarily, the chosen material for the designed bioscaffold is compatibility with the MakerBot Thing-O-Matic 3D Printer. According to the MakerBot support website, the printer can extrude three different types of material: ABS, PLA, and PVA (MakerBot Industries, 2012). These materials may be used to create the tissue scaffold directly, or to create a mold which can be used in conjunction with a hydrogel to produce a fractal tissue scaffold.

ABS is a thermoplastic that has excellent impact resistance, machinability, and thermoforming characteristics (Curbell Inc., 2008). Other key characteristics include high strength, high stiffness, and low cost. ABS is mainly used for rapid prototyping, machine panels, tote bins, and common consumer plastic materials. It is neither biodegradable nor biocompatible. While it is a good material for prototyping, it does not meet some of our final proposed design constraints outlined in Chapter 3.

PolyLactic acid (PLA) is a biocompatible and biodegradable plastic that is also usable with the MakerBot Thing-O-Matic printer. This makes it a viable option for a scaffold construction material. Important properties of PLA are listed below in Table 1. It is assumed that the PLA sold by MakerBot in filament form will retain these properties.

Table 1: Properties of PolyLactic Acid (MatBase, 2009)

Material Properties		
Quantity	Value	Unit
Young's modulus	350 - 2800	MPa
Tensile strength	10-60	MPa
Elongation	1.5 - 380	%
Bending strength	0.89 - 1.03	MPa
Impact strength	0.16 - 1.35	J/cm
Physical Properties		
Quantity	Value	Unit
Melting temperature	150 - 160	°C
Glass temperature	45 - 65	°C
Density	1210 - 1430	kg/m ³
Water absorption	0.5 - 50	%

Polyvinyl alcohol (PVA) is another option for the printing of 3D tissue scaffolds. MakerBot supplies it in a form that is biocompatible and water-soluble, fully degrading within 24 hours in an aqueous environment. These properties make it resorbable in biological conditions. Table 2 outlines some of the properties of the water-soluble PVA supplied by MakerBot.

Table 2: Properties of Water Soluble Polyvinyl Alcohol (MakerBot Industries, PVA, 2012)

Product Characteristics	Value
Melt flow index (190°C, 2.16 kg)	1.5- 3.5g/10min
Melting point	160- 170°C
Glass Transition Temperature	45 - 55°C
Specific Heat	0.4 cal /g °C
Density	1.25 - 1.35 g/cm ³

Generally, many different classes of materials are used in the development and production of tissue engineering scaffolds. Natural and synthetic biomaterials each have their own advantages and disadvantages for a wide variety of applications. Table 3 outlines some of the major differences between the two types of biomaterials. Due to the requirement of using plastic filaments in the Thing-O-Matic printer, we are limited to printing only synthetic materials for which we can find a supplier.

Table 3: Natural and Synthetic Polymeric Materials (Ng *et al.*, 2012)

Types of scaffold materials	Comments	Examples
Natural materials	<i>Advantages</i> Low toxicity Low chronic inflammatory response Biological recognition and biodegradable	Alginates Chitosan Collagen Fibrin Fibronectin Gelatin
	<i>Disadvantages</i> Complexities associated with purification, immunogenicity and pathogen transmission Poor mechanical strength Difficult manipulation Easy denaturation Not available in large quantities Batch-to-batch variations	Glycosaminoglycan Laminin Poly(hydroxyalkanoates) Polysaccharides Silk
Synthetic materials	<i>Advantages</i> Large-scale and reproducible production Controllable design with desired mechanical properties, geometries and degradation time	Polycaprolactone Poly(ethylene glycol) Poly(ethylene terephthalate) Poly(lactic acid)
	<i>Disadvantages</i> Lack of cell-recognition signals	Poly(lactic-co-glycolic acid) Poly(propylene fumarate) Polyurethane

The main advantages of natural biomaterials are low probability of rejection and low toxicity. However, natural materials are hard to produce in large quantities and have poor mechanical strength. On the other hand, synthetic materials have controllable properties and geometries, as well as good reproducibility potential. The disadvantage of using synthetic materials is that they carry a higher chance of rejection by the body, causing problems with *in vivo* implantation.

For the purpose of this project, synthetic biomaterials are optimal because the degradation rates and mechanical properties of the polymers can be controlled. The only constraint for material selection is that the MakerBot Thing-O-Matic uses a thermal extrusion tip that works with thermoplastics in filament form (diameter < 3 mm). PLA and PVA are both delivered in this form, and any other thermoplastic that can be found in this form would also be a possibility. Any materials considered for use with the Thing-O-Matic, apart from the supported ABS, PLA, and PVA, would require further testing and method development before use.

2.4 Sterilization Techniques

When designing a device that will be used in cell culture and potentially implanted into a human body, sterilization is important to prevent contamination from foreign bodies, such as viruses, bacteria, fungi, and parasites. In our specific case, we will be using a variety of plastics – including ABS, PLA, and PVA – as well as hydrogels. To ensure that the hydrogels in which cells are cultured are sterile, the plastic used to create the mold must be

sterilized before cell seeding and dissolution of the mold material. Sterilization of the MakerBot Thing-O-Matic printer is not feasible, so the focus will be on directly sterilizing the mold immediately before use. A variety of sterilization techniques will be compared for utility, ease of use, and price to determine the optimal one.

A key method of sterilization that eliminates microorganism contamination that can ruin a cell culture is by using heat. While we can use heat to sterilize any of the steel lab tools we will be using, we cannot use it for our plastic molds because they are thermoplastics, which will readily soften and change shape if heated. Additionally, even temperatures lower than the melting point of the plastic can cause warping in the shape of the structure due to resulting heat inconsistency between different parts of the mold. Thus, heat can be eliminated as an option for sterilization.

A medical industry standard method of sterilization is by the use of ethylene oxide (EtO). This involves low-temperature addition of EtO gas to a chamber that contains the item to be sterilized. The low temperature is ideal for use with our thermoplastic molds, and the equipment required for EtO sterilization is already owned by WPI. A limitation of EtO sterilization is the amount of time it takes – approximately 15 hours for a full sterilization cycle. Our water-soluble PVA begins to degrade in as little as two hours, even at atmospheric humidity, so a 15-hour cycle is not feasible. While EtO is also harmful to life, there are no residual deposits found on sterilized items if a properly calibrated EtO sterilization chamber is used. Overall, EtO is a good option for the sterilization of thermoplastic tissue engineering molds, but the long timeframe is incompatible with our material choices (Conviser, 2000).

Another sterilization method is by the use of ortho-phthalaldehyde (OPA). OPA has a number of advantages over other sterilization methods, including stability at standard pH, low toxicity to humans, sterilization times less than one hour, and effective sterilization at room temperature. For example, the FDA has cleared OPA sterilization as effective at 25°C with as little as 5 minutes of contact time. OPA must be cleaned thoroughly off the items on which it is used because it stains skin and tissues gray. Overall it represents a low cost, low toxicity, and quick sterilization method that should be tested for compatibility with our molds (Centers for Disease Control and Prevention, 2008).

A final sterilization method we will consider for sterilization of our tissue engineering molds is the dry sterilization process (DSP). This method is used primarily in the beverages industry for the sterilization of plastic containers, but has also found use in the medical field. It uses 30-35% hydrogen peroxide at temperatures 10-15°C above room temperature to sterilize samples over a very short timeframe – as short as six seconds. This is one of the best choices of sterilization procedure, but it seems to be a specialized, closed process on which little information is available. This suggests major costs may be associated with successful implementation, but suppliers will be contacted for potential discounts (Centers for Disease Control and Prevention, 2008).

2.5 Fibroblast Physiology

Fibroblast cells are the most abundant cell type in the body. They are primarily responsible for synthesizing extracellular matrix and connective tissue and play a major role in wound healing. These cells produce types I and III collagen, which form aggregates to create larger collagenous structures. Fibroblasts also secrete glycoproteins and polysaccharides to form extracellular matrix. These cells are essential in the body's response to injury in the reparation of connective tissue. When injury occurs, the cells proliferate and fill the wounds to repair the body (Alberts *et al.*, 2002). In 3D conformations, fibroblasts may exhibit extended or retracted conformations, while in 2D cultures, they appear flattened when they have attached to the culture surface. It is important to understand that they do not appear to have the same conformations between the different dimensional cultures (Grinnell, 2005).

The NIH/3T3 fibroblast cell line was established in 1963 from Swiss mouse embryonic tissue by George Todaro and Howard Green at the New York University School of Medicine. The nomenclature, 3T3, refers to the protocol used to establish the line; 3-day transfer with inoculation of 3×10^5 cells. After about 20 generations, the cells became less contact inhibited, changed from diploid to tetraploid, and the growth rate of the cells increased. It took the scientists about three months culture time to establish this cell line with unlimited cell growth and new growth properties. The cells were cultured on tissue culture plates using Dulbecco's Modification of Eagle's Medium (DMEM) with 10% calf serum (Todaro & Greene, 1963).

2.6 Review of Three-Dimensional Tissue Engineering

The goal of tissue engineering (TE) is to create a method of regenerating damaged tissues *in vivo* using allogeneic cells or a patient's own cells. The current golden standard for treating tissue and organ disorders is organ transplantation. However, the needed amount of organs is much greater than the supply resulting in thousands of people going without treatment. TE combines the expertise and knowledge base of polymer chemistry, materials science, cell and molecular biology, and clinical medicine (Holzwarth & Ma, 2011) to satisfy the unmet needs for tissue engineered constructs in the clinics. The current research focus in tissue engineering is to develop a 3D scaffold that is reproducible, biomimetic of the extracellular matrix and mechanical surroundings of the tissue, support thick tissues without developing a necrotic core, has a controlled pore size, geometry, interconnectivity, spatial distribution, is biocompatible, resorbable, porous, and provides a structure that guides cells into differentiation, proliferation, and *in vivo* signaling (Miller *et al.*, 2012). The current state of literature suggests these qualifications can be better achieved by using a combination of microstructures and nanostructures (Ng *et al.*, 2012). The combination of these two physical attributes holds the potential to more accurately mimic *in vivo* structures, and influence cell adhesion, proliferation, morphogenesis, and differentiation (Ng *et al.*, 2012). The variation in mechanical, chemical and physical scaffold characteristics causes the cells to behave in different ways. Researchers aim to discover the ideal combinations of properties a scaffold requires to replicate *in vivo* structures. The properties that impact cells on 3D scaffolds are: chemistry, topography, geometry, functionalization with biological molecules, porosity, pore size, pore configuration, fiber diameter, scaffold dimension, scaffold configuration, degradability, mechanical strength, ionic charges, and electrical conductivity. The required properties for optimal cell viability depend on the cell type being cultured (Ng *et al.*, 2012).

3D tissue scaffolds have many advantages over 2D scaffolds, most notably the ability to mimic the dimensional structure of the human body. Growing cells on a 3D scaffold impacts numerous components of the culturing conditions. These components include; cell attachment to the scaffold and the formation of bridges between fibers, slower proliferation rate due to surface attachment, longer *in vitro* culturing periods due to the

high surface area, rapid function execution, amount of healthy non-apoptotic cells, smaller more spherical structures, increased production of ECM and adhesion proteins, *in vivo* ECM mimicry, and 3D cell morphology (Ng *et al.*, 2012). The combination of the correct physical and chemical properties in a scaffold will allow for tissue and organ regeneration *in vitro*, posing a possible alternative to organ transplantation with a patient's own cells.

2.6.1. Tissue Engineering Approaches

The broad base of ideal components in a TE scaffold resulted in numerous approaches to the solution. There are four categories of TE scaffolds; gel-like scaffolds, constant geometry and structure scaffolds, fibrous scaffolds, and amorphous foam scaffolds. Each scaffold offers its own advantages and disadvantages to mimicking the organization of native structures. To determine which scaffold is appropriate for a certain situation, the native shape, mechanical properties, ability to direct cell-cell and cell-matrix interactions, and the extent of porous structures for efficient mass transport should be evaluated and compared to the desired *in vivo* structure. Some of the fundamental components for scaffold success are porosity allowing cell penetration and nutrient/waste removal (approximately 5-10 times that of the cell diameter) (Peltola *et al.*, 2008), mechanical properties matching application, biocompatible, biodegradable, and the scaffold contains nanofibrous features that attempts to mimic collagen, the largest component of the ECM (Holzwarth & Ma., 2011).

2.6.2. Hydrogels

Hydrogels are water-swollen, cross-linked polymeric structures containing covalent bonds between monomers, physical cross-links from chain entanglements, and van der Waals interactions between chains. Hydrogels are the TE scaffold of choice for soft tissue replacement due to their mechanical and chemical properties. Hydrogels are composed of mostly water, and have characteristics similar to that of ECM including flexibility, water retention capabilities, rubbery and soft consistency, and permeability of oxygen and metabolites. In addition, hydrogels have a minimal tendency to adsorb proteins, can be modified to create specific protein affinity, and self-assemble upon temperature modification. These characteristics allow hydrogels to be tailored to specific locations in

the body (based on protein surroundings), and form a gel upon injection into the body (Vlierberghe *et al.*, 2011).

Hydrogels are classified by characteristic variations of preparation methods, mechanical and structural characteristic, and overall charge. These broad categories result in hydrogels that are homopolymeric, copolymeric, neutral, anionic, cationic, amorphous, semicrystalline, hydrogen bonded, supramolecular and hydrocolloidal. These property variations provide options for selection based on body and cell characteristics.

2.6.3. Fibrous Scaffolds

Fibrous scaffolds are the conglomerations of individual fibers into 3D composites. Fibers can be combined to mimic the collagen components of the extracellular matrix. Synthetic and natural polymeric structures can be used to create fibrous scaffolds that mimic the *in vivo* cellular microenvironment, and have good structural penetration, porosity, chemical and thermal stability, mechanical strength, and physical properties. Fibrous scaffolds can be created using various methods. These methods are fiber bonding, needle punch, electrospinning, 3D printing, and micro embossing. All of these methods allow for the ability to control pore size; one of the main benefits of fibrous scaffolds is the ability to create pores with constant pore size (Ng *et al.*, 2012).

2.6.4. Amorphous Foam Scaffolds

The final type of 3D tissue engineered scaffolds is an amorphous foam scaffold. Particulate leaching, phase separation, gas foaming, and solid freeform fabrication are all methods that can be used to create amorphous foam scaffolds. Amorphous foams offer the ability to create highly porous scaffolds; however, none of the methods used to create foam scaffolds can create constant pore diameters that would be desired for consistent tissue morphology.

2.6.5. Three-Dimensional Tissue Engineering Scaffold Fabrication Methods

The various fabrication methods for creating a 3D TE scaffold are grounded in the bottom-up approach. Nature, including the human body, is composed of small simplistic sub-units, that when combined in 3D conformations create complex structures. Some examples include: nephrons, muscle fibers, and the liver lobules (Suri *et al.*, 2011). The fabrication methods that are used to create TE scaffolds are: solvent casting, particulate

leaching, gas foaming, fiber meshes, fiber bonding, phase separation, melt molding, emulsion freeze drying, freeze drying, solution casting, micro embossing, 3D printing, electrospinning, needle punch, and solid freeform fabrication (rapid prototyping) (Ng *et al.*, 2011; Peltola *et al.*, 2008).

2.6.6. Rapid Prototyping

Rapid prototyping (RP) is one fabrication method for developing 3D TE scaffolds. It is based on an additive process in which complex structures are constructed layer by layer based on a CAD model. RP is one avenue of addressing the inability to control pore size, geometry, interconnectivity, and spatial distribution of 3D scaffolds. Stereolithography, 3D printing, selective laser sintering, and fused deposition modeling all fall under the RP umbrella. These methods are employed to make scaffolds for hard tissue replacement. RP has several advantages that make it a good option for 3D scaffold fabrication; speed, customization, efficiency, patient specificity, economical, reduced constraints allowing the creation of complex geometries, composition variation, positional variation, controlled porosity, and does not require the use of organic solvents. Despite these advantages, there are some drawbacks to RP including the material fabrication compatibility, material entrapment within the scaffold during fabrication, high temperatures used during creation, and the unknown compatibility with sterilization techniques. While further investigation is needed for RP, the advantages outweigh the disadvantages, making RP a feasible option to pursue for TE scaffold fabrication (Peltola *et al.*, 2008).

2.7 Previous Publications and Approaches

Tissue engineering has rapidly developed since its commencement and is ever-changing. Researchers publish new work and discover novel methods for fabricating 3D scaffolds every year. Fortunately, a portion of this work has been accomplished through 3D printing. This section outlines some of the work that has been generated and the different approaches each research team took in regards to building a 3D scaffold.

While there are many ways to approach this issue, one method is using rapid casting of patterned networks. In this paper, the research team printed a rigid 3D construct using a 3D printer and carbohydrate glass filaments (Miller *et al.*, 2012). Once the lattice was printed, extracellular matrix (ECM) and cells were poured around the device encapsulating

the entire construct. Then media allowed for the dissolution of the lattice, leaving behind the patterned vasculature within. Once flow rate of media through the vasculature was established, cell viability tests were performed. Using this method, cells that were exposed to media within and around the scaffold were viable thus reducing the amount of necrotic core that can form within these scaffolds. This is an important proof-of-concept test that combines both geometric patterns and vasculature with rapid 3D printing.

Additionally, instead of creating a sacrificial lattice, the fabrication of multilayered systems with channels is a possibility. In this review by Lee *et al.* (2010), a natural hydrogel was created from collagen and, using a 3D bioprinter, multiple collagen layers were printed. In between these layers, a sacrificial gelatin pattern was printed that would be liquefied after the layered construction was complete. This enabled the tissue scaffold to have media perfusion in the X, Y directions, but not in the Z direction. This is a clever approach because hydrogels more accurately mimic soft tissue and can be used to create a more realistic environment for cell culture.

While Lee *et al.* (2010) did not culture cells on their hydrogel scaffold; Liu *et al.* (2008) cultured human mesenchymal stem cells (hMSC) on a collagen hydrogel. This team, instead of directly printing their scaffold, printed a mold to fill with collagen (Lee *et al.*, 2010). Once the mold was dissolved, only the desired collagen structure remained. Ultimately, this group found that, by crosslinking the hydrogel, they were able to create better cell adhesion and proliferation on the collagen scaffold.

Although hydrogels are a useful tool for tissue engineering applications, they are very difficult to handle and manufacture. Their fragility and limited diffusion capabilities must be addressed. Huang *et al.* (2011) discussed recent advances in the fabrication and functionality of these scaffolds. The surface to volume ratio of cells to media flow has been a major issue in the tissue engineering field. However, by creating porous hydrogels, one allows for cell growth, tissue invasion, and nutrient transport. While the mechanical properties of hydrogels are driven by pore size and density, pores can be manufactured and controlled by methods such as particulate leaching, freeze drying, gas foaming, phase separation, and electrospinning. It is also important to consider pore distribution. Another method reviewed was embedding the hydrogels in microfluidic channels. These constructs can closely mimic natural tissues and recreate their spatial complexities while maximizing

perfusion capacity. Micro-needle templates, fiber templates, soft lithography, photopatterning, and bioprinting are all techniques used to create the microfluidic layered channels. The reviewed methods each have their advantages and disadvantages, such as changes in repeatability, accuracy, and ease of use, which must be considered when making a final selection.

While hydrogels can be made from many different types of materials, usually they are either made from purely natural or synthetic materials. Shim *et al.* (2011) used a combination of these two types of materials to form a hybrid scaffold. In this novel approach, synthetic biomaterial slabs were printed and hydrogel was infused between every other slab to form an alternating pattern. Then, layer-by-layer, this processing was repeated, rotating each of the next layers 90° and stacking them to the desired height. By doing so, a natural hydrogel scaffold was created which was supported by a synthetic biomaterial frame that included pores for cell growth and proliferation (Shim *et al.*, 2011).

Another approach to creating a 3D tissue scaffold is by layering polydimethylsiloxane (PDMS) in a microfluidic device. By using PDMS, high gas permeability can be obtained, enabling cells to attach and proliferate (Leclerc *et al.*, 2003). The main advantage of this technique is the ability to create the microfluidic device using molds, thus being able to culture cells directly onto this device. Leclerc *et al.* (2003) also created a protocol for cell culture in PDMS microfluidic devices, including sterilization procedures and surface treatments

Many of the researchers listed in this section have taken different approaches to solving the same issue. They have each had some measure of success and their research is key in deciding which direction to pursue in the completion of this project.

Chapter 3. Project Strategy

The goal of this project is to design and model a 3D tissue engineered scaffold using an inexpensive 3D printer in order to culture NIH/3T3 cells and eliminate necrotic cores within the scaffold. This chapter outlines the steps and methods used to create and prioritize the objectives and constraints of this project in accordance with our client statement. Lastly, a project approach section outlines our goals for our project and a strategy for completing them.

3.1 Initial Client Statement

Our initial client statement as summarized by our advisor and client, Professor Domhnull Granquist-Fraser:

“Cells developing in three-dimensional (3D) tissue scaffolds rapidly develop a necrotic core. To improve scaffold function, a vascularized network could be incorporated into the system. We aim to optimize the scaffold material and geometry by use of a MakerBot Thing-O-Matic 3D printer. In addition, the surface to volume ratio of media to cells throughout the scaffold will be maximized.”

After creating this initial client statement from Professor Fraser’s summary of the project, the team developed a list of questions to ask at the next meeting with the team’s advisor. The questions asked helped to clarify the problem and what the client wanted so that the design process could progress.

The next part of this was to decide who the stakeholders would be for the final design and product. By doing so, the scope of the project was revealed and certain objectives that were not otherwise clear were solidified. While Professor Domhnull Granquist-Fraser is the main advisor and client for this product, other clients could be other researchers and professors in the Biomedical Engineering department that would benefit from the creation of a 3D, rapidly produced scaffold. The ultimate users of this device are research teams and doctors working on tissue regeneration for large-scale wounds. The design team consists of Kellie Chadwick, Kali Manning, Johan Skende, and Sarah Walker. All members worked to clarify the problem in order to satisfy the needs and wants of the client and potential end users.

3.2 Objectives and Constraints

After the team completely understood the initial client statement, objectives and constraints were created based on these needs. Objectives are tasks and goals for the project to ensure the creation of a quality product. They should be met by the final design. Constraints must be incorporated into the final design for the project to be deemed a success. Below are lists of the objectives and constraints for this project and descriptions for each:

Objectives:

- **Optimal Geometry:** The geometry of the scaffold must recreate a fractal pattern and evenly disperse media through the scaffold in order to reduce the necrotic core.
- **Optimal Material:** The material used for the scaffold must be relatively inexpensive, be biocompatible, resorbable, be compatible with the MakerBot Thing-O-Matic, and be able to be sterilized.
- **Reproducibility:** The scaffold design should be modeled in SolidWorks, be able to be mathematically modeled in MatLab, have a consistent surface area to volume ratio, and have a consistent precision rate.
- **Rapid Production:** The scaffold must be made using the MakerBot Thing-O-Matic and be created within a designated time frame.

Constraints:

- Manufacturability
- Biocompatible
- Resorbable
- Stay within budget (\$500)
- Scaffold must be printed on MakerBot Thing-O-Matic
- Must be smaller than 100 mm x 100 mm x 100 mm (Build Platform size)
- Stay within 28 week time limit

3.2.1. Quantitative Analysis of Objectives

After the team established all objectives for this project, visual models were made so the team could prioritize all of the wants and needs of the client. Pairwise Comparison Charts and objectives trees were consulted to determine the importance and hierarchy of the team's design goals. Below are the models used in analyzing the objectives.

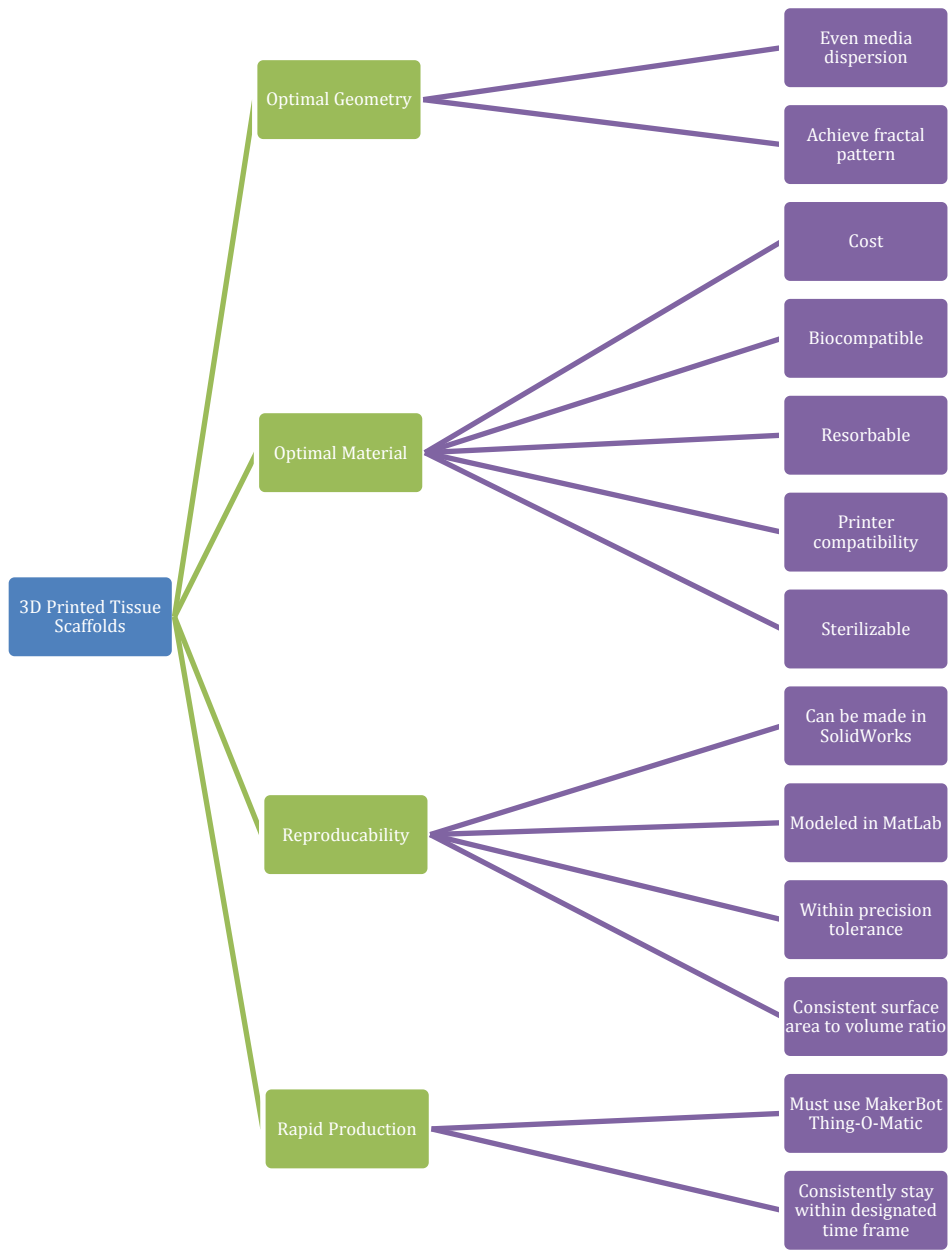


Figure 3: Objectives Tree

The above objectives tree (Figure 3) breaks down all of our main objectives into sub-objectives therefore more clearly defining what each objective encompasses.

Table 4: Pairwise Comparison Chart

	Optimal Geometry	Optimal Material	Reproducibility	Rapid Production	Totals
Optimal Geometry		0.5	1	1	2.5
Optimal Material	0.5		1	1	2.5
Reproducibility	0	0		1	1
Rapid Production	0	0	0		0

The Pairwise Comparison Chart in Table 4 indicated that the most important objectives were creating the most optimal 3D tissue scaffold geometry while using the best material for the application. Reproducibility scored lower than these objectives because natural fractals incorporate a level of randomness, so even if they are not reproduced perfectly each time, they will still be fractal. Rapid production was a desire expressed by the client and the team will work to accomplish this as well if the other objectives are met first.

3.3 Revised Client Statement

After meeting with the client and reviewing the objectives and constraints, the team revised the initial client statement to read:

“Cells developing in three-dimensional (3D) tissue scaffolds rapidly develop a necrotic core. To improve scaffold function, an optimal geometry can be incorporated into the system. We aim to optimize the scaffold material and geometry by use of an inexpensive 3D printer. To do this, the team will create a biologically inspired geometric 3D CAD model to design and mathematically optimize the surface to volume ratio of media to cells throughout the scaffold. The team will also develop a novel technique to fabricate the scaffold and grow cells in vitro.”

This statement more accurately represents the ultimate goal of the project and describes what aspects the final design should have.

3.4 Project Approach

In order to complete this project and be successful, the project constraints must be met. The following describes the methods used to accomplish each of these goals. The main constraint of this project is printing the scaffold with the MakerBot Thing-O-Matic. This

constraint was set by the client; it is essential to the successful design of our tissue scaffolds. The scaffold printed on the MakerBot must be smaller than 100 mm x 100 mm x 100 mm, as that is the size of the effective print area on the heated build platform of the Thing-O-Matic. This can be accomplished by limiting the size of the design in CAD and ensuring a central location of the scaffold on the build platform. Additionally, any design that is created must be printable within the limited abilities of the MakerBot Thing-O-Matic.

Another primary constraint of this project is scaffold material selection. The material chosen must be compatible with the MakerBot Thing-O-Matic. The MakerBot Thing-O-Matic only supports the use of ABS plastic, PLA, and PVA. Material selection is also reliant on the biocompatibility and non-toxic degradability of each plastic. While PLA and PVA are biocompatible, ABS plastic is not and therefore that material must not be used in the tissue scaffold. In addition, PLA and PVA are biodegradable, while ABS plastic is not. Thus, our material choices are limited to those that are compatible with the Thing-O-Matic and meet the other design constraints – PLA and PVA.

In general, this project must stay within the 28-week time limit of the MQP as designated by the Worcester Polytechnic Institute (WPI) and indicated in our Gantt Chart (Appendix A). The budget for this project is \$500, given to the team by the Biomedical Engineering Department at WPI. This means that the cost of all materials used for the scaffold must be less than \$500 unless special permission or funding is obtained, or materials are donated.

Chapter 4. Alternative Designs

Design alternatives in any engineering project are key to the design process and provide important information and considerations to all aspects of the project. In this section, design functions and variations of the design are outlined to determine the optimal final design. In this particular project, two rounds of design alternatives must be considered. Firstly, the manufacturing and fabrication methods of creating a 3D tissue scaffold are discussed. This is an important part of the process because while there are many methods used to manufacture these scaffolds so that they do not develop a necrotic core, there are only a few options when using an inexpensive 3D printer. Secondly, the actual biomorphic structure that will be used in the scaffold will be discussed and determined. Many fractal patterns are found in nature, and we must determine if there is a correlation between the surface area to volume ratios of each fractal and the resulting cell growth and proliferation data (Smith *et al.*, 1996).

4.1 Needs Analysis

One of the most important requirements in a design project is determining what the client wants and needs from the design. Based on this consideration, functions were brainstormed from the final client statement as stated in Chapter 3. In particular, the driving force for this project is the need for a 3D tissue scaffold that does not develop a necrotic core due to insufficient nutrient delivery. To accomplish this, we will test biomorphic fractal geometries to determine if the surface area to volume ratios are linked to cell proliferation and growth. This biomorphic fractal geometry must be mathematically modeled, imported into a 3D CAD program, placed in an appropriate configuration for 3D printing, and exported for printing on the MakerBot Thing-O-Matic.

Based on our project constraints, the final design should be biocompatible, resorbable, manufacturable with the MakerBot Thing-O-Matic, and smaller than the size of the printer's build platform (100 x 100 x 100 mm). These constraints represent requirements of the project that must be fulfilled to have a successful outcome.

The team created a design matrix to determine the relative importance of the needs and wants of the client, which can be seen in Table 5. The assigned weights are based on a 1

to 10 scale, 1 being the least important and 10 being the most important. This will aid in prioritizing the needs to produce a design in line with the clients' needs.

Table 5: Needs Analysis

Need	Priority Level (1-10)
Does not develop a necrotic core	10
Biologically inspired geometry	5
Optimal geometry	7
Optimal material	9
Biocompatibility	10
Resorbable	7
Build Size (100x100x100mm)	10
Manufactured using the MakerBot Thing-O-Matic	10

4.2 Functions and Specifications

Determining functions and specifications is a necessary and important aspect of any engineering design project, to ascertain what the design must do and by what it is limited. We determined four main functions for our fractal 3D tissue scaffold: it must not develop a necrotic core, must maintain cell viability, have uniform media dispersion and nutrient flow, and mimic fractal geometries found in nature.

Our first function specifies that our scaffold must not develop a necrotic core. The overall goal of this project is to develop a 3D tissue scaffold that does not develop a necrotic core, unlike some current industry applications. The scaffold must also maintain cell viability. If the majority of cells die, we must review and revise our cell culture protocol, such as our material and media selections. The nutrients in the cell culture media must be evenly dispersed for all of our cells to survive, proliferate, and differentiate. This can be achieved by our delivery system as well as our geometric structure. The shape of our scaffold must mimic a fractal biomorphic structure as directed by our client statement. Fractal patterns in nature have been shown to have the optimal surface area to volume ratio, which can be applied to media flow in channels (Smith *et al.*, 1996).

Specifications stemming from our functions are that the inner cell viability must be greater than 50%, the scaffold or material must be resorbable and biocompatible, the geometric structure should be able to be rapidly produced within an hour, and that the size of the structure should be less than 100 x 100 x 100 mm.

The cell viability, a measure of necrotic core formation and severity, must remain greater than 50% to be deemed acceptable. If more than half of the cells have died, the design and/or cell culture protocol must be reconsidered. The material used to create the scaffold must be biocompatible and resorbable in order to be implantable *in vivo*. If it is not compatible, there is a chance for rejection and cell death. If it is not resorbable, there could be complications from particles released in the body or mechanical disadvantages associated with the selected material. The scaffold should be printed, sterilized, and seeded within one hour to be considered rapid production. This rate has been determined by the team as a goal for the overall project. The size of the structure is limited by the Thing-O-Matic's build platform and cannot be any larger than 100 x 100 x 100 mm. The above functions and specifications are all critical to the successful completion of our design and the creation of alternative designs.

4.3 Design Alternatives

The nature of our project required two separate design iterations. The first round of design alternatives generation was performed to determine which method of fabrication best fits our objectives, goals, functions, constraints, and specifications. Our team came up with four design alternatives for this determination. Our second round of design alternatives generation focused on designing the geometry of our scaffold. We used MatLab to mathematically determine what design was most appropriate. The team designed a series of fractal models to find the most optimal design. We built the fractals and then simulated the surface area to volume ratio to find the model with the highest ratio. Based on these two iterations, the final design was chosen and pursued with further testing. The final design verification test will be a live dead assay of the cells to determine cell viability. All of the design methods explained are compatible with this final verification method.

4.3.1. Fabrication Alternatives

As previously stated, the team chose four fabrication methods based on the 3D printing constraints to create a scaffold. These four methods were printed biomaterial tissue scaffold, hydrogel mold, sacrificial lattice, and cells embedded in the material.

Printed Biomaterial Tissue Scaffold

This design approach is the most classic of our alternatives, applying the approach of directly printing the tissue scaffold. The printed material would serve as a structural scaffold. The material used in this model is either PLA or water-soluble PVA. However, since neither of these materials can culture cells directly on their surface, the scaffold would need to be coated in collagen. The cells could then be seeded on the collagen, and the scaffold submerged in media (DMEM with 10% FBS (fetal bovine serum)). Over time, the biomaterial scaffold will degrade, leaving the collagenous structure with cells remaining. The cells would be cultured between 10 and 14 days, culminating in a live dead assay. Figure 4, shown below, illustrates a simple schematic of this process.

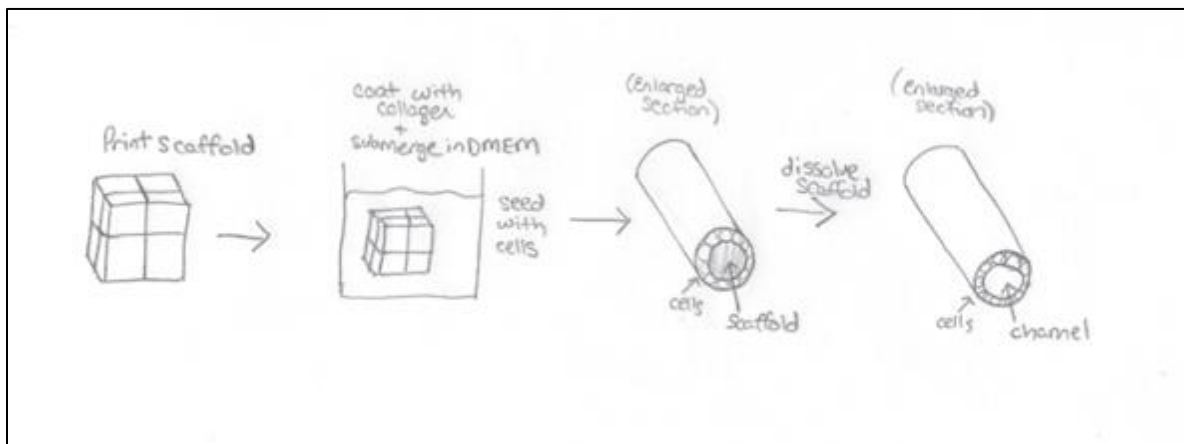


Figure 4: Schematic of Printed Biomaterial Tissue Scaffold

Hydrogel Mold

This design approach requires printing a mold for the scaffold. The inverse of the scaffold structure will be printed with a resorbable material (either PLA or water soluble PVA). The resulting void will be used as a mold for a hydrogel. This hydrogel will serve as the scaffold. Cells will be seeded onto the hydrogel, and then the hydrogel will be set. The setting procedure must be rapidly accomplished to assure the scaffold will not start degrading before setting can be achieved. The hydrogels therefore could be thermal set hydrogels, which swell at body temperature. Gradually, the mold will degrade leaving behind the hydrogel cell complex submerged in media. The hydrogel will not resorb,

serving as the structure of the tissue. Figure 5 below shows a step-by-step schematic of the fabrication process using a hydrogel mold.

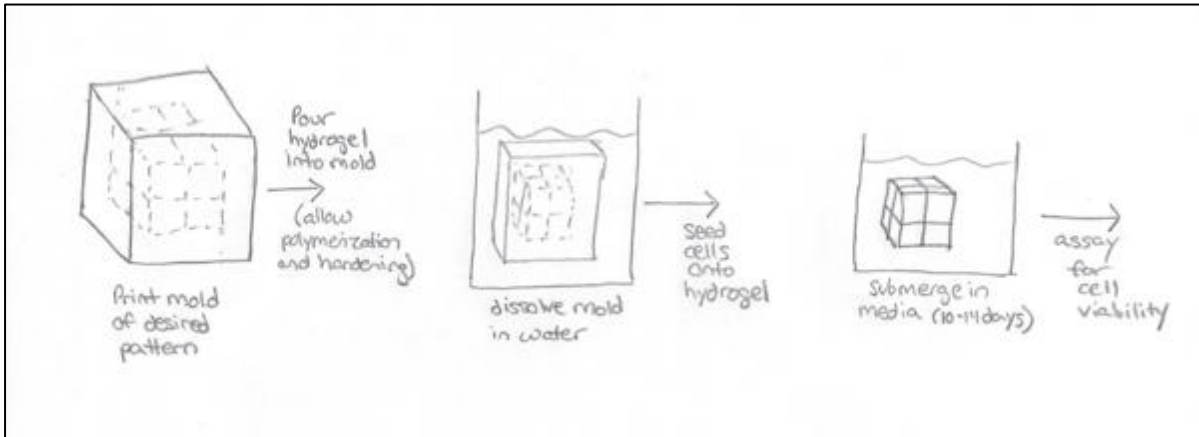


Figure 5: Schematic of Hydrogel Mold

Sacrificial Lattice

The third fabrication method is printing a sacrificial lattice. This would be used to create a network of interpenetrating channels within the scaffold. The desired network would be printed (with either PVA or water-soluble PLA), and then coated with ECM or collagen. The cells would then be seeded on the collagen, and the printed lattice degraded. After degradation, the scaffold would consist of a collagen base with interpenetrating channels for media dispersion. A brief schematic of this fabrication process is shown below in Figure 6.

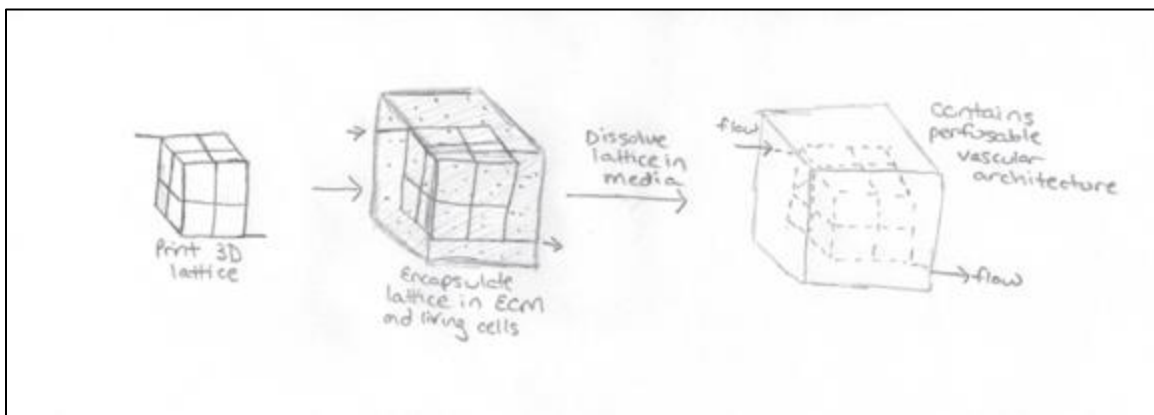


Figure 6: Sacrificial Lattice Schematic

Cells Embedded in Biomaterial

The final fabrication method was inspired by the Bioplotter®, a 3D printer that prints cells and the scaffold material simultaneously. This would remove intermediate steps required in the three previous designs. Figure 7 displays a schematic of this design alternative.

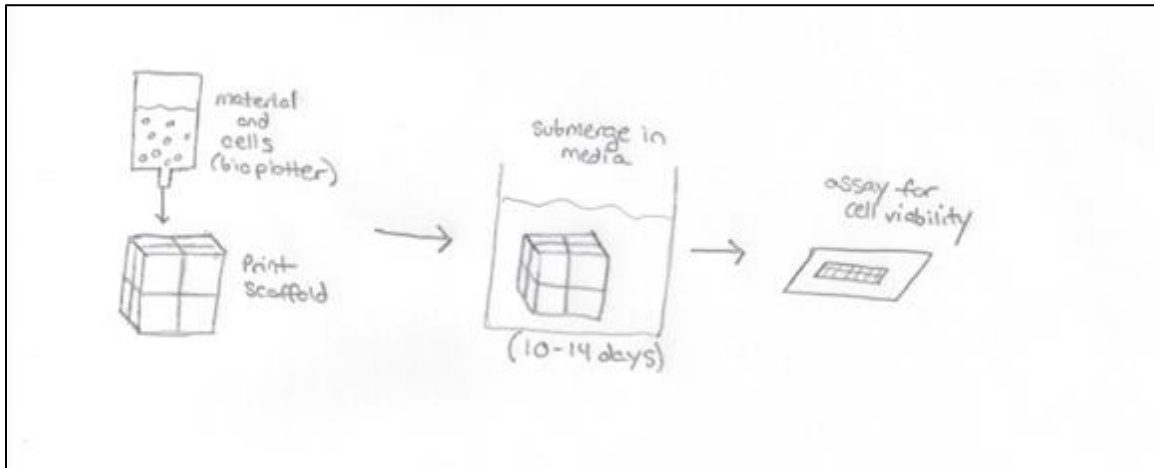


Figure 7: Embedded Cells Schematic

4.3.2. Geometric Alternatives

The development of these alternatives was based on nature inspired geometric fractals. Organisms that employ fractal geometries in nature maximize their ability to deliver nutrients. This is the motivation for basing our selections on nature inspired fractals. Some of the many natural fractal geometries we will be considering for inspiration are trees, coral, Xenophyophores, and nerves and blood vessels. These fractals are shown below in Figure 8 through Figure 11.

a

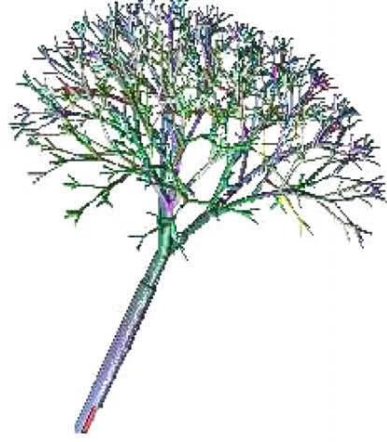


Figure 8: Tree Fractal (Chandra & Rani, 2009)



Figure 9: Coral (Anonymous, 2012)

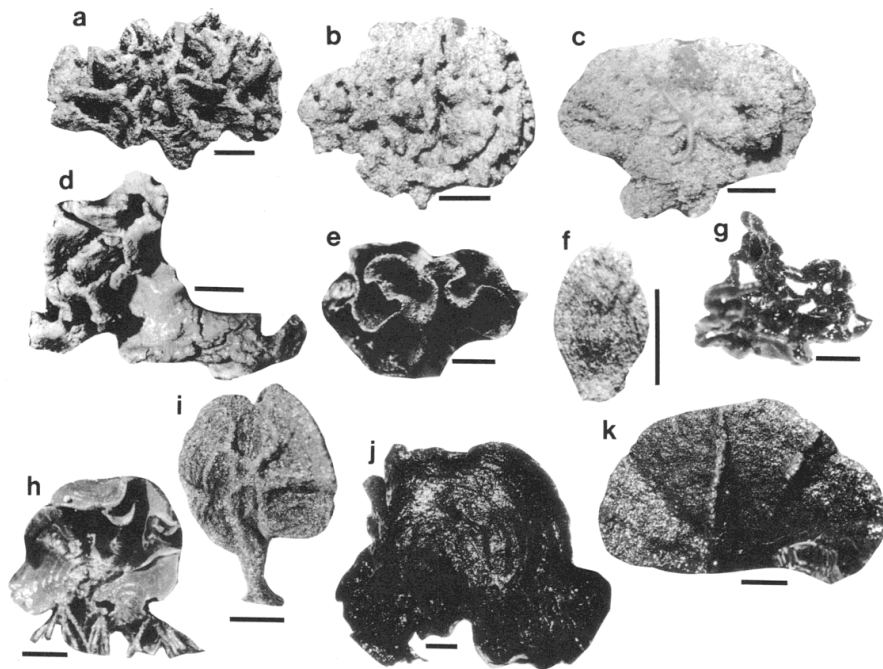


Figure 10: Variation in Xenophyophore Morphologies (Levin, 1994)

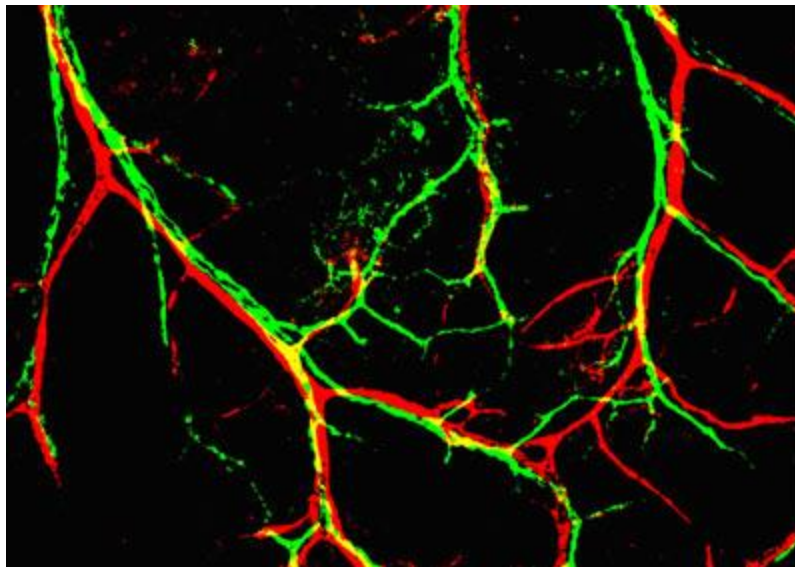


Figure 11: Nerves (National Institute of Health)

4.4 Feasibility Study

There are several aspects of this design project that must be evaluated for feasibility. The broad categories are material feasibility, fractal geometry feasibility, and printer capability. Verification of material feasibility will include classifying the degradation of ABS, PLA, and PVA in water. Printing process feasibility, reproducibility, and accuracy will be determined by printing in ABS, PLA, and PVA using the MakerBot Thing-O-Matic 3D printer. Test prints of both PLA and PVA – the materials that will be used for the prototype and final experiment respectively – will be used to determine the optimal extrusion rate, temperature, build platform material, infill %, number of shells, layer height, and raft. These numbers, once determined, will be kept constant for the remainder of the experimental validation.

Our product design is based around printing a 3D fractal shape as a mold, then allowing that shape to dissolve in water after it has served as the template for a cell-laden hydrogel. Of all of the materials compatible with the MakerBot Thing-O-Matic, ABS shows no degradation in water, so it is not appropriate for the final design. PLA does degrade, but over a period of months, which is not compatible with our target timeframe. Therefore, PVA is the only material appropriate for our target design, and will be the only one considered. The degradation of the PVA filament will be tested in water to determine the feasibility of our final design.

Next, we will evaluate whether our target fractal geometries can be printed using our MakerBot Thing-O-Matic 3D printer. We will accomplish this by attempting to print each design at different settings (Extrusion Speed, Filament Diameter, Shells, and Infill %) until the optimal settings are found that enable each design to be printed. Filament diameter is especially important because, although the filament we are using will remain at a constant diameter, changing the software value will cause the printer to extrude either more or less than what is programmed in the .GCODE file. This strategy can be used to clean up fractal molds that are messy and irreproducible because they are printed with more plastic than the shape requires. Surface area and volume for each fractal will be determined by using the Netfabb Cloud utility to process each .STL file. This utility returns surface area and volume ratios for each fractal. These values will be processed by an algorithm we create to

generate the surface area and volume for the fractal hydrogel scaffolds created from each PVA mold.

4.5 Experimental Methods

All of the following methods were conducted in accordance with standard guidelines and protocols provided by various sources.

4.5.1. NIH/3T3 Cell Culture Protocol

All cell culture work done throughout the entirety of this project followed the standard cell culture protocols. Cells were cultured in Dulbecco's Modified Eagle Medium (DMEM) containing Fetal Bovine Serum, Glutamax, and Penn-Strep with concentrations according to Table 6. The primary experiments conducted were with regard to the selected hydrogel. These experiments included gelation time, thickness, cell density studies, and cell dispersion studies. The team worked with NIH/3T3 cells throughout the entirety of the project. The following sections will explain those studies and their purpose in more detail.

Table 6: Complete Media Protocol

Component	Stock Solution	Volume (mL)	Final Concentration
DMEM basal media		88.0	
Penn Strep	100X	1.0	1X
L-Glutamine/Glutamax	200 mM	1.0	2 mM
FBS		10.0	10%
Total Volume		100.0	

Subculturing

NIH/3T3 cells were cultured on 100 mm tissue culture plates (CellTreat) at 37°C and 5% CO₂ until achieving ~80% confluency. At this point the cells were passaged. The protocol followed for passaging the NIH/3T3 cells is as follows:

1. Aspirate media
2. Rinse cells with 5mL DPBS
3. Aspirate DPBS
4. Add 3mL of 0.05% trypsin
5. Incubate for 5 minutes at 37°C

6. When cells are floating and circular in conformation neutralize the trypsin with 2mL of complete media (Table 6)
7. Transfer the cell suspension into a 15mL conical tube
8. Centrifuge the cells at 200g for 10 minutes to form a pellet
9. Aspirate the media from the pellet and re-suspend in 5mL of complete media
10. Add 1mL of the re-suspended cell suspension to a 100mm tissue culture plate
11. Add 9mL of complete media to the tissue culture plate

Cell Isolation

NIH/3T3 cells were isolated from 100mm tissue culture plates for use in experiments according to the following protocol:

1. Aspirate media
2. Rinse cells with 5mL DPBS
3. Aspirate DPBS
4. Add 3mL of 0.05% trypsin
5. Incubate for 5 minutes at 37°C
6. When cells are floating and circular in conformation neutralize the trypsin with 2mL of complete media (Table 6)
7. Transfer the cell suspension into a 15mL conical tube, and remove 50µL for cell counting.
8. Centrifuge the cells at 200g for 10 minutes to form a pellet
9. Aspirate the media from the pellet and re-suspend in desired amount of complete media based on cell counting calculations
10. Use the cells as needed for the experiment

4.5.2. Hydrogel Protocols and Preliminary Data

Prior to selecting a hydrogel to perform the final test with, the team ran experiments with three hydrogel kits, Extracel (Glycosan Biosystems Inc.) HyStem-HP, and HyStem-C (Sigma Aldrich). The various studies, outlined below, were done to determine the compatibility of the hydrogels for our testing purposes. These preliminary experiments verified that all gels were compatible for our experimental purposes.

Gelation Study

The team performed a study to determine how short the gelation time for the Extracel Kit could be without interfering with cell viability. In the scope of this project, the solution needs to be able to gel before the PVA mold degrades. The components of the

Extracel Kit are Gelin-S, Glycosil, and Extralink. Gelin-S is a thiol-modified gelatin, Extralink is a thiol-reactive crosslinker, and Glycosil is thiol-modified sodium hyaluronate. According to Glycosan Biosystems Inc., if medium is added to the samples, gelation time will increase. If the ratio of components is altered, or the pH is changed, gelation time can be manipulated. Specifically, if the ratio of Extralink to Glycosil and Gelin-S increases, the gelation time should decrease. Because these molds will be used in the body, changing the pH is not feasible for the purpose of this project as it will impact cell viability. Based on published data that can be seen in Table 7 below, the team performed several experiments to test different ratios of the components.

Table 7: Published data on Gelation time (Extracel™ and Extracel™-HP Gelation Time Variation, Glycosan Biosystems Inc., 2011)

Glycosil (mL)	Extralink (mL)	Extralink Vol	Gelation (min)
0.5	0.063	8	16
0.5	0.125	4	11
0.5	0.250	2	9

To perform this study, the team reconstituted the hydrogel according to the Glycosan Biosystems Inc. protocol (Appendix B), stopping at step 5. The team combined the solutions into microcentrifuge tubes in different ratios according to Tables 8 and 9 below. The solutions prepared according to Table 8 were made without media, and the solutions made according to Table 9 included media. A constant 1:1 ratio of Gelin-S to Glycosil was used because Gelin-S is unable to form a gel on its own. Once the solutions are prepared, 50 µl drops were placed on a tissue culture plate to time until gelation occurred. The team defined gelation as the point at which if the outer edge of the gel droplet was pulled back with a micropipette tip and released, the gel will retract back into its original shape.

Table 8: Gelation Study 1 without Media

Test	Glycosil (µl)	Gelin-S (µl)	Extralink (µl)	Ratio (E:G)
1	20	20	10	1:4
2	18.75	18.75	12.5	1:3
3	16.7	16.7	16.7	1:2
4	12.5	12.5	25	1:1
5	8.35	8.35	33.3	1:0.5

Table 9: Gelation Study 1 with Media

Test	Glycosil (µl)	Gelin-S (µl)	Extralink (µl)	Medium (µl)	Ratio (E:G)
1	20	20	10	10	1:4
2	18.75	18.75	12.5	10	1:3
3	16.7	16.7	16.7	10	1:2
4	12.5	12.5	25	10	1:1
5	8.35	8.35	33.3	10	1:0.5

This study was performed a second time (referred to as Gelation Study 2) with different amounts of reconstituted solutions. The preparations of these tests are shown in Table 10.

Table 10: Gelation Study 2

Test	Glycosil (µl)	Gelin-S (µl)	Extralink (µl)
1	20	20	10
2	20	20	20
3	20	20	30
4	20	20	40

Upon performing the gelation studies, the team observed the time it took for each droplet of Extracel hydrogel to gel. If gelation did not occur within 20 minutes, timing was stopped because that data is not useful for this project. The tables (11, 12, and 13) below show the results from gelation study 1 without media, with media, and gelation study 2, respectively.

Table 11: Gelation Study 1 without Media Results

Test	Glycosil (µl)	Gelin-S (µl)	Extralink (µl)	Ratio (E:G)	Time (min:sec)
1	20	20	10	1:4	19:30
2	18.75	18.75	12.5	1:3	9:20
3	16.7	16.7	16.7	1:2	16:40
4	12.5	12.5	25	1:1	20+
5	8.35	8.35	33.3	1:0.5	20+

Table 12: Gelation Study 1 with Media Results

Test	Glycosil (µl)	Gelin-S (µl)	Extralink (µl)	Medium (µl)	Ratio (E:G)	Time (min:sec)
6	20	20	10	10	1:4	17:15
7	18.75	18.75	12.5	10	1:3	15:30
8	16.7	16.7	16.7	10	1:2	10:54
9	12.5	12.5	25	10	1:1	15:30
10	8.35	8.35	33.3	10	1:0.5	20+

Table 13: Gelation Study 2 Results

Test	Glycosil (μl)	Gelin-S (μl)	Extralink (μl)	Time to gel (min:sec)
11	20	20	10	18:20
12	20	20	20	20:00+
13	20	20	30	20:00+
14	20	20	40	20:00+

As one can see from the tables above, trial 2 produced a hydrogel with the lowest gelation time (Table 11). The team was also able to achieve multiple gelation times under 20 minutes, which is ideal for this project. One problem that was solved with the second gelation study was that in trials 4 and 5, 20 μl barrier pipette tips were used by accident – this did not allow enough of the Extracel solution to be mixed into the hydrogel. However, in general the results were not as expected. Table 14 below published by Glycosan Biosystems Inc. displays standard component variations and their corresponding gelation times.

Table 14: Glycosil : Gelin-S (Extracel™ and Extracel™-HP Gelation Time Variation, Glycosan Biosystems Inc., 2011)

Glycosil (mL)	Gelin-S (mL)	Extralink (mL)	% Gelin-S	Gelation (min:sec)
0.500	0.00	0.125	0	10:00
0.375	0.125	0.125	25	11:00
0.250	0.250	0.125	50	15:00
0.125	0.375	0.125	75	20:00

Thickness Study

In order to determine how thick the hydrogel can be while still being able to accurately view the seeded cells, we performed a thickness study. Different volumes of the Extracel hydrogel were placed in a 96-well plate with NIH/3T3 cells seeded onto the surface. Each well in the plate had an area of 0.33 cm^2 . The team decided to test samples with thicknesses of 100 μm , 200 μm , 300 μm , 400 μm , 500 μm , 1 mm, and 2 mm on a plate. NIH/3T3 cells were then seeded onto the surface of the hydrogel after gelation occurred.

To perform this study, the Extracel hydrogel was reconstituted in coordination with the Glycosan Biosystems Inc. protocol (Appendix B). The components were added to each

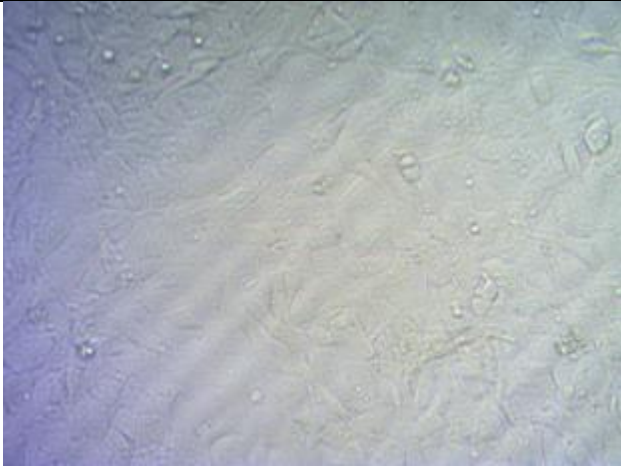
well in the desired volumes according to Table 15, and the gel was allowed to form. 250 μ l of NIH/3T3 cell suspension in 5 mL media was seeded to the surface of each well, and the samples were allowed to culture for one day before they were imaged with a microscope.

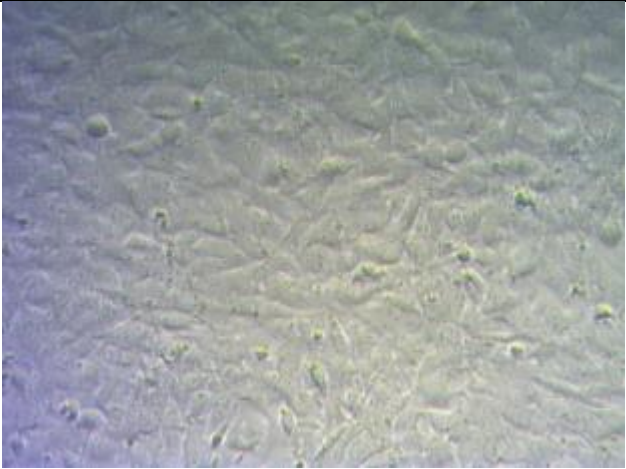
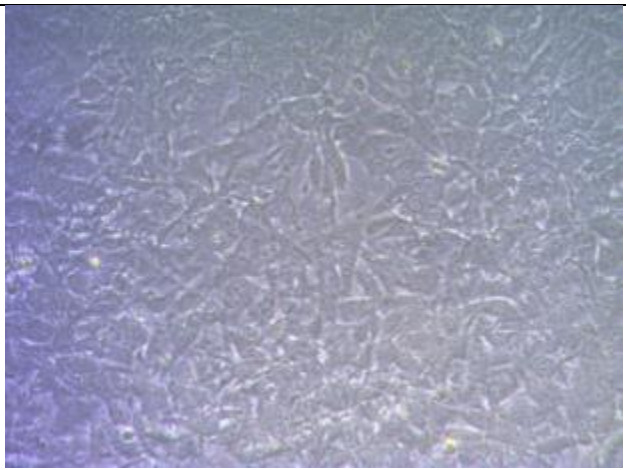
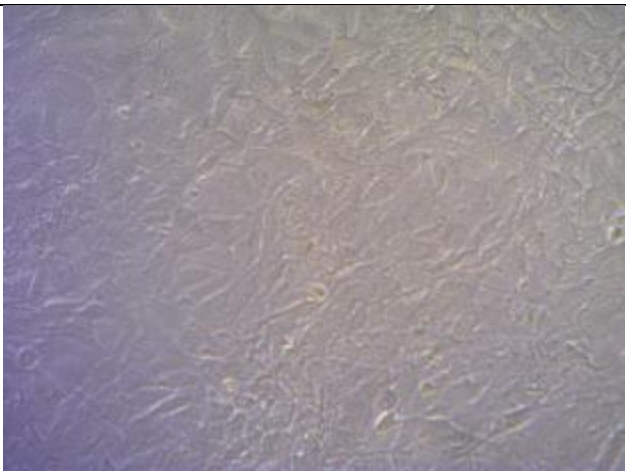
Table 15: Thickness study

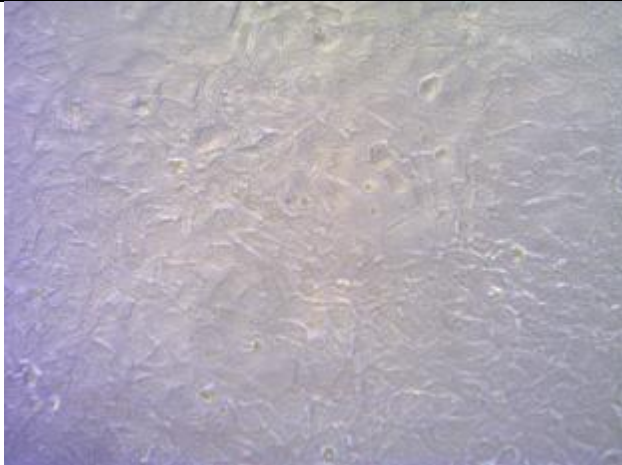
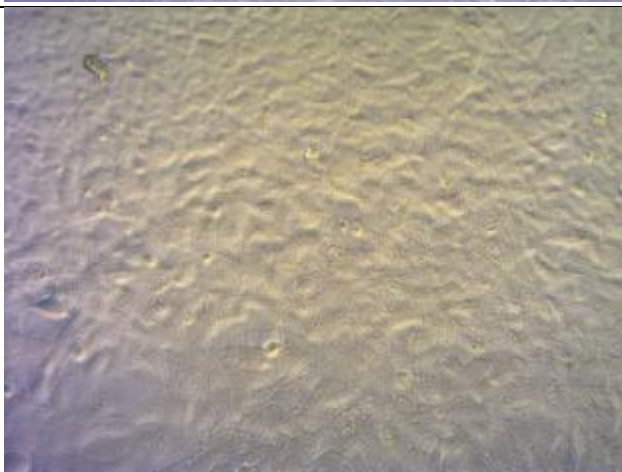
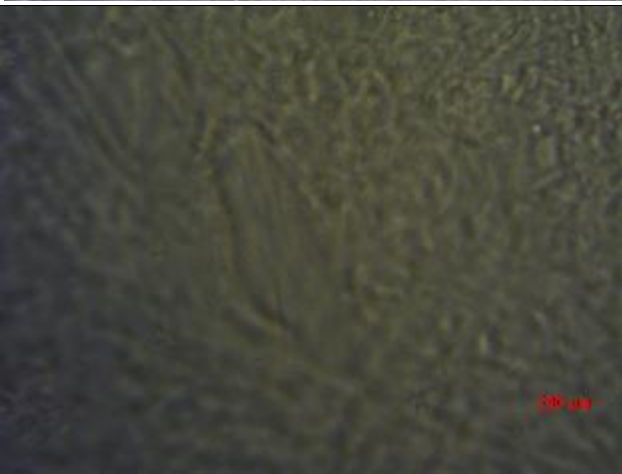
Trial	Area (cm ²)	Desired Thickness (cm)	Needed Volume (μ L)	Gelin (μ L)	Glycosil (μ L)	Extralink (μ L)
1	0.32	0.1	3.20	1.28	1.28	0.64
2	0.32	0.2	6.40	2.56	2.56	1.28
3	0.32	0.3	9.60	3.84	3.84	1.92
4	0.32	0.4	12.8	5.12	5.12	2.56
5	0.32	0.5	16.0	6.40	6.40	3.20
6	0.32	1.0	32.0	12.8	12.8	6.40
7	0.32	2.0	64.0	25.6	25.6	12.8

The images of the cells after one day on culture can be seen below in Table 16.

Table 16: Thickness Study 1 Results

Thickness	Day 1	
100 μ m		

200 μm			
300 μm			
400 μm			

500 μ m			
1 mm			
2 mm			

As can be seen in the images above, the cells were highly confluent after one day of seeding. Because of this, we performed this study a second time to improve upon the first set of results. The volumes of each component were minimally changed as the area of the 96-well plate was recorded incorrectly for the first trial. Table 17 below shows the

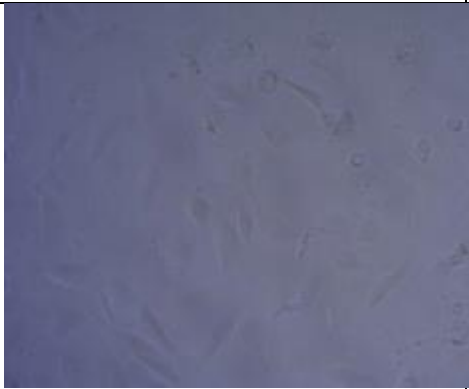

amounts of each component that were used. An eighth well was used as a control with no hydrogel; the cells were seeded directly onto the culture surface.

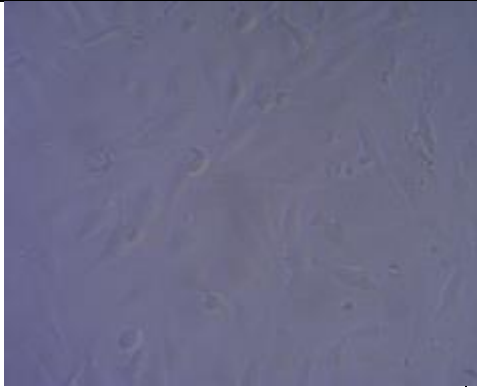


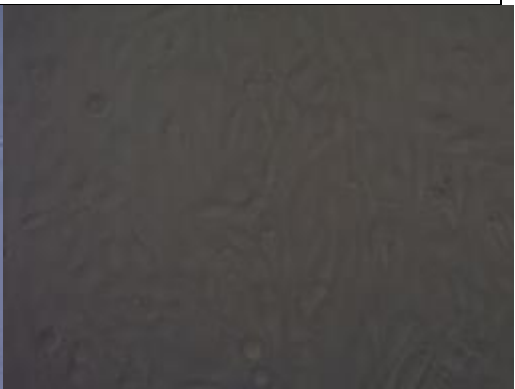


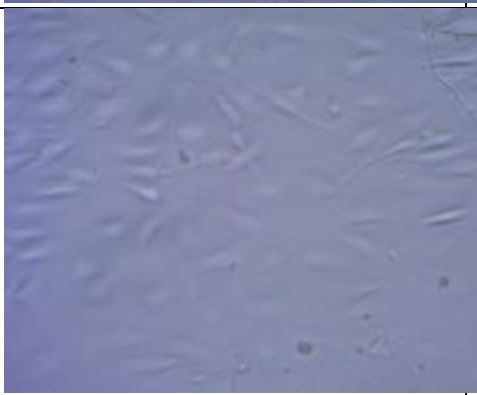

Table 17: Volume of Extracel™ Hydrogel Components

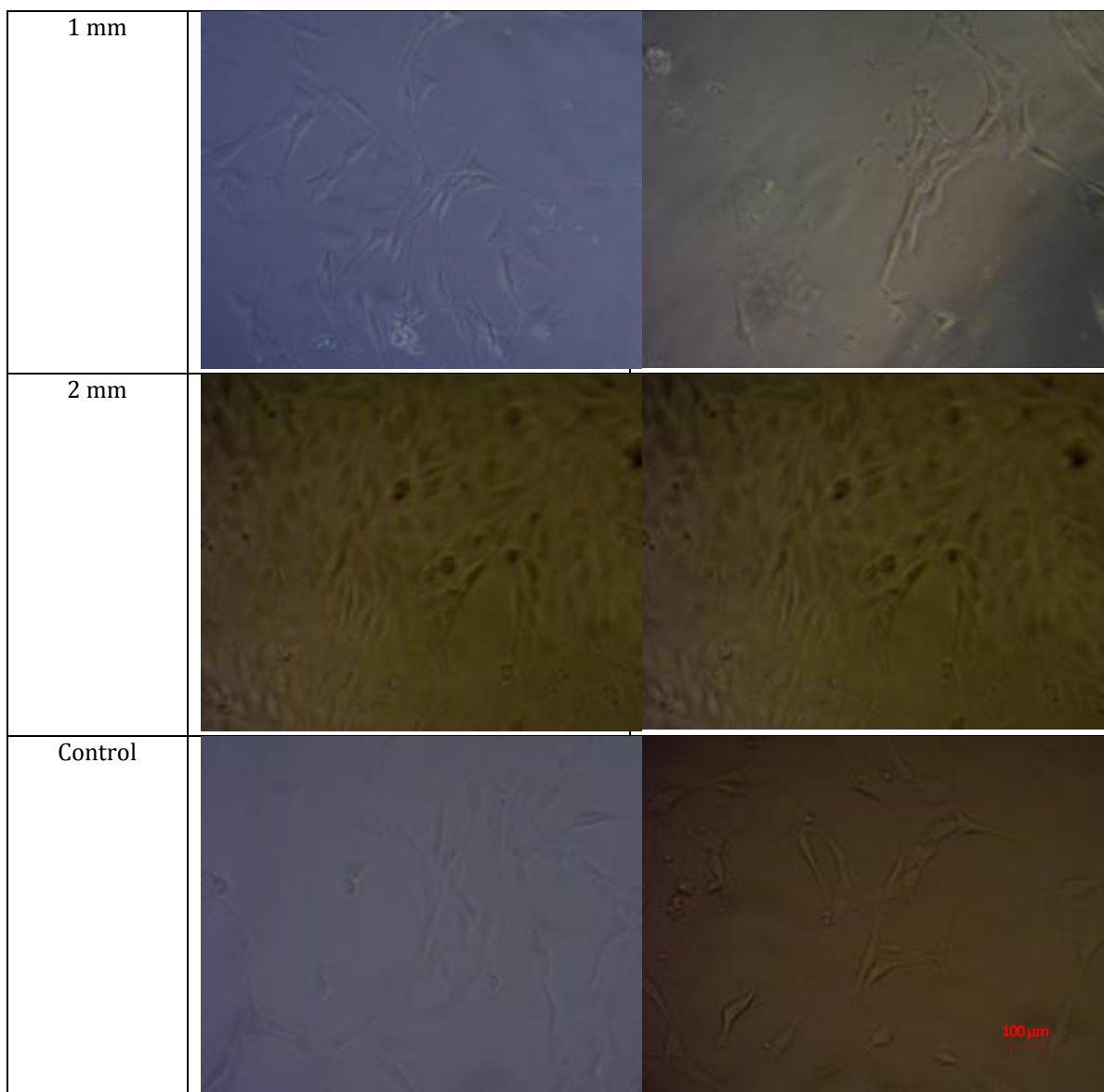
Trial	Area (cm ²)	Desired Thickness (mm)	Needed Volume (μL)	Gelin & Glycosil (1:1 ratio) (μL)	Extralink (μL)
1	0.33	0.1	3.30	2.64	0.66
2	0.33	0.2	6.60	5.28	1.32
3	0.33	0.3	9.90	7.92	1.98
4	0.33	0.4	13.2	10.56	2.64
5	0.33	0.5	16.5	13.2	3.30
6	0.33	1.0	33.0	26.4	6.60
7	0.33	2.0	66.0	52.8	13.2
8 - control	0.33	0	0.00	0.00	0.00

The correct amount of cells to seed was determined by cell counting. It was found that a 1 mL suspension of cells had about 222,500 cells, so we used 0.0449 mL of cell suspension in addition to 155.1 μL of media to each well to seed 10,000 cells. The results of this study after 1 and 2 days of culture are shown below in Table 18.

Table 18: Thickness Study 2 Results

Thickness	Day 1	Day 2
100 μm		

200 μm		
300 μm		
400 μm		
500 μm		



At 10,000 cells per well proliferation of the NIH/3T3 cells is evident at 2 days of culture. In addition, cells can be viewed at all thicknesses; however viewing is ideal between 100 μm and 500 μm .

Cell Density Study

NIH/3T3 cells were incorporated into Extracel, HyStem-C and HyStem-HP hydrogels at thicknesses of 0.25mm and 1mm at densities of 1,000, 2,000, 5,000, and 10,000 cells per well. The experiment followed the protocol outlined below, for the exact amounts of various components see the paper section about the 3D Density Experiment.

1. Isolate NIH/3T3 cells (see isolating cells protocol)
2. Reconstitute hydrogel components according to their respective protocols (Appendices B, H, and I respectively)
3. Extract the necessary volume of each hydrogel component using a sterile 3mL syringe and 20 gauge needle and put in microcentrifuge tubes
4. Save the unused reconstituted hydrogel components in -20°C
5. Add the gel components without the crosslinking agents (Extralink) for each hydrogel type to a 96-well plate in 0.25mm and 1mm thicknesses in triplicate (see Table 19 for a diagram of where each gel amount should be placed).
6. Add the required amount of cells to each well in triplicate (see Table 19 for cell densities). Top off the cell suspension in each well with media to bring the total cell suspension volume in each well to 50µL
7. Add Extralink to each well and mix to disperse the cell suspension
8. Image each well daily to view cell proliferation

Table 19: 3D Density 96-well plate Arrangement

	1	2	3	4	5	6	7	8	9	10	11	12
A Extracel 0.25mm	1,000	1,000	1,000	2,000	2,000	2,000	5,000	5,000	5,000	10,000	10,000	10,000
B Extracel 1mm	1,000	1,000	1,000	2,000	2,000	2,000	5,000	5,000	5,000	10,000	10,000	10,000
C HyStem-C 0.25mm	1,000	1,000	1,000	2,000	2,000	2,000	5,000	5,000	5,000	10,000	10,000	10,000
D HyStem-C 1mm	1,000	1,000	1,000	2,000	2,000	2,000	5,000	5,000	5,000	10,000	10,000	10,000
E HyStem-HP 0.25mm	1,000	1,000	1,000	2,000	2,000	2,000	5,000	5,000	5,000	10,000	10,000	10,000
F HyStem-HP 1mm	1,000	1,000	1,000	2,000	2,000	2,000	5,000	5,000	5,000	10,000	10,000	10,000
G Control (no hydrogel)	1,000	1,000	1,000	2,000	2,000	2,000	5,000	5,000	5,000	10,000	10,000	10,000
H	-	-	-	-	-	-	-	-	-	-	-	-

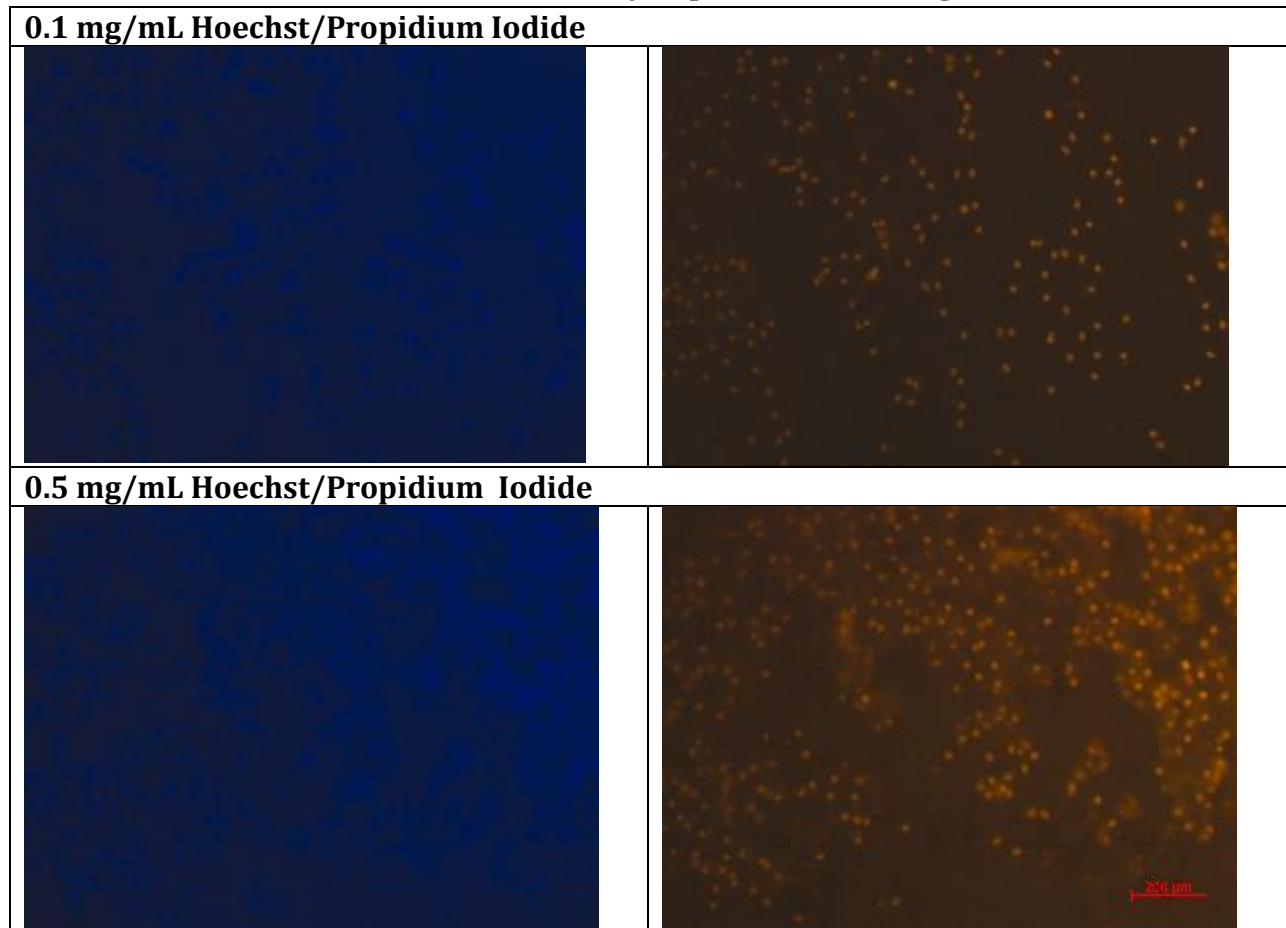
After concluding the cells could be viewed when seeded on the surface of the gel, the next step in the preliminary experiments was to incorporate the cells into the hydrogel, validate a protocol for cell incorporation, and determine which hydrogel to continue conducting research with. Glycosan Biosystems Inc. and Sigma Aldrich were generous, and

provided kits of Extracel, HyStem-C and HyStem-HP to our project team for preliminary research. These were the three hydrogels used in this experiment, and the protocol followed was the 3D Density Experiment.

Staining and Extraction of 3D Density Experiment

The purpose of this experiment was to determine if the cells in Extracel from the 3D Thickness Experiment were alive, and if they could be extracted from the hydrogel. Wells B11 and B12 of the 96-well plate were stained with Hoechst and Propidium Iodide at concentrations of 0.1mg/mL and 0.5mg/mL. Table 20 shows the wells imaged after 30 minutes of exposure to the stains.

Table 20: 3D Density Experiment Staining



As can be seen by the images above, the cells were dead. The cause of cell death was unknown. In addition to staining the wells, a 10X collagenase/hyaluronase solution made

by Glycosan was used. The protocol was adjusted to the volume of the 96-well plate based off of the protocol listed in Appendix K.

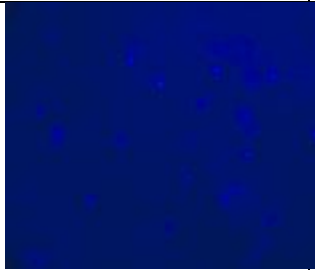
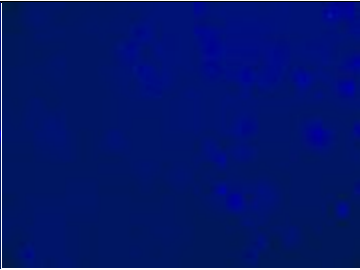
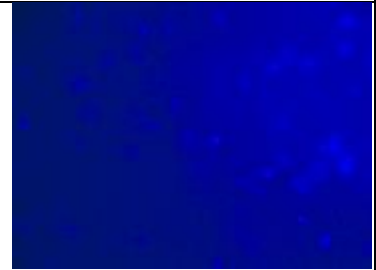
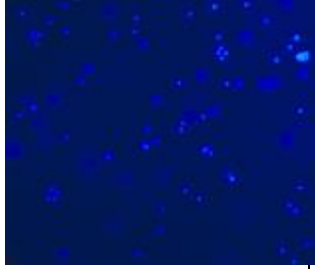
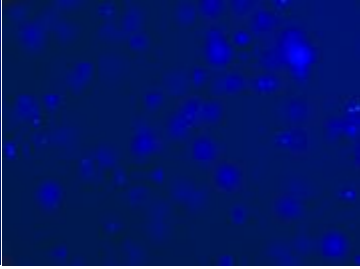
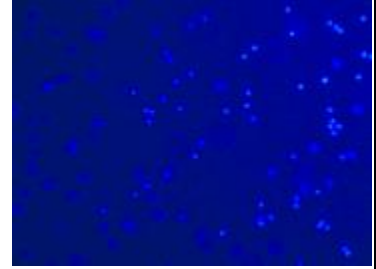


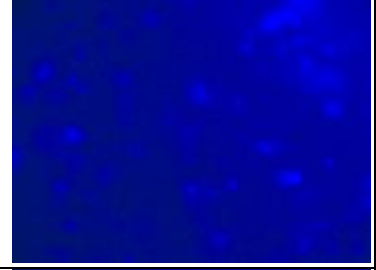

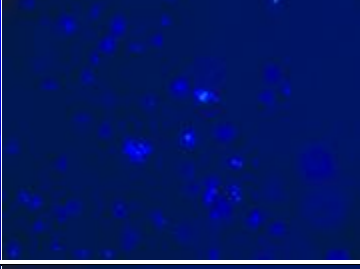
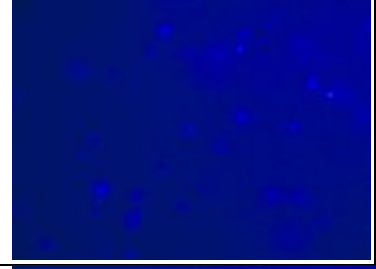


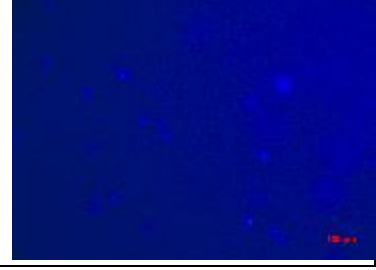
Because the team did not have a tissue culture plate (TCP) with a removable insert, the gel could not be removed from the TCP. 200 μ L of the diluted enzyme solution was put in each well and incubated overnight, and still the gel could not be removed from the well using a pipette tip. Based on this, if the team wanted to remove the gel and extract the cells, and TCP with a removable tissue culture insert would be needed.

This experiment showed that all three of the gels performed the same, and we could move forward with any of them. We chose to move forward with the Extracel Kit. This experiment also revealed a complication with mixing the cells with the hydrogel. We observed that mixing the cells with the hydrogels at time point zero, the cells settled to the bottom of the plate during the 15-18 minutes of gelation period (Figure 20). Adding the cells to gel mixture at a later time point may help avoid this problem.

3D Cell Dispersion Experiment

The purpose of this experiment was to try and achieve uniform 3D cell dispersion throughout the hydrogel. To achieve this, we allowed the gel to start crosslinking and then added the cell suspension at different time points (0, 4, 8, 12 and 16 minutes of gelation) before plating in culture wells. The protocol followed is detailed under 3D Cell Dispersion Experiment. As can be seen in Table 21 below, 3D cell dispersion was achieved at all time points tested. Addition of cells to the gel after, 8 and 12 minutes of gelation resulted in an even distribution of cells. The 3D dispersion is apparent by the inability to focus on all the cells simultaneously, but rather having to move through the gel to view all the cells. Based on these results, in future experiments the cell suspension was added to the gel between 8 and 12 minutes post initiation of gelation.

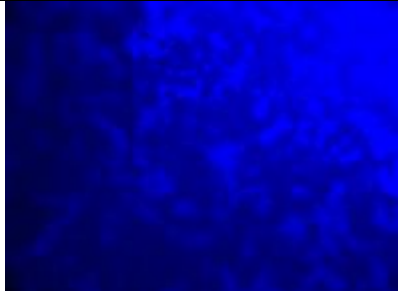
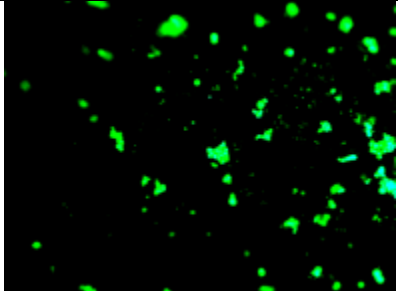
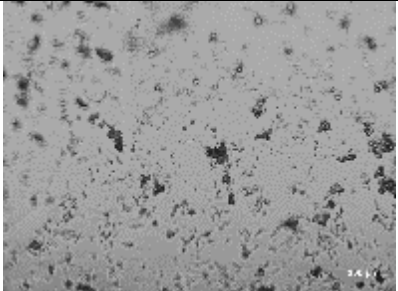
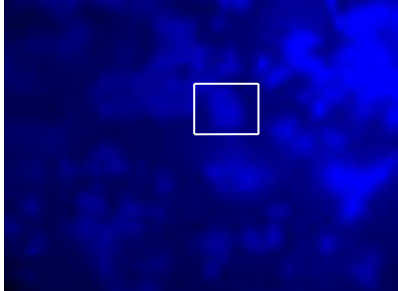
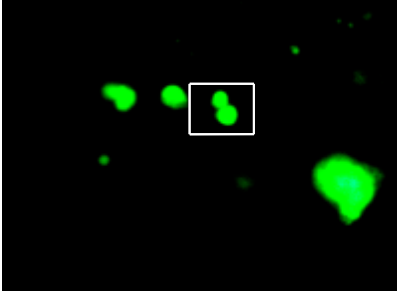
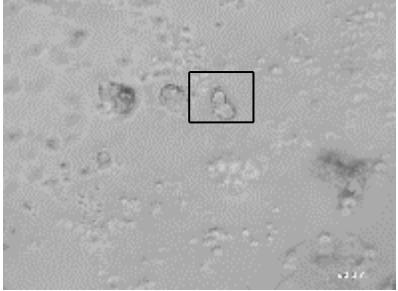
Table 21: 3D Cell Dispersion

Time Post Gelation	Day 1	Day 1	Day 2
0 minutes			
4 minutes			
8 minutes			
12 minutes			
16 minutes			

A follow-up to this experiment was to determine if the cells in the 3D dispersion were alive and proliferating. After monitoring the gel for 10 days, we observed that the cells maintained a spherical conformation, as opposed to the normal fibroblast phenotype observed while growing on a 2D tissue culture plastic surface. We believe that this change

in phenotype is due to the three-dimensionality of the gel as well as due to a drastic change in stiffness that the cells are used to growing immediately prior to the hydrogel. In order to assess the viability and proliferative ability of cells, we conducted a BrdU cell proliferation assay (Table 22). The BrdU assay followed the protocol in Appendix E.

Table 22: Staining of 3D Cell Dispersion

Hoechst	BrdU	Phase Contrast
10X		
		
40x		
		

As can be seen above, the cells in the gel were alive and proliferating. The proliferating cells could be seen as growing in small to large clumps. This is clearly seen in the 40X images and is highlighted by boxes focusing on one area of cell aggregation. We hypothesize that the change in dimensionality and stiffness resulted in a lag period where the cells needed time to accustom to the new environment before starting to proliferate. Because the cells are in a 3D environment, cells are now able to grow in all directions to form clumps as opposed to a monolayer growth on regular tissue culture plates.

Hydrogel Selection

Based on the results of the experiments discussed above, the team determined all three hydrogels (Extracel, HyStem-C, and HyStem-HP) to be compatible for the final test. As such, the team decided to move forward with Extracel for the duration of the experiment.

4.5.3. Material Degradation Study

In order to assess the degradation rate and the factors that affect water-soluble PVA and PLA degradation, we developed a protocol that is described below. Three one inch long sections of each 1.75 mm filament were cut off of the material stock and were immediately used in each experiment.

The main factor that will effect degradation is the media or water that it is dissolved in. Each set of filaments were placed in individual beakers containing 10 ml of water or complete DMEM media. The water and media were assessed at room temperature (21°C) and in an incubator at 37°C. The degradation rate was carefully monitored in 15 minute intervals until the filaments had dissolved.

Factors that could influence the degradation rate are ultra-violet (UV) light and oxygen. For these factors three filaments from each material class were placed in an incubator under germicidal (UV) light for five days. Alternatively oxygen effects were measured by placing the filaments in an open container exposed to the atmosphere.

After a period of two hours the PVA filaments in both temperatures and solvents (water and DMEM) had dissolved. From recording data at each 15 minute time point it was determined that DMEM media at 37°C was the optimal method for degrading the PVA. PLA showed minimal to no degradation in either solvent at any temperature. Neither oxygen nor UV light affected the degradation rate significantly after the two hour period. A note made by the team was that movement of the solvents also sped up the degradation time. The rotation or movement of the solvent is key in a clean dissolution of PVA.

From these results it was determined that PVA degrading in DMEM media in a 37°C incubator was the fastest option for material degradation. Rotation of the media can be achieved by a rotator plate or a shaker that can be used in an incubator.

4.5.4. 3D Printer Protocols and Preliminary Data

A variety of tests and file processing methods had to be established in order to achieve consistent print quality and fractal reproduction from the MakerBot Thing-O-Matic printer. These methods will be detailed in the following sections. They were vital in ensuring that the Thing-O-Matic was capable of printing fractal structures at a small scale that are otherwise on the very edge of its capabilities as a 3D printer. This is especially the

case with PLA and PVA, which are considered experimental materials for the Thing-O-Matic.

Test Prints

To achieve the best print quality and reproduction possible, the Thing-O-Matic must be properly calibrated. First, the extruder tip and build platform positions were calibrated. The ReplicatorG software has a built-in script named Calibration. When run, this script asks the user to manually center the build platform, and then positions the extruder tip in the middle of the platform and just barely above it. Once done, the printer saves this position as the zero point. This calibration was performed before each day of printing. Because the .GCODE files that contain the code for each 3D object printed are generated based on this zero position, each of those files had to be regenerated every day to ensure optimal print quality.

Next, the printing accuracy had to be properly calibrated. This was performed by printing a 20 mm x 20 mm x 20 mm solid cube of ABS, then measuring it with precision digital calipers. The X, Y, and Z axis motor revolutions per mm were then adjusted to ensure that the 20 x 20 x 20 mm cube was accurately reproduced. This calibration was performed after the printer tip had been serviced and when the printer filament material was changed, first to PLA then to PVA.

It is important to note that the Thing-O-Matic, as a low-cost, early generation 3D printer initially designed for ABS printing only, is incapable of fully reproducing each fractal shape accurately each time to a very fine degree of detail, even with calibration. However, it serves its purpose as a proof of concept device. Newer generations of 3D printers at the same price range as the Thing-O-Matic deliver significantly better quality and reproducibility, so even better results are possible. It is worth noting that any inaccuracies or variation in the printing of the 3D fractal .STL files impose a sense of randomness to the fractals being printed. This randomness is a feature of fractals found in nature, which are categorized as plasma fractals. Thus, printing inaccuracies actually contribute to the effectiveness of each fractal mold shape and may even provide extra pores in which cells may adhere and additional channels through which nutrition can be

delivered. The resulting prints are not only fractal in nature, but they incorporate more biomorphic features because of these slight irregularities.

Final .STL Processing and .GCODE Generation

The process of converting the fractals into molds, then producing .STL and finally .GCODE files requires significant computational power and a number of steps. First, the generated fractal shapes are opened as Mesh files in SolidWorks using the ScanTo3D function. Then, an assembly is created with the generated fractal shapes and the mold shell, shown below in Figure 12. The outer dimensions of this shape are 20 mm x 20 mm, the inner dimensions of the space are 15 mm x 15 mm, and the walls are 2.5 mm thick. The fractal was then placed within this mold, and the entire assembly was exported as a single .STL file using SolidWorks.

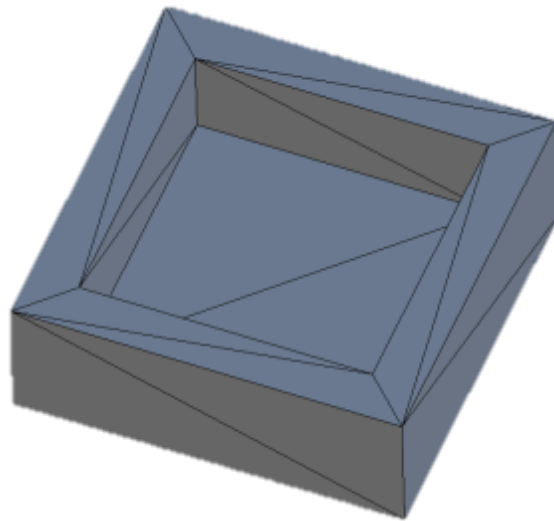


Figure 12: The base mesh for the fractal molds. Also used as the control.

Limitations in the SolidWorks .STL export script resulted in initial files that did not print correctly through ReplicatorG. These files were uploaded to the Netfabb Cloud Service (cloud.netfabb.com) which is an automated .STL repair utility. In addition to repairing the .STL files, this service provided surface area and volume values for each fractal mold. The resulting .STL files were opened with ReplicatorG 0037 and exported to the .GCODE format using Skeinforge 50 that was built into the ReplicatorG software. The .GCODE files were then printed normally using the Thing-O-Matic.

Because of the lengthy processing steps required to import a fractal mesh into SolidWorks and the file size and processing time limitations in the Netfabb service, the types of fractals that could be used were limited. Fractals chosen could not be too complex, and could not have excess amounts of detail or large recursion indexes ($n > 3$). This was not an issue for us due to the resolution limitations of the Thing-O-Matic, but it will be a limitation in the future if more capable 3D printers are utilized.

Chapter 5. Final Design and Validation

5.1 Conceptual Final Design

The selection of the final design was based on the design’s ability to achieve all of the previously stated constraints, objectives, and functions. This achievement was evaluated on various levels from binary, to a numerical range between 1 and 100. These multiple evaluations produced a numerical score for each design. The highest scoring design was selected for further development.

5.1.1. Fabrication Method Selection

The following tables and charts describe how we selected our final fabrication method. First, we used our Functions/Means tree to develop the Functions/Means Matrix, shown below in Table 23. This relates the functions to each design alternative. If the design achieves the function in that row, the means by which it does so are written. This eventually determined how successful we believed each design could be.

Table 23: Functions/Means Matrix

Functions	Printed Scaffold	Hydrogel Mold	Sacrificial Lattice	Embedded Cells
Must Not Develop Necrotic Core	Fractal Geometry, Controlled degradation of scaffold	Fractal geometry, surface characteristics for soft tissues	ECM/Surface characteristics, fractal geometry, controlled degradation of scaffold	ECM/growth factors incorporated
Maintains Cell Viability	All	All	All	All
Even Flow of Nutrients	Submerge in media	Submerge in media, porosity	Submerge in media	Submerge in media
Mimics Biological Structure	Fractal geometry, material, Surface Area : Volume	Fractal geometry, Surface Area : Volume	Fractal geometry, Surface Area : Volume	Surface Area : Volume

Next, we created a matrix relating each design to the constraints that we previously specified. Table 24 below shows this matrix. It is a binary system displaying a ‘Y’ if the design meets the specified constraint and an ‘N’ if it does not. As shown, the embedded cells design does not meet all of our specified constraints. The resources needed to create a scaffold of this nature are beyond the scope of our project and the material would not be

compatible with the MakerBot Thing-O-Matic 3D printer. At this point, we went ahead with the three designs that did meet all of our constraints.

Table 24: Matrix of Design Constraints

Constraints	Printed Scaffold	Hydrogel Mold	Sacrificial Lattice	Embedded Cells
Manufacturability	Y	Y	Y	N
Biocompatible	Y	Y	Y	Y
Resorbable	Y	Y	Y	Y
Within Budget	Y	Y	Y	Y
MakerBot Compatible	Y	Y	Y	N
Size Limitation	Y	Y	Y	Y
Time Limit (28 Weeks)	Y	Y	Y	Y

Next, we created a Pairwise Comparison Chart (PCC), as shown in Table 25, comparing the functions of our project. We determined that cell viability and the lack of a necrotic core were equally the most important functions of our design. In ranking the other functions, even nutrient flow was next, followed lastly by mimicking a biological structure.

Table 25: Pairwise Comparison Chart of Design Functions

	Must not develop a necrotic core	Maintains Cell Viability	Even Nutrient Flow	Mimics biological structure	Totals
Must not develop a necrotic core		0.5	1	1	2.5
Maintains Cell Viability	0.5		1	1	2.5
Even Nutrient Flow	0	0		1	1
Mimics biological Structure	0	0	0		0

Finally, we created a weighted matrix of our design alternatives to determine which fabrication method would best fit our project. The multipliers were determined based on the PCC. Then, each function for each design was given a score between 0 and 100 based on the information presented in our Functions/Means Matrix in Table 26. The scores were initially arbitrary, but then became subjective relative to the other alternative designs.

Table 26: Function/Means Matrix

Functions	Printed Scaffolds	Hydrogel Mold	Sacrificial Lattice	Embedded Cells
Must Not Develop Necrotic Core	Fractal Geometry, Controlled degradation of scaffold	Fractal geometry, surface characteristics for soft tissues	ECM/Surface characteristics, fractal geometry, controlled degradation of scaffold	ECM/growth factors incorporated
Maintains Cell Viability	All	All	All	All
Even Flow of Nutrients	Submerge in media	Submerge in media, porosity	Submerge in media	Submerge in media
Mimics Biological Structure	Fractal geometry, material, Surface Area : Volume	Fractal geometry, Surface Area : Volume	Fractal geometry, Surface Area : Volume	Surface Area : Volume

As can be seen in Table 27, all three of the evaluated designs are feasible options; however, the hydrogel mold is the best option. In addition to the features displayed in the previous tables, the hydrogel mold is also a unique attempt at solving this problem with a 3D printer. The hydrogel mold will also allow a variety of cell type options because its mechanical characteristics are similar to that of biological tissue. In addition, this provides more material options outside of PVA and water-soluble PLA, the only two materials both biologically and MakerBot-compatible.

Table 27: Weighted Design Matrix

Functions	Printed Scaffold	Hydrogel Mold	Sacrificial Lattice	Embedded Cells
Must Not Develop Necrotic Core (X 2.5)	90 = 225	100 = 250	95 = 237.5	X
Maintains Cell Viability (X 2.5)	100 = 250	100 = 250	100 = 250	X
Even Flow of Nutrients (X 0.75)	75 = 56.25	90 = 67.5	70 = 52.5	X
Mimics Biological Structure (X 0.25)	80 = 20	80 = 20	65 = 16.25	X
TOTAL:	551.25	587.5	556.25	X

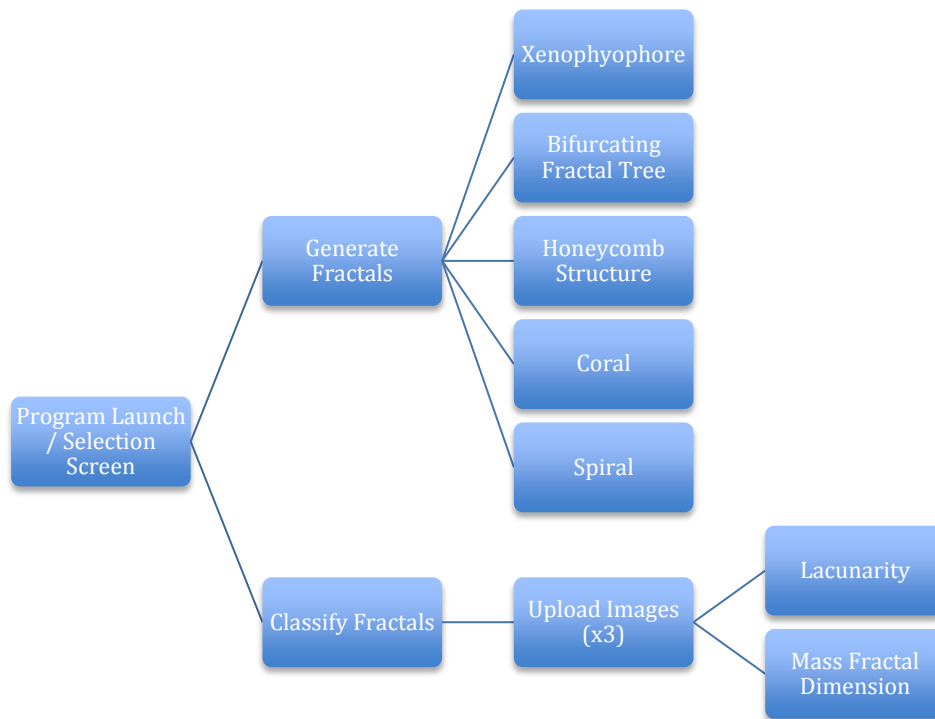
The hydrogel mold will require further verification testing before being pursued in testing validation. These verifications include specifically the ability of the hydrogel to maintain the selected geometric structure after the mold dissolves.

5.1.2. Fractal Classification and Generation

The MathWorks Matlab computational software package was used for the classification and generation of 3D fractals for this project. The classification and generation algorithms used are a combination of original programming and code from the Matlab Central File Exchange (www.mathworks.com/matlabcentral/fileexchange). The entire system will be detailed below, including code samples and licensing information.

The basic program design is outlined in Figure 13 below. The user is first presented with an opening screen that asks the user to either Generate Fractals or Classify Fractals. If the user chooses to generate a fractal, they are taken to a window that allows them to select from any of the fractal generation algorithms that are available. Upon choosing an algorithm, the user is taken to a window that allows for input of any of the parameters

available in the fractal generation script and a button that generates a .STL file of the 3D fractal that can then be imported into ReplicatorG and printed with the MakerBot Thing-O-Matic 3D printer. When available, the user will also be supplied with some of the default or common parameters that can be used with each algorithm. If the user chooses to classify a fractal, they are taken to a window that allows them to upload three images of the fractal: Top, Front, and Right. The user may then generate a report that classifies the fractal by lacunarity (L) or by fractal dimension (D).



**Figure 13: Flow Chart of Fractal Generation and Classification Program in MatLab.
See Appendix C for code.**

The user interfaces with the fractal generation and classification software by way of a Graphical User Interface (GUI) written using the MatLab GUIDE utility. An example of the user interface can be seen below in Figure 14. This GUI utilizes buttons, scrolling lists, and selection boxes because they are common interface elements in modern software packages, thus improving the inherent ease of use in this software.

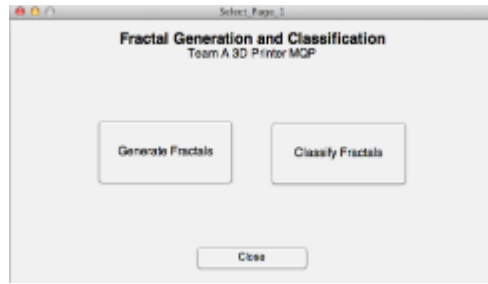


Figure 14: Function Selection Screen

The window for the fractal classification section of the program can be seen below in Figure 15. The two available classification tests are lacunarity and fractal dimension. Three images are uploaded for each test – one image of the top, one image of one side, and one image of another side turned 90 degrees. Each image should be 1000 px x 1000 px in size. The chosen algorithm will be run on each of the images and the results for each image will be averaged together to achieve a 3D fractal score for each parameter. The fractal dimension and lacunarity algorithms used were found on the MathWorks File Exchange, and are available for use under Appendix L.

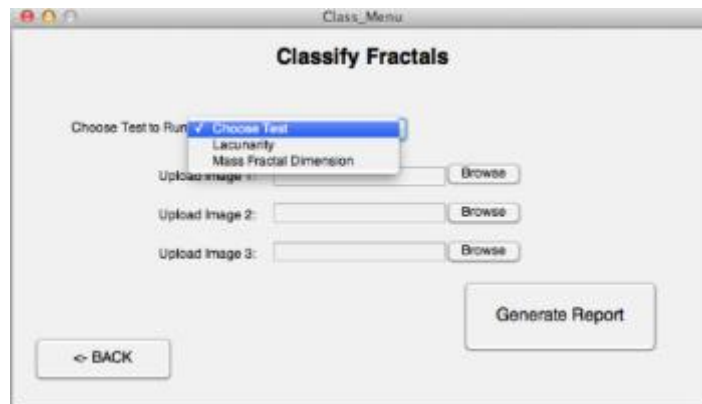


Figure 15: Fractal Classification Window

The four fractal geometries chosen for the first round of testing, as well as many other geometries considered, were generated with either MathWorks Matlab or Incendia software packages, or modeled directly within SolidWorks. As part of the initial research

stage, a fractal generation algorithm was written which can be used in a general sense to generate iterated function systems for any base shape if provided with coordinates.

The general fractal generation algorithm which was written for this project is presented in Appendix C, though most fractals generated with this algorithm were not tested due to equipment limitations in the Makerbot Thing-O-Matic 3D printer. All code is written for MathWorks MatLab.

This algorithm can be used with any set of vertices and faces defining a 3D seed shape for the fractal. The program outputs a 3D plot of the target geometry which can then be exported using a Matlab to .STL conversion program. Many different geometries were tested with this algorithm, but the only ones generated that were used in final testing were the Sierpinski triangle and Menger Sponge (cluster fractal), using triangle and cube base shapes, respectively.

A bifurcating fractal tree is one of the most simple fractal shapes, yet it can model some of the most complex biological phenomena, including vasculature and neural networks. Due to its simplicity, the bifurcating tree that we used was manually modeled directly in Dassault Systemes SolidWorks.

The most geometrically complex fractal used for this project was the fern fractal. This fractal was an experiment in using more complex fluid surface shapes, rather than stricter geometries, while maintaining self-similarity at different levels. Due to its difference from the other shapes we considered, the above algorithm was insufficient, so the Incendia software package was used. Incendia is a program that can generate complex fractal shapes given any user defined base shapes and algorithms, then output them as .STL files.

5.1.3. Fractal Selection

The fractal geometries that were selected for testing were chosen based on optimization of surface area to volume ratio, integration of biomorphic design, and ability to be printed using the MakerBot Thing-O-Matic. Four of the most promising fractal geometries that could be successfully and rapidly (<30 min) printed using the Thing-O-Matic in both PLA for prototyping and PVA for testing were selected.

The first fractal selected was the Menger sponge, a fractal in the Cluster fractal category. This fractal is built by starting with a cube and iteratively subtracting smaller cubes from the larger one, increasing the surface area to volume ratio. This also forms a self-similar model. Iteration of the generation algorithm can be carried out as many times as desired, producing increasingly better surface area to volume ratios. This is limited by the capabilities of the Thing-O-Matic printer to $n=2$ or $n=3$. A cross-section of the Menger Sponge that will be used in our experimental testing can be seen below in Figure 16.

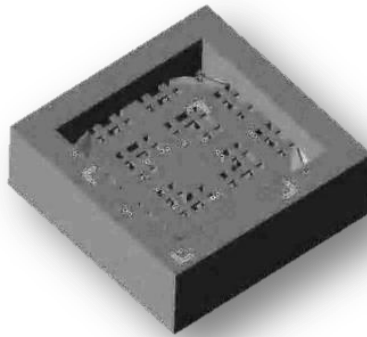


Figure 16: Menger Sponge Fractal Cross-Section

Another set of fractal systems that were explored are Iterated Function Systems (IFS). These fractal geometries are biomorphic in nature because they mimic some common biological shapes – such as plant leaves, roots, and branches, blood vessels, and neural networks. Any function may be iterated to create such a 3D structure, but the two specific ones chosen were a tree and a fern. Figure 17 is an IFS fractal model of a fern, which was chosen to model the nutrient transfer that occurs in plants. Figure 18 is an IFS fractal of a bifurcating tree, designed to model tree roots and branches in a simplified mathematical manner.

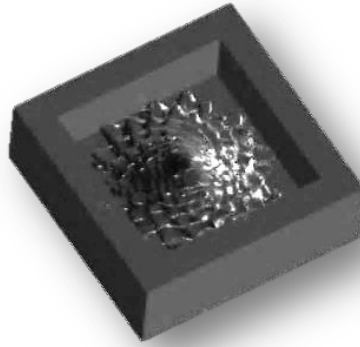


Figure 17: An Iterated Function System Fractal Modeling a Fern

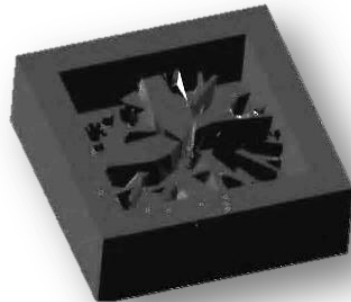


Figure 18: A Bifurcating Fractal Tree

The final fractal chosen for testing is the Sierpinski triangle. This is a simple variation on the Menger sponge in that it is also a cluster fractal. It is generated using the same algorithm as the Menger Sponge, but using a pyramid as the base shape instead of a square. This fractal is designed to optimize surface area to volume in much the same way as the Menger sponge and, if this category proves successful in testing, many other primitive 3D shapes could be processed with the same algorithm to potentially generate additional effective geometries. An example of the Sierpinski triangle in 3D can be seen below in Figure 19.

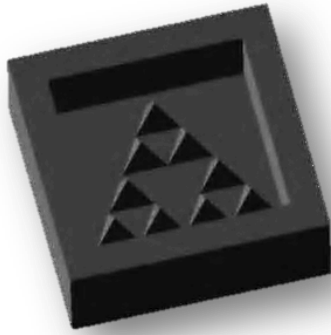


Figure 19: Three-Dimensional Sierpinski Triangle Fractal Shape

5.2 3D Printing of Fractal Molds

The 3D printing protocol for all fractal molds produced in PVA was determined then kept consistent to ensure reproducibility of mold quality and comparability of results. The MakerBot Thing-O-Matic printer was equipped with a Heated Build Platform covered with Blue Painter's Tape, though the heated platform was powered off for PVA printing. The printer was kept in a Plexiglas enclosure that was mostly sealed using tape. A Nitrogen purge of the enclosure was performed prior to printing, and a steady flow of Nitrogen was maintained during printing to lower the humidity in the print environment.

Printing was conducted at room temperature (22° C) with the extruder tip set to 210° C. Fractal molds were printed at 50% infill, 0.3mm layers, 1 shell, with a raft, at 20mm/s plastic extrusion speed. Each fractal mold was printed three times per test, and the resulting documents were sterilized in 70% ethanol and UV light.

5.3 Surface Area to Volume Ratio Calculations

An essential part of our data analysis was a comparison of the surface area to volume ratios of each fractal we used and the resulting cell growth in each one. The following describes how we calculated the surface area to volume ratios of the resulting gel using data from the fractal molds.

As part of the .STL generation process, each file was submitted to the Netfabb Cloud Service (cloud.netfabb.com) that repairs submitted .STL files and provides the Surface Area and Volume of the mold geometry. Using this service, we obtained a set of numbers from which we calculated the surface area and volume of the gel fractals themselves. We also

used the amount of gel added to each scaffold as a starting point. The full set of data for each scaffold is included below in Table 28.

Table 28: Surface Area and Volumes for Fractal Molds and Hydrogel

Fractal Mold Name	Surface Area (cm ²)	Volume (cm ³)	Volume of Gel (cm ³)
Control	16.60	1.67	1.03
Cluster	22.95	1.89	0.50
Fern	20.11	1.84	0.58
Sierpinski	17.39	1.71	0.40
Tree	21.2	1.80	0.90

The surface area to volume (SA:V) ratio was an essential metric that we used to classify the theoretical effectiveness of a fractal shape to provide nutrition to cells in a tissue scaffold. Basic values used in the calculation of the SA:V ratio were calculated by submitting the fractal scaffold .STL files to the online Netfabb Cloud Service, which repairs .STL files and provides the surface area and volume of the model. The following values computed by the program were used:

$$SA_{control} = \text{Surface Area of the Control Geometry Mold (Slab)}$$

$$SA_{fractal} = \text{Surface Area of the Fractal Mold}$$

The following values were constants for each fractal mold:

$$\text{Area of Mold Surface} = 1.5\text{cm} * 1.5\text{cm} = 2.25 \text{ cm}^2$$

$$\text{Area of Top} = 1.5\text{cm} * 1.5\text{cm} = 2.25 \text{ cm}^2$$

$$\text{Area of Mold Sides} = 1.5\text{cm} * \text{Height} * 4$$

Where the height was determined based on the volume of hydrogel added to each mold, in the following manner:

$$\text{Volume} = \text{Width} * \text{Height} * \text{Depth}$$

$$\text{Volume} = 1.5\text{cm} * 1.5\text{cm} * \text{Height}$$

$$\text{Height} = \frac{\text{Volume}}{2.25 \text{ cm}^2}$$

Thus, the surface area of only the fractal geometry surface in each mold can be defined as:

$$SA_{surface} = (SA_{fractal} - SA_{control}) + \text{Area of Mold Surface}$$

And the surface area of the full hydrogel scaffold generated from the mold can be represented by:

$$SA_{scaffold} = SA_{surface} + \text{Area of Mold Sides} + \text{Area of Top}$$

This method was used to find the surface area and volume of each gel tissue scaffold, and then compute the surface area to volume ratios of the resulting hydrogel tissue scaffolds. The final values for each scaffold are presented below in Table 29.

Table 29: Surface Area, Volume, and SA:V Ratio for all hydrogel scaffolds

Scaffold Name	Surface Area (cm ²)	Volume (cm ³)	SA:V Ratio (cm ⁻¹)
Cluster	12.77	0.50	25.5
Fern	20.11	0.58	17.2
Sierpinski	17.39	0.40	16.2
Tree	11.85	0.90	13.2
Control	7.24	1.025	7.06

5.4 Hydrogel Protocol

The final step that needed to be completed before creating the scaffolds was to calculate the amount of cells to be seeded within each scaffold. From previous studies it became apparent that the cells would need to have quite a high density because they are in 3D conformations. The team found previously that the cells did not grow and proliferate as fast within the gel as they typically do on tissue culture plate surfaces. This may be attributed to the fact that they are not as close together so they cannot communicate through chemical signals or factors as well as they can on 2D surfaces, in addition to a lower stiffness than TCP.

Based on observations and suggestions from the team's advisor, it was determined that the scaffolds should be seeded with cells at a density of 10,000 cells per monolayer. In the case of NIH/3T3 cells, a monolayer is 20 μm thick, because NIH/3T3 cells are normally 18 μm in size (Invitrogen, 2013). The number of monolayers was determined by measuring the approximate thickness of the mold. From this information, we extrapolated the number of cells needed per mold. Information for the volume of the gel components of each mold,

the total volume, the number of monolayers, the area of an entire cross section, the thickness, and the number of cells to be seeded are presented below in Table 30.

Table 30: Volume of Gel and Cell Density Components of Scaffolds

Fractal /Mold	Volume (μL)	Volume of Glycosil and Gelin-S (μL)	Volume of Extralink (μL)	Area (cm ²)	Thickness (μm)	Number of monolayers	Total # of cells
Cluster	500	400	100	2.25	2220	111	1,110,000
Fern	580	464	116	2.25	2580	129	1,290,000
Sierpinski	400	320	80	2.25	1780	89	890,000
Tree	900	720	180	2.25	4000	200	2,000,000
Control	1025	820	205	2.25	4560	228	2,280,000
TOTALS		2724	681				7,570,000 (X3)

Once the calculations for cell densities were complete, printing of the molds began. The molds were printed in polyvinyl-alcohol (PVA) inside a closed Plexiglass printer enclosure after a nitrogen purge was performed. A total of 15 PVA molds (3 of each of the following fractals: cluster, fern, Sierpinski, tree, and control) were printed. The molds were rinsed under a hood in 70% isopropyl alcohol for less than 10 seconds. The molds were then placed in weigh boats and exposed to ultraviolet light for 20 minutes for sterilization before the hydrogel was added.

While the molds were being printed, volumes of each hydrogel and cell suspensions were prepared for each mold in microcentrifuge tubes. Once the molds were sterilized and the gel components prepared, Extralink, Glycosil, and Gelin-S were combined for an individual mold. After waiting for 8 minutes, the volume of cell suspension and any additional media calculated in Table 31 was added into the molds. The cell suspension contained 2,280,000 cells / 0.5 mL. The components were mixed via pipetting before being added to each mold. While waiting for each mold to set, more molds were prepared until all 15 were complete. For a detailed outline of this protocol, see Appendix J.

Table 31: Final volumes of gel components and cell suspension.

Mold (Fractal)	Gelin-S & Glycosil (μL)	Extralink (μL)	Cell Suspension (μL)	Additional Media (μL)
Cluster	400	100	48.7	51.3
Fern	464	116	56.6	43.4
Sierpinski	320	80	39.0	61.0
Tree	720	180	87.7	12.3
Control	820	205	100.0	0

5.5 Cell Maintenance Protocol

After the molds had sufficiently gelled, they were placed in 100 mm tissue culture plates with 50 mL of DMEM and placed on a rotator inside of an incubator. Four hours later, the media was aspirated to remove as much dissolved PVA as possible, and replaced with 45 mL of new DMEM before returning the plates to the rotator. The following day, after the majority of the PVA had dissolved, the molds were removed from the 100 mm tissue culture plates, and placed in 30 mm tissue culture plates with 10 mL of media. Each successive day, half of the media was aspirated and replaced with new DMEM. The only day that this did not occur was on the fourth day of culture. On the fourth day, the molds were rinsed in media by submersion and transferred to new 30 mm tissue culture plates with 10 mL of fresh growth media. During every day of culturing, phase contrast microscopy photographs were taken until the samples were fixed for histology on day 16.

5.6 Hydrogel Transfer and Washing

The day after the hydrogel scaffolds were molded, and on the fourth day of culture, we replated the scaffolds to ensure that there was as little PVA left in and around the scaffolds as possible. In order to do this, each mold was washed by submersion in DMEM. Polypropylene flexible spatulas were sterilized and used for picking up, rinsing, and replating the hydrogel. A photograph of the rinsing setup may be seen below in Figure 20.



Figure 20: Setup of Scaffold Rinsing on Day 4 of Culture

5.7 Cell Imaging

After the hydrogel scaffolds were created, phase contrast images were acquired every day for 16 days of culture at 10X magnification using a Zeiss Axiovert 40 CFL inverted fluorescent microscope. During the first 2-3 days of culture, it was difficult to visualize any cells because of the presence of PVA in the mold. After a week to 10 days in culture and removal of PVA, cells were more visible as evidenced by formation of cell clusters.

5.8 Cell Fixation and Sectioning Protocol

On day 16 of culture, the hydrogels were fixed and prepared for cryostat sectioning on the Leica CM3050 Cryostat Microtome (see Appendix F for the SOP) following the procedure outlined below.

1. Immediately after the experiment is over, place the hydrogel tissue scaffolds into individual cassettes and label with the appropriate identifying data.
2. Fix the hydrogels using methanol-free formaldehyde (this is to allow for actin staining) in a volume 10-15 times greater than that the specimen for 4-8 hours.
3. Wash your specimen under running tap water for 10 minutes.

4. Place the cassettes into freshly made 30% sucrose solution (100mL DI Water, and 30.0g of sucrose) in a leak proof container.

Just prior to beginning sectioning, the samples were placed under running water for 10 minutes. The samples were then attached to a chuck using optimal cutting temperature (OTC) compound. The hydrogel was cut in 20 micron sections, taking 16 sections from the top portion of the gel, 32 sections from the center of the gel, and 16 sections from the bottom of the gel. After completion of sections, the OTC was dissolved, the hydrogel was placed back in its cassette, and into 100% ethanol for storage.

5.9 Cell Staining Protocols

Two staining procedures were performed on select slides containing cryostat sections - hematoxylin and eosin (H&E) and AlexaFluor 488-Phalloidin with DAPI as counter-stain. H&E staining followed the procedure in Appendix G and stained the nuclei and cytoplasm. The AlexaFluor and DAPI staining followed the protocol outlined below, and stained for the actin cytoskeletal structure and alignment, and nuclei respectively. Before beginning the actin staining procedure, slides to be stained were placed on a test tube rack with paper towel beneath it. Between each step pour off the respective liquid, and then gently shake off the excess before proceeding to the next step.

1. Rinse the slides twice with 1mL DPBS+. Each rinse lasting 5 minutes.
2. Add 1mL 1% BSA blocking solution. Incubate at room temperature for 10 minutes.
3. Rinse twice with 1mL DPBS+.
4. Add 500 μ l of AlexaFluor 488-Phalloidin. Incubate at room temperature for 20 minutes.
5. Rinse twice with 1mL DPBS+.
6. Counterstain using 1mL of 200ng/mL of DAPI. Incubate at room temperature for 10 minutes.
7. Rinse twice with 1mL DPBS+.
8. Mount the slides with a coverslip using Cytoseal.


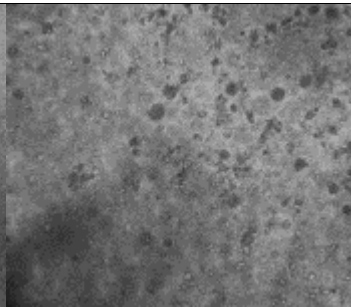
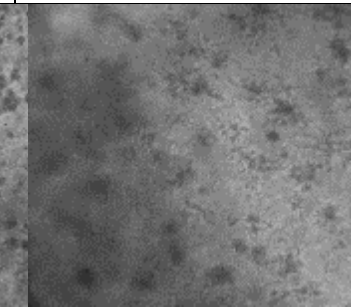
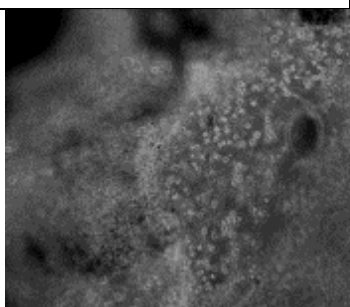
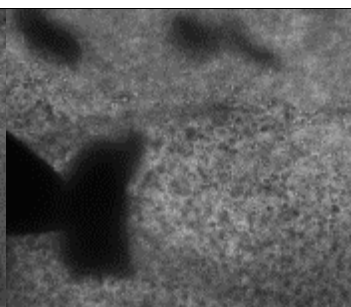
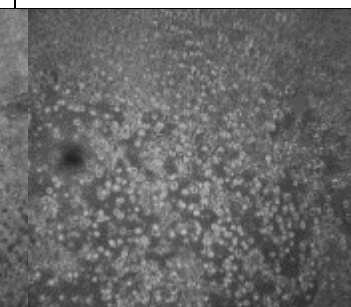
Chapter 6. Design Verification

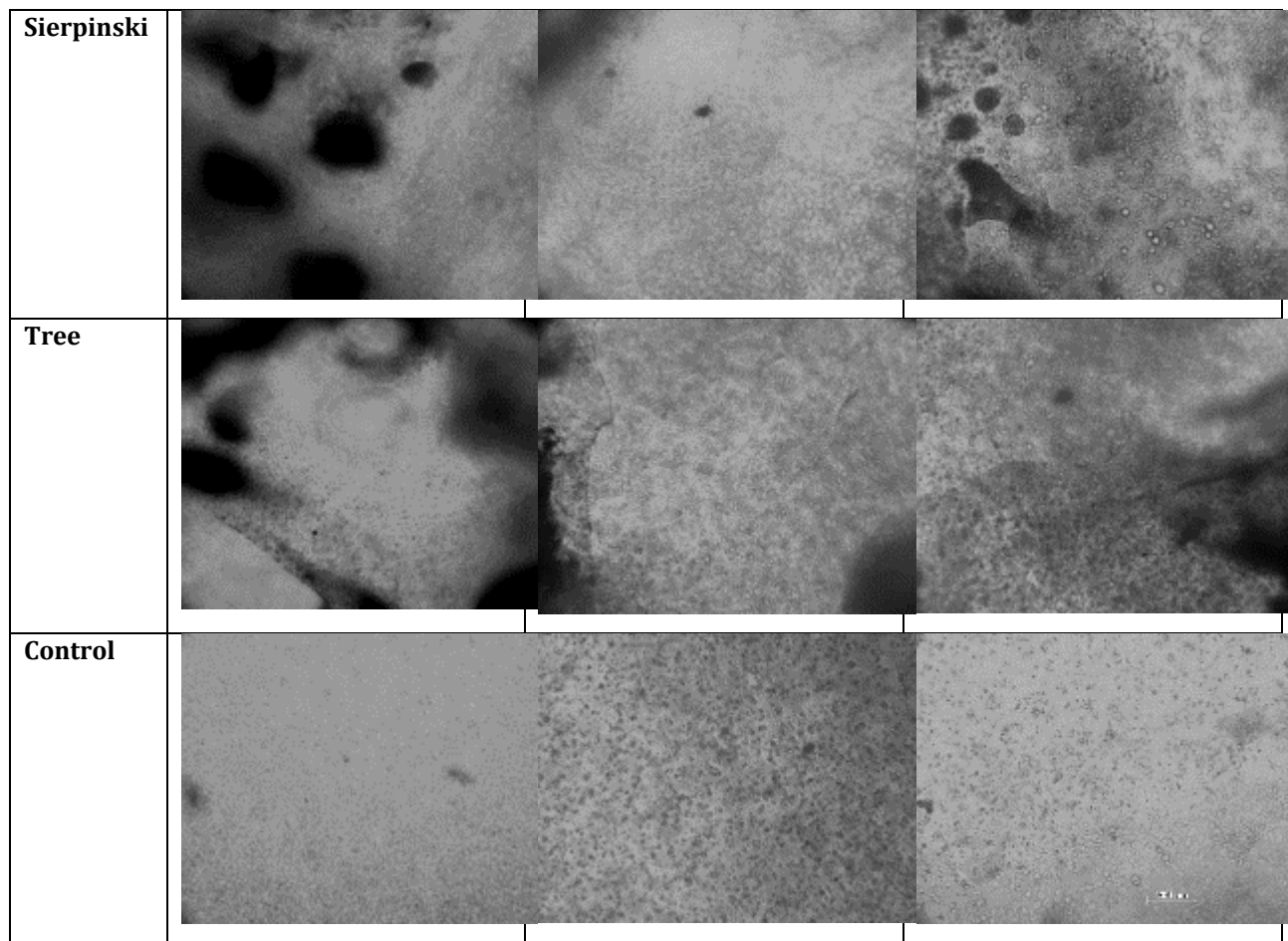
After the final experiment was executed following the protocols outlined above, the results of microscopy, histology, and staining were analyzed to determine if the experiment was successful. While there was no way to quantify the number of cells, analysis of the images showed that the cells remained in a 3D conformation within the hydrogel for the entirety of the experiment.

6.1 Cell Images Over Time

All hydrogels were reviewed and imaged daily to monitor the degradation of the PVA (black spots/regions on the images in Table 32), and the state of the cells. The cells were closely monitored for the initiation of proliferation. As can be seen by the formation of clumps, proliferation was visible on day 10 of culture (Table 32). The formation of clumps confirmed the cells were alive and adjusting to the 3D hydrogel environment. The length of time for proliferation to start could be attributed to the cells adjusting to the mechanical properties of the hydrogel, which is much softer than a TCP, and also adjusting to the distance with regards to cell-to-cell communication.

Table 32: Microscopy Images of Hydrogels from Days 5, 10, and 16

Hydrogel /Day	Day 5	Day 10	Day 16
Cluster			
Fern			



6.2 Cell Viability / Histology Results

Histology was performed to view the middle of the hydrogel. The gels were prepared as outlined in Section 5.8, and the depth of the sections taken was based on the number of cuts made. The sections were 20 μm in thickness, and the depth was counted starting when the hydrogel was first cut with the blade. Unfortunately, there was no way to make the hydrogel completely level on the chuck. Sections from the top, middle, and bottom were taken. In addition, some of the hydrogels cut more cleanly than others, some formed crystals, and disintegrated when coming in contact with the blade. This occurred with the tree fractal in particular. Despite these difficulties, we were able to obtain clean histological sections for staining and further analysis.

A portion of the slides were stained with H&E to view the nuclei (purple) and cytoplasm (pink). As can be seen in Figure 21, cells could be visualized at various depths, distributed uniformly as a 3D construct. The hydrogel (mesh-like structure stained purple)

is holding the cells in place; the nuclei in the foreground are dark purple circles, and cytoplasm can be seen in the background as light pink circles. This section of the Fern mold was 1500 μm deep, in the middle of the scaffold. This image confirms the presence of cells in the middle of the gel, validating our procedure.

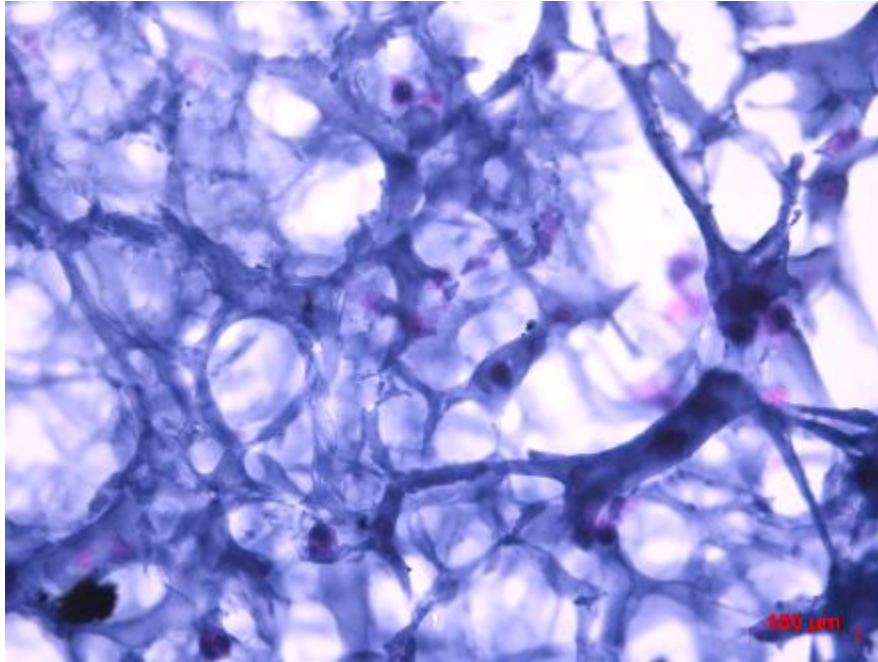


Figure 21: H&E staining of fern section

A few sections were stained with AlexaFluor-488 conjugated phalloidin (AF) to stain the actin cytoskeleton and counterstained with DAPI for staining the nuclei. Upon viewing the slides stained with AF and DAPI, multiple tube-like structures were identified in the Sierpinski and cluster gels, and at least one was found in the tree and fern gels. Representative images of these structures from the cluster gel at a depth of 1200 μm are shown in Figure 22 below. As can be seen by the images, the cells are clearly aligning in an organized structure that includes branching (bottom rows). This discovery was unexpected, but promising. The cells formed these structures in approximately 6 days (proliferation started on day 10 of culture, and the gels were fixed on day 16), and at depths of approximately 1200 microns from either end of the scaffold. Such formations were also found in the control gels at about the same depth. However, as can be seen in Figure 23, the organization of the structures in control is not as robust as the fractal

scaffolds. The majority of the control gels had single scattered cells as can be seen in the image in Figure 24.

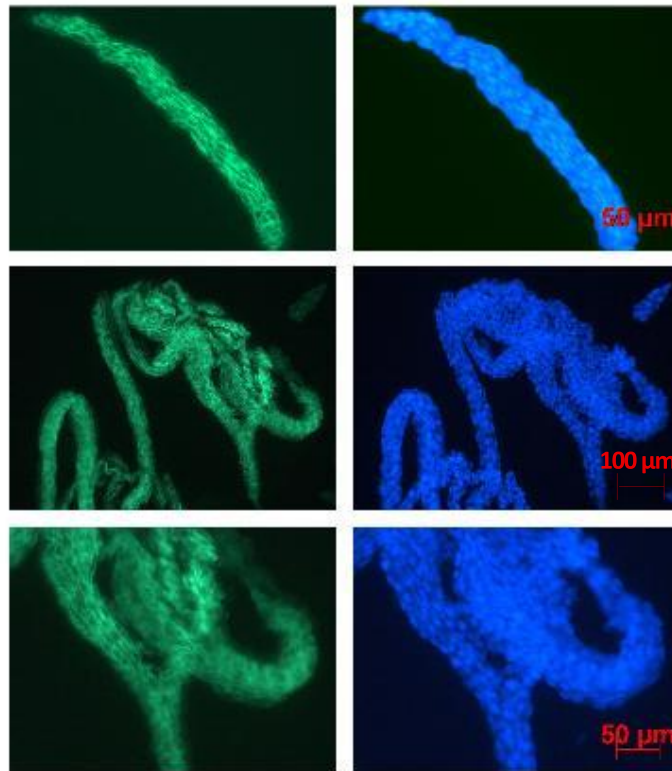


Figure 22: Actin (*left*) and DAPI (*right*) staining of tube-like formations in cluster section (40X top and bottom, 20X middle)



Figure 23: Actin (*left*) and DAPI (*right*) of cell clusters in control section (32X)

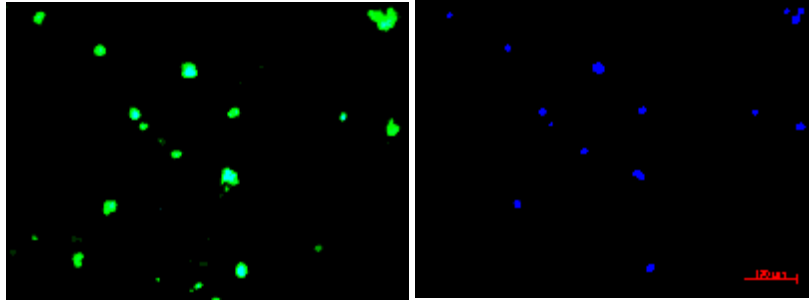


Figure 24: Actin (*left*) and DAPI (*right*) of cells in control section (20X)

6.3 Confocal Microscopy Results

With the discovery of tube-like formations, the actin stained sections were subjected to confocal microscopy on the cluster gel in attempts to further validate their identity. Confocal microscopy showed that the structures transcended the entire 20 μm thickness of the section, proving they are 3D. Figure 25 shows a portion of a tube-like structure in the cluster gel. This image more clearly shows the cytoskeletal alignment (green) of the cells. Further testing is required to confirm the identity of these structures.

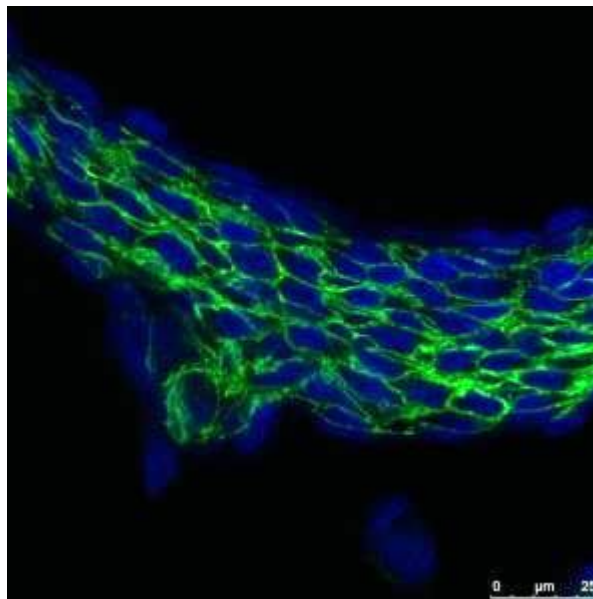


Figure 25: Actin and DAPI stain at 63X and 1.8 zoom of tube-like formation in cluster section

Chapter 7. Discussion

This chapter discusses the specific aims that were met throughout the project, including all of the manufacturing aims and limitations, the hydrogel scaffold and cell incorporation data, and how the process of the manufacturing and testing our final design went.

7.1 Review of Raw Data

Imaging the cells over time enabled us to see the proliferation and alignment of the NIH/3T3 cells. The aggregation of cells seen on day 10 of the images signifies that not only are the cells alive, they are proliferating. Also, the appearance of the cell aggregates can be seen at all depths of the scaffold, meaning that cells that are not immediately exposed to the media are surviving and growing. While the proliferation of the cells is slower than expected, complete media with the addition of growth factors could speed up the process.

The validation of our cell incorporation method was evident in the H&E stained hydrogels. The existence of cells in the middle of the gel confirms that cells remained suspended in the gel over an extended period of time and did not settle to the bottom of the scaffold.

The unexpected result of tube-like formations in the histological sections of the cluster, Sierpinski, fern, and tree fractals follow the premise that the scaffolds with high surface area to volume ratios will exhibit more cell growth than scaffolds with low ratios, such as the control slab. While the identity of the alignments are unknown at this time, the presence of these structures in multiple areas throughout the Sierpinski and cluster scaffolds rule out any procedural error or random effect. This pattern is interesting not only because it follows a tight-junctioned, tube-like structure, but also because the only varying factor in all of the tested scaffolds was geometry and resulting surface area to volume ratio. If, after further testing, it is confirmed that the structures are in fact hollow and are epithelial in nature, then the main factor for this type of cell differentiation and alignment will be scaffold geometry.

7.2 Limitations

The team faced several limitations while performing this study. The major challenge throughout this project was that the printer was outdated and significantly better technology is currently available at the same price point. Not only was it not able to achieve sufficient resolution, the printer malfunctioned numerous times throughout the course of the project. Troubleshooting technical problems was more difficult because the printer was user-assembled, not pre-assembled in a factory. The Thing-O-Matic was designed with the intention that ABS plastic be used; not PLA or PVA. It was also designed to be used with 3 mm filament, but in order to create smaller features, the team chose to use 1.75 mm filament. The motor deformed the smaller, weaker filament, producing printer blockages that occasionally resulted in inconsistent print quality. There were also significant issues in how the computer software was integrated with the printer. These problems would severely hinder the marketability of the system that was produced, but the team was able to work through them to gather results. Newer 3D printer technologies do not possess the same limitations and significantly improve the reproducibility and manufacturability of the 3D fractal molds.

The ability of PVA to solubilize and degrade in a matter of minutes to hours can be considered a limitation in our project. We were unable to show the fractal nature of the hydrogel using microscopy. We assume that the fractal nature allowed the cells to proliferate better and form the complex structures compared to control scaffolds by virtue of better nutrient delivery through the channels created by the fractals. One factor that may have contributed to this problem is the swelling property of hydrogels that may narrow the channels and hence not be detected by phase contrast microscopy. Additionally, the micron level fractal geometry may be destroyed by squeezing pressures exerted on the gel during histological sectioning.

Another limitation faced was the inability to quantitatively evaluate cell growth in our final tissue scaffolds. A possible method to quantify cell populations in each scaffold is to use a Quant-iT PicoGreen dsDNA Kit from LifeTechnologies (Li *et al.*, 2012). Alternatively, scaffolds could be digested to isolate cells and quantified using hemocytometer or automated cell counting systems.

7.3 Manufacturability

Our tissue scaffold design and methods have shown promising results, so it is worth considering the manufacturability of this product, and what must be changed and improved to optimize the manufacturing of these tissue scaffolds. Primarily, manufacturability can be significantly improved with a 3D printer using newer technology. Additionally, newer technology will enable more complex fractal generation and increase fractal reproduction reliability.

An improved 3D printer can help with every aspect of the PVA mold production. A better printer can enable the use of more complex fractals, can make them more reproducible, and can help produce them faster and on a larger scale. A printer designed for printing PVA can also enable the molds to be printed smaller and with thinner walls, optimizing degradation times. Higher processing power may lead to more complex fractal geometries with higher surface area to volume ratios.

7.4 Political, Ethical, and Sociological Ramifications

This section will discuss various hopes and concerns that this study may affect in many different aspects of society. Though the premise of this project focused on the economic feasibility of a 3D printer, the team also assessed the environmental impact, societal influences, political ramifications, ethical concerns, health and safety issues, and sustainability of the fabrication process developed.

The printer that this project was based on is economically feasible for a wide variety of research, clinical, or hospital settings. The Thing-O-Matic is very affordable, priced under \$2,000 USD, and facilities with little resources may not have a very difficult time attaining the equipment needed. For those organizations that may have sufficient resources, it should be advised that they use more durable printers with better resolution and more up-to-date software and hardware. Should this fabrication process of creating 3D scaffolds succeed in further research, it is hopeful that 3D printers become more widely available and manufactured on a larger scale. The main economic concern affiliated with this study stems from the laboratory resources used – the method used to care for and culture the scaffolds *in vitro* could be much more efficient with a lesser use of DMEM and cell culture

materials. The amount of training and expertise required will also play a role in the economic impact of this process.

This project presents both positive and negative environmental impacts. These concerns also tie into the sustainability of the process that was developed. The material that is used as the mold for our scaffold, PVA, is degradable; however the particles may negatively affect the environment. It has been shown that, when red pepper plants are cultivated in soil containing PVA, it retards their growth (Lee & Kim, 2001). Another environmental concern is attributed to the plastic waste created from cell culture resources. In the academic year the team worked on this project, cell cultures were passaged at least once a week for approximately 20 weeks, which translates to at least 40 cell culture plates if we kept two plates of cells at all times. These materials are not recycled as they are biohazard waste. An environmental advantage of this project is that the printer wastes very little material as compared to subtractive fabrication processes. Because the molds are manufactured on-site, only what is needed is printed. There is also less transportation needed to ship the molds as the plastic filament is bought in a more economic manner, so less fossil fuel is used. In rural communities or hard to reach places around the globe, this could be a more daunting task that would need many more resources in order to transport the materials.

Socially, the fabrication process that we developed would impact the world and tissue engineering in a few different ways. The printer and resources needed would be less expensive, and should be more available to research facilities, clinics, hospitals, and surgical units. The medicine itself presents a rapid production time because the molds are manufactured on-site and could be defect specific. The fabrication process itself is relatively simple and the materials used are not extremely difficult to acquire, so this technology may become easier to acquire, even for those with limited insurance plans.

As stated previously, the low cost of this printer would create more opportunities for availability of this technology throughout the world. It is also relatively simple to fabricate the scaffolds using this method and with commercialization of this process, it would become more streamlined. Despite this streamlined process, a surgeon is still required for implantation. Regarding the printer itself, there are a wide variety of online forums and helpful directions for building, repairing, and adjusting the mechanics and resolution of the

printer. Politically, this could greatly improve healthcare throughout the world and tissue engineering research.

The ethical concerns of using this technology include plagiarism, piracy of code, and religious concerns. Due to the nature of the programming used to generate and classify the fractal structures and use the 3D printer, the resulting code can be easily distributed illegitimately. While all copyright information was carefully reviewed in this project, other adaptations or similar research could infringe upon copyright information if due care is not exercised. The potential for this project to result in tissue regeneration *in vivo* may disagree with the beliefs of certain religions that believe God is the only creator of life.

In terms of health and safety issues, more long-term testing as well as *in vivo* testing will need to be completed before this process could enter clinical trials or become commercialized. The team has not found evidence of long-term *in vivo* tests using the Glycosan Extracel hydrogel. According to Glycosan Biosystems Inc., their Extracel product is intended only for research purposes. These tests, as well as any cytotoxicity tests, would need to be performed in accordance with FDA regulations. Though the research presented proves that we were able to create a 3D hydrogel tissue scaffold, future tests would need to prove that it would survive and integrate within the body.

In regards to sustainability, the amount of waste generated by this process is not ideal; however the process itself can be modified and adapted to future works. The amount of plastic used without the ability to be recycled has a negative impact on the environment. However, with the optimization of the manufacturing process, the development of these hydrogel tissue scaffolds could occur in one place. In addition, the process was created with change in mind. The experimental protocols for printing molds can be optimized based on the desired needs, and capabilities of the printer. With these changes available, the process developed is applicable to many situations.

Chapter 8. Conclusions and Recommendations

Our design consists of two primary components, computational modeling and the fibroblast cell culture within the hydrogel scaffold. This section reviews the conclusions drawn from each design aspect and provides recommendations for continuations of this project.

8.1 Objectives

The main objective of this project was the optimization of 3D tissue scaffold geometry, material, and surface area to volume ratio. This objective was clearly met through the proliferation and alignment of cells within the scaffolds and specifically the alignment seen in the scaffolds having the highest surface area to volume ratios.

Computational background and CAD modeling was also an important aspect of this project. The team was able to model each scaffold using MatLab, Incendia, Netfabb Cloud, and SolidWorks and mathematically calculate the surface area to volume ratio for each scaffold group.

The fabrication technique we used is not optimal for large-scale manufacturing, but is adapted for our smaller-scale research purposes. The fractal generation and production procedures can be feasibly adapted to faster, larger-scale 3D printers with minimal modification.

The use of an inexpensive 3D printer met our last objective of cost and therefore all of our objectives derived from the client's needs were met by this research. We exceeded the project budget initially assigned to us due to the cost of the hydrogel, so a more cost-effective alternative should be identified for further experimentation.

8.2 Future Improvements and Recommendations

While the overall goals of this project were met, improvements can be made to better the manufacturability and results of this project. Firstly, a 3D printer that has better reproducibility and accuracy should be purchased. With growing interest in 3D printing, there are many companies offering low-cost printer options that will yield higher quality results than the MakerBot Thing-O-Matic printer can provide. Printing in a sterile environment will also reduce the risk of contamination when cells are introduced. The

team chose the patterns we used not only because of their fractal nature but due to their ability to be easily printed. With a newer model printer, more fractal options can be explored and the surface area to volume ratio can be greatly varied.

The type of hydrogel used may also be explored. If a natural hydrogel or other synthetic hydrogel matrix is proven to work similarly to, or even improve the results found in this study then it may be a better option due to economic costs.

Confirmation of the amount of living cells should be quantified using live/dead staining. While we were able to qualitatively show that cells were proliferating and aligning, no quantitative data was gathered. This will be the next step in validating the results of this study.

A major aspect of this project that should be further developed is the confirmation of the identity of the tube-like structures. Immunocytochemical analysis using a panel of specific markers across various tissues would be required to identify the structures. Further, the cell seeded scaffolds need to be cultured over a longer period of time to allow the structures to grow, differentiate, and mature before final analysis. The formation of more pronounced and robust structures in fractal scaffolds compared to the control slab scaffold is highly significant because it supports the hypothesis that higher surface area to volume ratios enable robust cell growth compared to necrotic cores reported in previous studies. This suggests better nutritional supply to cells that are embedded deep in 3D scaffolds. It is also imperative to determine if various stiffness of the hydrogel can affect or influence cell growth and formation of other structures. If the geometric difference was the main factor in the possible alignment and differentiation of these cells, then this would be an important result that engineers and scientists could use to benefit their research.

8.3 Future Printer Selection

An important future consideration in this project is the purchase of an improved 3D printer to achieve better resolution, print speed, and consistency. In this section, currently available affordable 3D printers (< \$5000) will be compared to our current device – the MakerBot Thing-O-Matic. It is important to note that, during our time with the Thing-O-Matic, we were unable to achieve the claimed resolution and speed, and we were not able to have consistent prints in any material other than ABS. While most of the currently

available printers do not explicitly support PVA printing, and therefore might not demonstrate the same reproducibility and resolution as they do with ABS, they are likely to be better than the Thing-O-Matic due to improved extruder tip designs.

Newer affordable 3D printers have begun to focus on Resin-based 3D printing methods. While these new printers provide significantly better resolution and part reproducibility, the resin cartridges are significantly more expensive than plastic filaments and none of commercially affordably available resins are water-soluble or biocompatible like PVA. Therefore, we will focus on identifying an improved fused deposition 3D printer to use with PVA, as we are doing now. Priority will be given to positional and printing resolution, as well as printing speed to improve the manufacturability of the water-soluble PVA molds. Cost will only be considered to stay under the \$5000 limit and if very similar printers are being compared. Platform size will not be considered important because the PVA molds we are printing are relatively small.

The market has recently been flooded with affordable fused deposition printers. This increased competition has led to significant improvements in resolution, speed, consistency, and overall print quality. Smaller nozzles, more accurate motors, better temperature control, smoother platforms, and tighter tolerances on stepper extruders have all improved print quality and speed. A comparison of many of the currently available 3D printers is contained in Table 33 below.

Table 33: Affordable 3D Printer Specifications and Prices.

Printer Name	X/Y Min. Resolution (mm)	Min. Layer Thickness (mm)	Extrusion Speed (mm/min)	Cost (USD)
MakerBot Thing-O-Matic	0.10	0.30	1000	\$1250
Makerbot Replicator 2	0.10	0.10	5000	\$2199
The Ultimaker	0.05	0.04	5000	\$1900
RepRap Prusa Mendel 3D	0.10	0.30	Based on Config.	\$1225
Stratasys Mojo	0.178	0.178	Not reported	\$9900
3D Touch	0.125	0.125	Not Reported	\$3000

Based on the results from the Table above, the Ultimaker appears to have the best layer thickness, resolution, extrusion speed, and price. Additionally, reviews indicate that the Ultimaker seems to meet and even exceed its reported resolutions and speeds. Thus, it should be used for future PVA molds printed for this project. No printers were found between the \$3000-\$5000 price range, as professional 3D printers such as the Stratasys Mojo begin around \$10,000 with little improvement over the \$2500 affordable, consumer-grade printers.

8.4 Impact

This research is unique in its computational and biologically inspired approach to achieving optimal tissue scaffold geometry, maximizing media availability to cells throughout a scaffold. Our results indicate that 3D structures with higher surface area to volume ratios and fractal dimensions enable greater nutrient perfusion in a tissue scaffold and allow for cell alignment and proliferation. By using an inexpensive 3D printer, we reduced fabrication cost and enabled the repeatable fabrication of complex fractal geometries.

Glossary

- **3D Printing:** The creation of a three-dimensional shape by stacking two-dimensional layers by a variety of different methods.
- **Fused Deposition Printing:** 3D printing by the extrusion of layers of melted plastic that fuse together before cooling down and hardening into a three-dimensional shape. This is the method of 3D printing being used for this project.
- **Biomorphic:** Design that attempts to emulate principles found in nature.
- **Biomimetic:** Design that copies natural shapes and processes.
- **Thermoplastic:** A plastic that becomes deformable above a specific temperature, then becomes solid again once below that temperature.
- **Media / DMEM:** A liquid containing the nutrients necessary for cell growth in culture. DMEM stands for Dulbecco's Modified Eagle's Medium and is one of the many different kinds of media that are commercially available.
- **Hydrogel:** A hydrophilic network of polymers that readily absorbs large amounts of water.
- **Fractal:** A geometric structure in any number of dimensions that is self-similar at different levels of zoom.
- **Self-Similar:** A term describing a structure that is similar to itself. Geometric similarity describes structures that have the same shape.
- **Tissue Scaffold:** A structure designed to promote the growth of three-dimensional tissues.

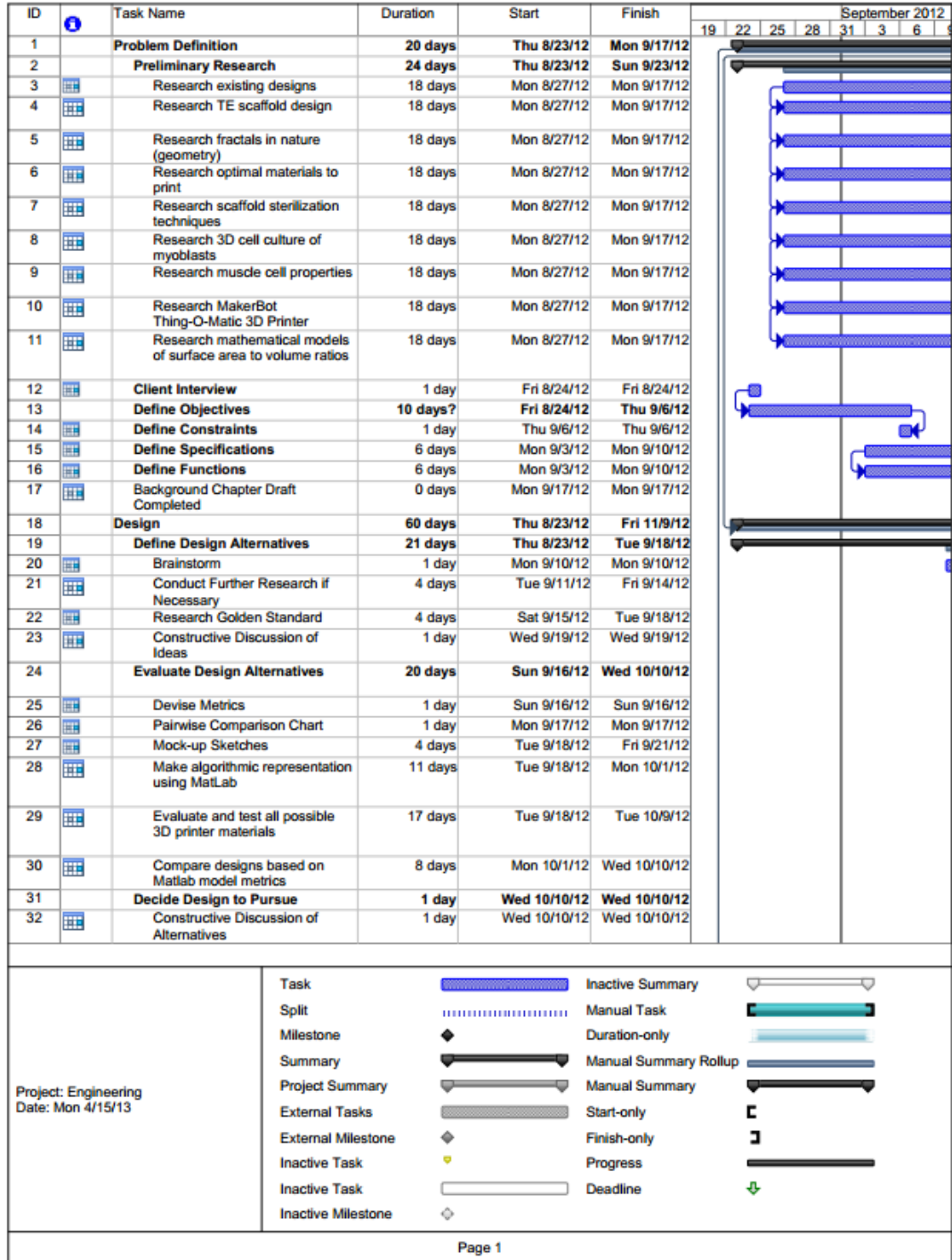
References

- Alberts, B., Johnson, A., & Lewis, J. (2002) *Fibroblasts and Their Transformations: The Connective-Tissue Cell Family*. Molecular Biology of the Cell - 4th edition. New York, NY: Garland Science.
- Centers for Disease Control and Prevention. (2009) *Guideline for Disinfection and Sterilization in Healthcare Facilities*. Healthcare Infection Control Practices Advisory Committee (HICPAC), Web. 09 Apr. 2013. <http://www.cdc.gov/hicpac/Disinfection_Sterilization/8_0Iodophors.html>
- Chandra, M., & Rani, M. (2009). *Chaos, solitons & fractals*. The Interdisciplinary Journal for Nonlinear Science, Nano and Quantum Technology, 41, 1442.
- Conviser, Stephen. (2000). *The Future of Ethylene Oxide Sterilization*. Infection Control Today. Web. 09 Apr. 2013 < <http://www.infectioncontrolday.com/articles/2000/06/the-future-of-ethylene-oxide-sterilization.aspx>>
- Curbell Plastics Inc. *ABS*. Curbell Plastics Inc., 2008. Web. 01 Sept. 2012. <<http://www.curbellplastics.com/technical-resources/pdf/abs-pop-datasheet-curbell.pdf>>.
- Grinnell, F. (2005). *Fibroblast biology in three-dimensional collagen matrices*. Trends in Cell Biology. 13(5), 264-269.
- Holzwarth, J. M., & Ma, P. M. (2011). *3D nanofibrous scaffolds for tissue engineering*. Journal of Materials Chemistry, 21, 10243-10251.
- Huang G., Zhou L., Zhang Q., Chen Y., Sun, W., Xu, F., Tian, J., (2011). *Microfluidic hydrogels for tissue engineering*. Biofabrication, 3(1), 012001.
- Invitrogen. *Cell data sheet - NIH/3T3*. Invitrogen Countess. <www.invitrogen.com/etc/medialib/en/filelibrary/cell_tissue_analysis/pdfs.Par.38126.File.dat/NIH-3T3.pdf>.
- Leclerc, E., Sakai, Y., & Fujii, T. (2003). *Cell culture in 3-dimensional microfluidic structure of PDMS (polydimethylsiloxane)*. Biomedical Microdevices. 5(2). 109-114.
- Lee, J. A., & Kim, M. N., (2001). *Effect of Poly(Vinyl Alcohol) and Polyethylene on the Growth of Red Pepper and Tomato*. Journal of Polymers and the Environment. 9(2), 91-95.
- Lee, W., Lee, V., Polio, S., Keegan, P., Lee, J., Fischer, K., Yoo, S. (2010). *On-demand three-dimensional freeform fabrication of multi-layered hydrogel scaffold with fluidic channels*. Biotechnology and Bioengineering, 105(6), 1178-1186.
- Levin, L. A. (1994). *Paleoecology and ecology of xenophyophores*. Society for Sedimentary Geology, 9(1), 32.
- Li, H., Wijekoon, A., Leipzig, N. D. (2012). *3D Differentiation of Neural Stem Cells in Macroporous Photopolymerizable Hydrogel Scaffolds*. PLoS ONE 7(11).
- Liu, C. Z., Xia, Z. D., Han, Z. W., Hulley, P. A., Triffitt, J. T., & Czernuszka, J. T. (2008). *Novel 3D collagen scaffolds fabricated by indirect printing technique for tissue engineering*. Journal of Biomedical Materials Research Part B: Applied Biomaterials, 85B(2), 519-528.

- MakerBot Industries. *PVA*. MakerBot Industries, (2012). Web. 16 Sept. 2012. <<http://wiki.makerbot.com/pva>>.
- MatBase. *Polylactic Acid (PLA) Material Properties of Agro Based Polymers*. MatBase, 2009. Web. 06 Sept. 2012. <<http://www.matbase.com/material/polymers/agrobased/polylactic-acid-pla/properties>>.
- Miller, J.S., Stevens, K.R., Yang, M.T., Baker, B.M., Nguyen, D.H., Cohen, D.M., Toro, E., Chen, A.A., Galie, P.A., Yu, X., Chaturvedi, R., Bhatia, S.N., Chen, C.S. (2012) *Rapid casting of patterned vascular networks for perfusable engineered three-dimensional tissues*. *Nature Materials*. 11, 768-774.
- Naderi, H., Matin, M., Bahrami, A. (2011). *Review paper: Critical Issues in Tissue Engineering: Biomaterials, Cell Sources, Angiogenesis, and Drug Delivery Systems*. *J Biomater Appl*. 26, 383-417.
- Ng, R., Zang, R., Yang, K. K., Liu, N., & Yang, S. (2012). *Three-dimensional fibrous scaffolds with microstructures and nanotextures for tissue engineering*. *The Royal Society of Chemistry*, 2, 10110-10124.
- Peltola, S. M., Grijpma, D. W., Melchels, F. P. W., & Kellomaki, M. (2008). *A review of rapid prototyping techniques for tissue engineering purposes*. *Annals of Medicine*, 40(4), 268.
- Rajagopalan, S., & Robb, R. A. (2006). *Schwarz meets schwann: Design and fabrication of biomorphic and durataxic tissue engineering scaffolds*. *Medical Image Analysis*, 10, 693.
- Shim, J., Kim, J. Y., Park, M., Park, J., & Cho, D. (2011). *Development of a hybrid scaffold with synthetic biomaterials and hydrogel using solid freeform fabrication technology*. *Biofabrication*, 3(3), 034102. doi: 10.1088/1758-5082/3/3/034102.
- Smith, T. G., Lange, G. D., & Marks, W. B. (1996). *Fractal methods and results in cellular morphology - dimensions, lacunarity, and multifractals*. *Journal of Neuroscience Methods*, 69, 123-136.
- Suri, S., Han, L., Zang, W., Singh, A., Chen, S., & Schmidt, C. E. (2011). *Solid freeform fabrication of designer scaffolds of hyaluronic acid for nerve tissue engineering*. *Biomedical Microdevices*, 13, 983.
- Todaro, G. J., & Green, H. (1963). *Quantitative studies of the growth of mouse embryo cells in culture and their development into established lines*. *Journal of Cell Biology*. 17(2), 299-313.
- Vlierberghe, S. V., Dubruel, P., & Schacht, E. (2011). *Biopolymer-based hydrogels as scaffolds for tissue engineering applications: A review*. *BioMacromolecules*, 12(5), 1387.

Appendix A: Gantt Chart

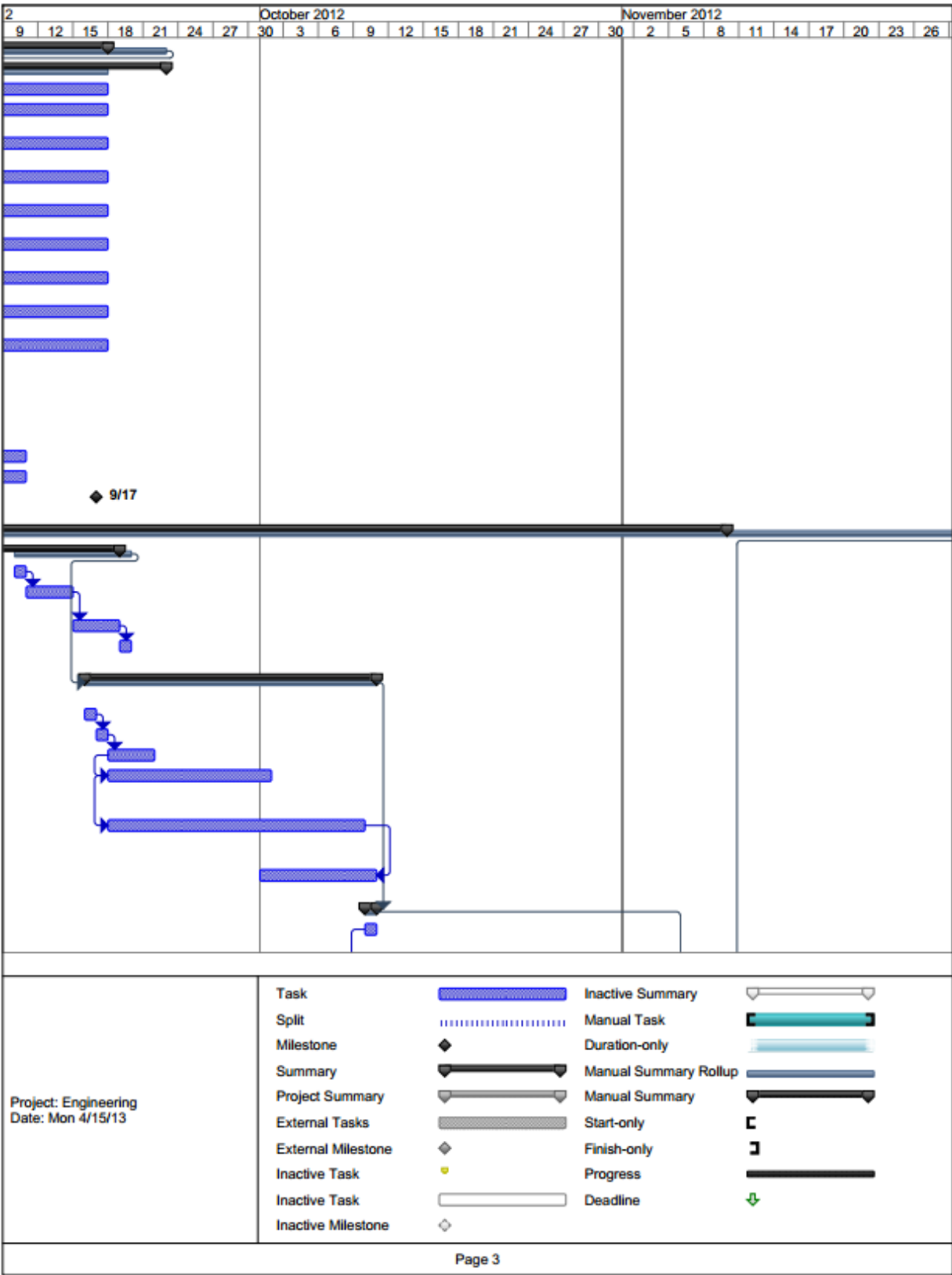
The Gantt chart for this project is included in the following pages, ordered left to right then top to bottom.

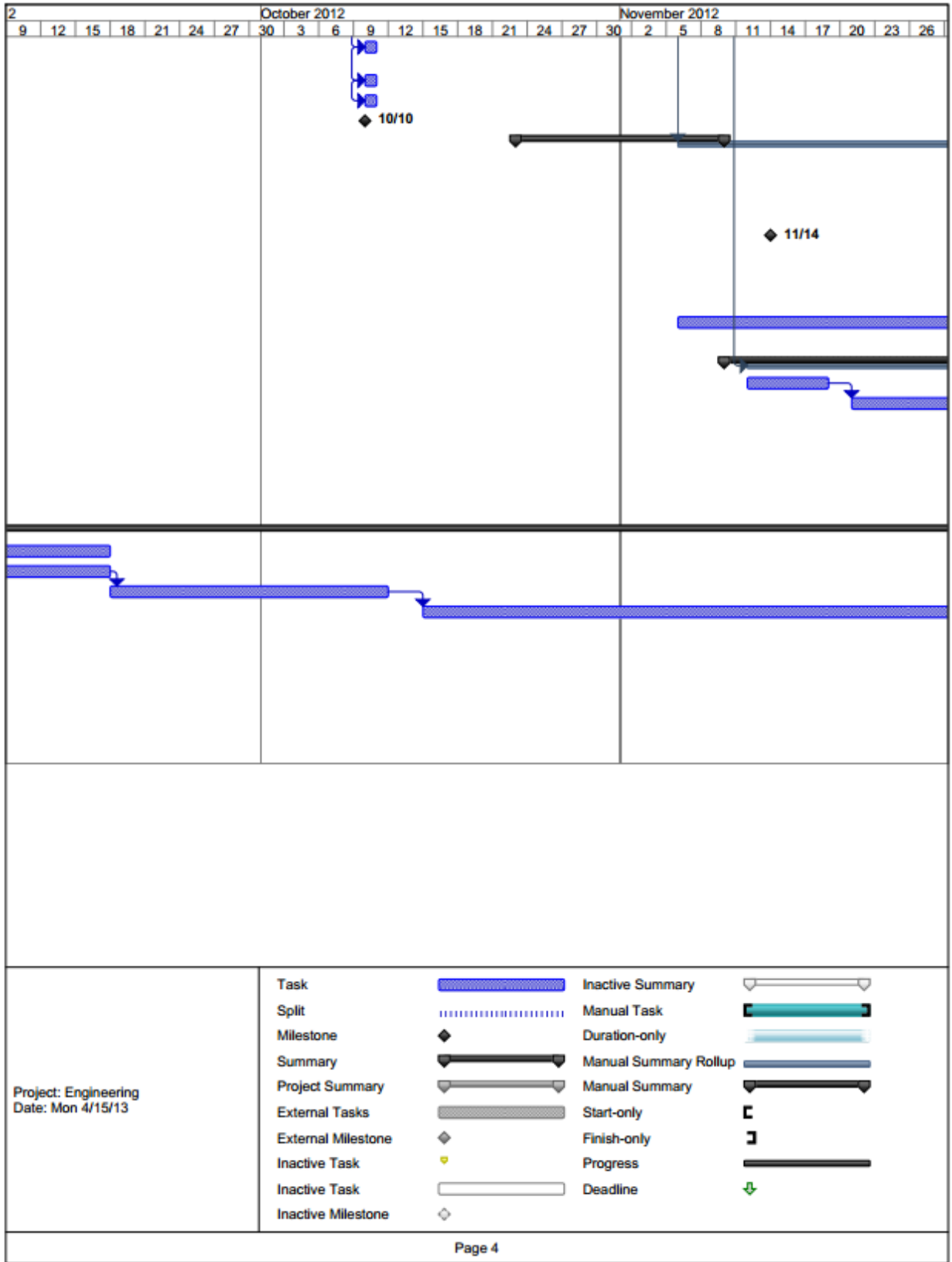


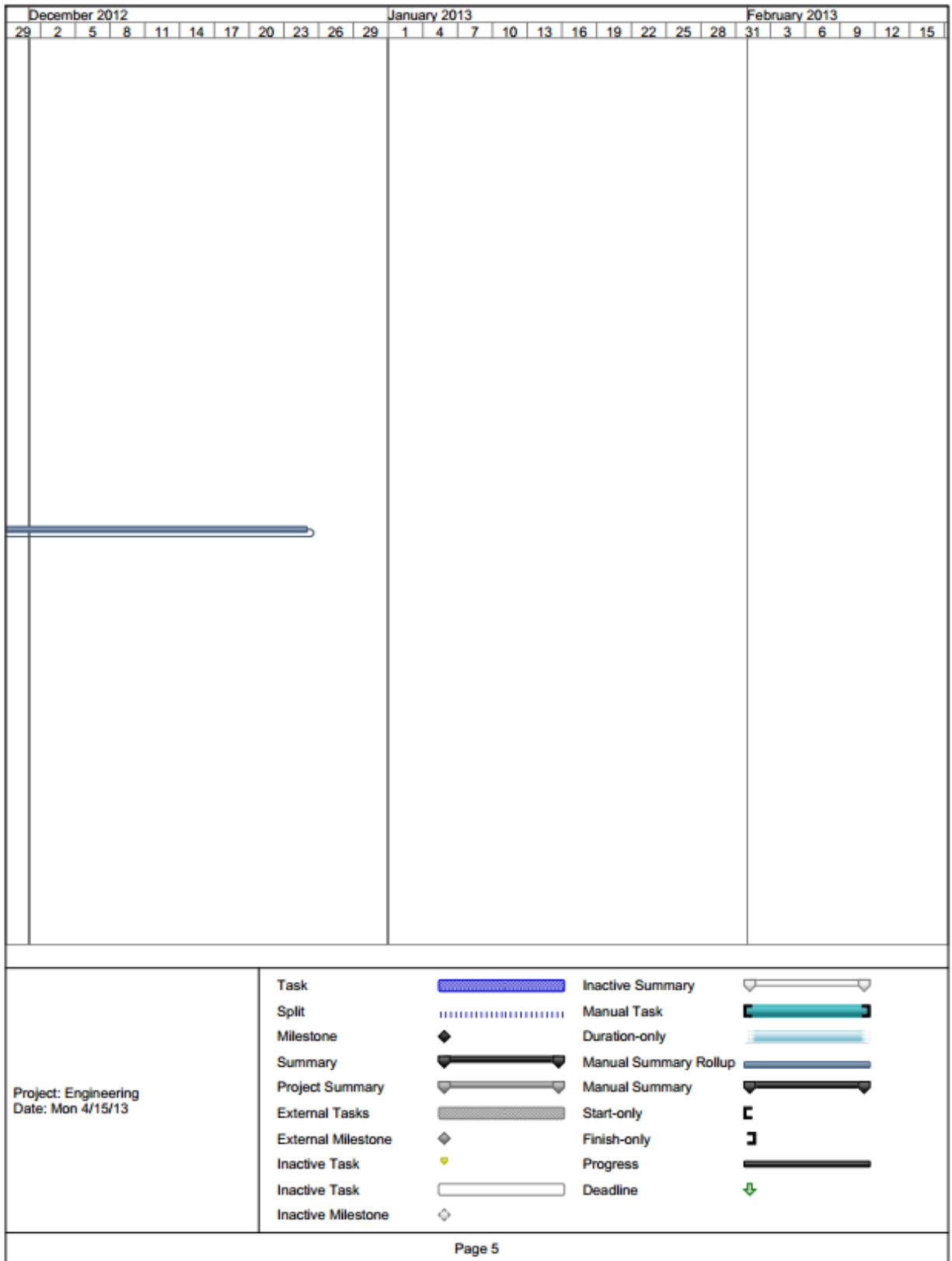
ID	Task Name	Duration	Start	Finish	September 2012							
					19	22	25	28	31	3	6	9
33	Select the one that best meets client needs	1 day	Wed 10/10/12	Wed 10/10/12								
34	Review with client	1 day	Wed 10/10/12	Wed 10/10/12								
35	Purchase Materials	1 day	Wed 10/10/12	Wed 10/10/12								
36	Final Design Chosen	0 days	Wed 10/10/12	Wed 10/10/12								
37	Detailed Design	14 days	Tue 10/23/12	Fri 11/9/12								
38	Solidworks Fractal Models	7 days	Fri 12/7/12	Fri 12/14/12								
39	Integrate CAD models with MakerBot printer	2 days	Sat 12/15/12	Mon 12/17/12								
40	Generate Prototype	5 days	Tue 12/18/12	Mon 12/24/12								
41	Design Specifications Finalized	0 days	Wed 11/14/12	Wed 11/14/12								
42	All Molds Printed in PLA and PVA	0 days	Fri 12/14/12	Fri 12/14/12								
43	Plastic Degradation Studies	2 days?	Fri 12/7/12	Sun 12/9/12								
44	Order and Test Hydrogels	30 days	Tue 11/6/12	Fri 12/14/12								
45	Hydrogel Choice Finalized	0 days	Fri 12/14/12	Fri 12/14/12								
46	Test Prototype	71 days	Sat 11/10/12	Wed 2/13/13								
47	Generate Testing Protocol	5 days	Mon 11/12/12	Sun 11/18/12								
48	Evaluate the prototype	50 days	Wed 11/21/12	Fri 1/25/13								
49	Make changes in design if necessary	10 days	Mon 1/28/13	Fri 2/8/13								
50	Review with Client	1 day	Mon 2/11/13	Mon 2/11/13								
51	Build Final Proof of Concept	3 days	Tue 2/12/13	Thu 2/14/13								
52	Proof of Concept Delivered	0 days	Thu 2/14/13	Thu 2/14/13								
53	Documentation	184 days	Thu 8/23/12	Tue 4/30/13								
54	Complete Chapter 2	20 days	Thu 8/23/12	Mon 9/17/12								
55	Complete Chapter 3	20 days	Thu 8/23/12	Mon 9/17/12								
56	Complete Chapter 4	19 days	Tue 9/18/12	Thu 10/11/12								
57	Complete Chapter 5	123 days	Mon 10/15/12	Mon 4/1/13								
58	Complete Chapter 6	11 days	Tue 4/2/13	Tue 4/16/13								
59	Complete Chapter 7	8 days	Mon 4/15/13	Wed 4/24/13								
60	Final Presentation Completed	0 days	Thu 4/18/13	Thu 4/18/13								
61	Complete Chapter 8	8 days	Mon 4/15/13	Wed 4/24/13								
62	Complete Chapter 1 (Introduction)	8 days	Mon 4/15/13	Wed 4/24/13								
63	Finalize Appendices	4 days	Thu 4/25/13	Tue 4/30/13								
64	Final MQP Report Delivered	0 days	Tue 4/30/13	Tue 4/30/13								

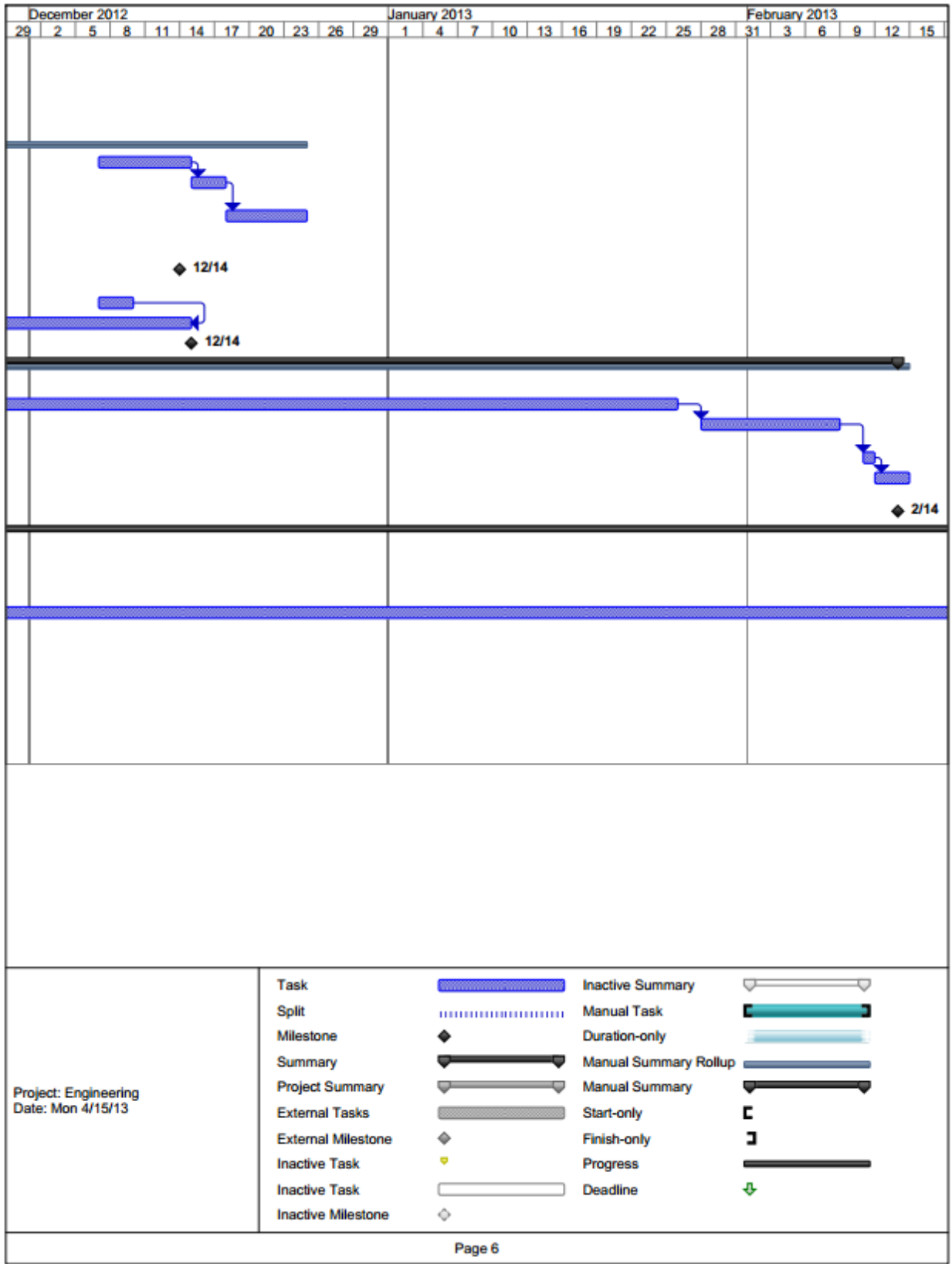


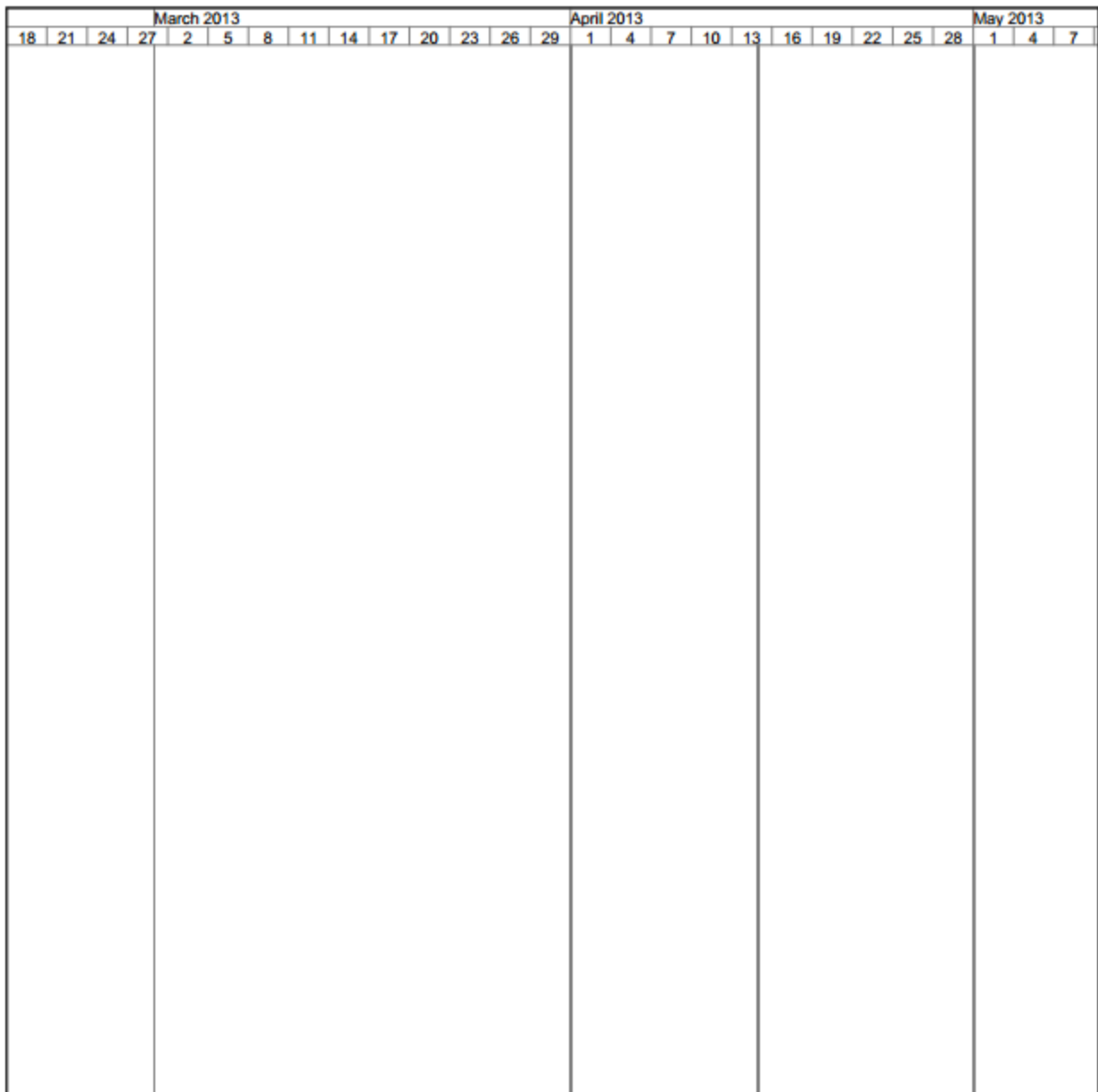
Project: Engineering Date: Mon 4/15/13	Task		Inactive Summary	
	Split		Manual Task	
	Milestone		Duration-only	
	Summary		Manual Summary Rollup	
	Project Summary		Manual Summary	
	External Tasks		Start-only	
	External Milestone		Finish-only	
	Inactive Task		Progress	
	Inactive Task		Deadline	
	Inactive Milestone			



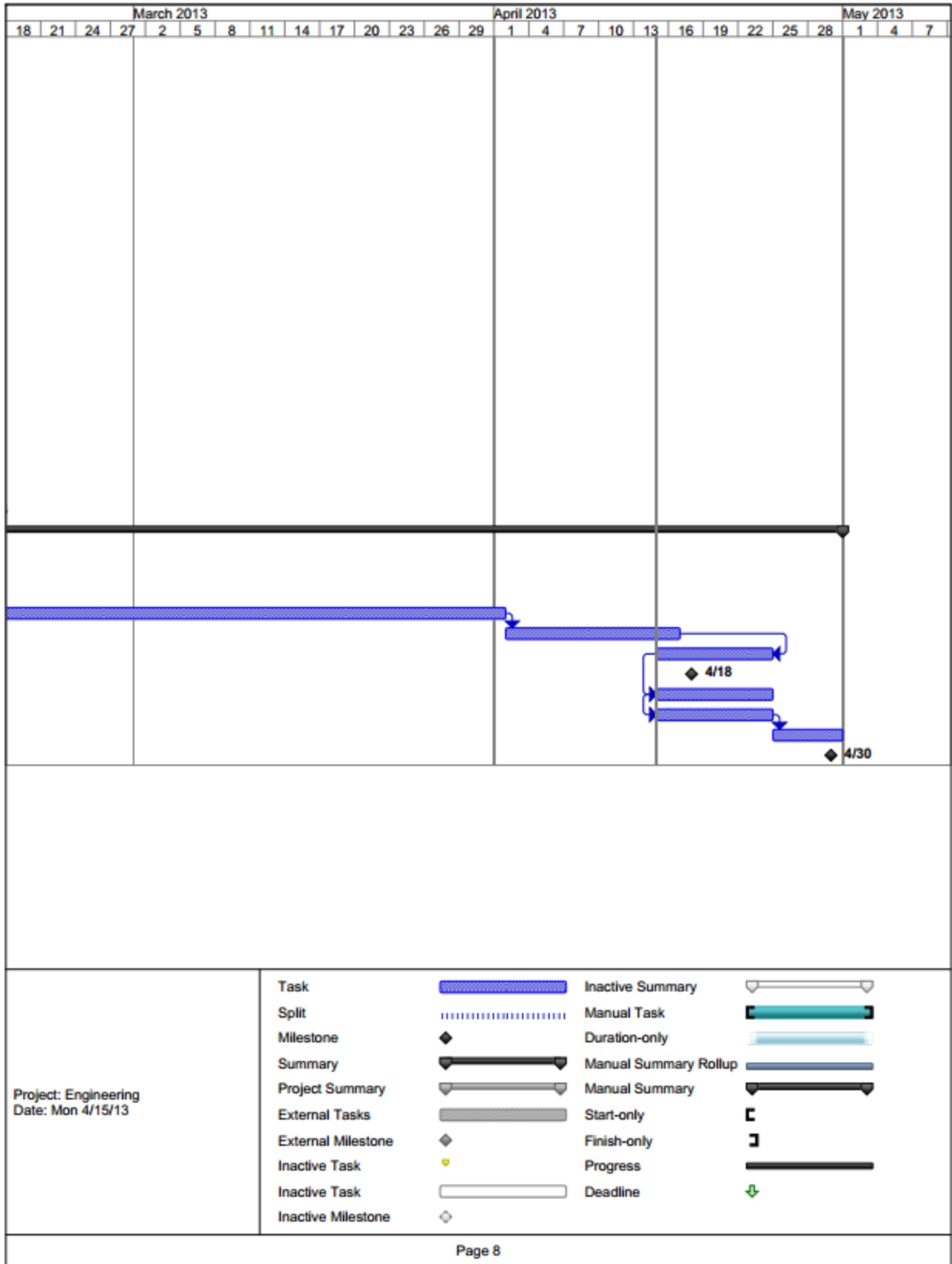








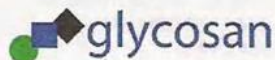
Project: Engineering Date: Mon 4/15/13	Task		Inactive Summary	
	Split		Manual Task	
	Milestone		Duration-only	
	Summary		Manual Summary Rollup	
	Project Summary		Manual Summary	
	External Tasks		Start-only	
	External Milestone		Finish-only	
	Inactive Task		Progress	
	Inactive Task		Deadline	
	Inactive Milestone			



Appendix B: Glycosan Biosystems Inc. Extracel Protocol

Extracel™ Hydrogel Kit (7.5 mL) Product Datasheet

FOR RESEARCH USE ONLY



PRODUCT DESCRIPTION

The Extracel Hydrogel Kit is composed of Glycosil™ (thiol-modified sodium hyaluronate), Gelin-S™ (thiol-modified gelatin), Extralink™ (PEGDA, polyethylene glycol diacrylate), and degassed deionized water (DG Water). Solutions of Glycosil and Gelin-S form a transparent hydrogel when mixed with Extralink. All lyophilized solids are blanket-ed by argon and under a slight vacuum.

STORAGE

Glycosil and Gelin-S

- ◆ Store Glycosil and Gelin-S in original vials at -20 °C for up to one year.
- ◆ Do not uncap the Glycosil and Gelin-S vials since both materials will cross-link in the presence of oxygen. Use a syringe to add DG Water and remove product from the vials.

Extralink

- ◆ Store Extralink in the original vial at -20 °C for up to one year.
- ◆ Reconstituted solutions can be stored at -20°C for ~ one month.

INSTRUCTIONS FOR USE

Glycosil, Gelin-S and Extralink solutions are prepared by dissolving the lyophilized solids in the DG Water. When reconstituted, the three materials will be in 1x phosphate buffered saline (PBS), pH ~7.4. Glycosil and Gelin-S vials contain 10 mg of material and when reconstituted according to instruction will produce a 1% (w/v) solution. Extralink vials contain 10 mg of material and when reconstituted according to instructions will produce a 2% (w/v) solution.

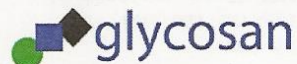
Note: Glycosan recommends reconstituting each vial in its entirety.

Glycosan BioSystems Inc.
1301 Harbor Bay Parkway
Alameda, CA 94502
1-877-636-4978
www.glycosan.com

Page 1 of 2
Form 003-051: Rev E
Modified Last: Sept. 20, 2011

Extracel™ Hydrogel Kit (7.5 mL) Product Datasheet

FOR RESEARCH USE ONLY



Extracel hydrogels (3 x 2.5 mL = 7.5 mL) should be prepared in the following manner:

1. Allow the Glycosil, Gelin-S, Extralink, and DG Water vials to come to room temperature.
2. Under aseptic conditions and using a syringe add 1.0 mL of DG Water to the Glycosil vial. Repeat for the Gelin-S vial.
3. Place both vials horizontally on a rocker or shaker. It will take ~30 minutes for the solids to fully dissolve. Warming to not more than 37 °C and/or gentle vortexing will speed dissolution. Solutions will be clear and slightly viscous.
4. Under aseptic conditions and using a syringe add 0.5 mL of DG Water to the Extralink vial. Invert several times to dissolve.
5. As soon as possible, but within 2 hours of making the solutions, mix equal volumes of Glycosil and Gelin-S. To mix, pipette back and forth to mix.
6. If encapsulating cells, resuspend cell pellet in 2.0 mL of Glycosil + Gelin-S. Pipette back and forth to mix.
7. To form the hydrogel, add Extralink to the Glycosil + Gelin-S mix in a 1:4 volume ratio (0.5 mL Extralink to 2.0 mL Glycosil + Gelin-S) mix by pipette.
8. If encapsulating cells, allow solution to react for 10 minutes then mix again by pipette to ensure even distribution of cells.
9. Gelation will occur within ~20 minutes.

Note: Each kit component has been manufactured under aseptic conditions and tested for bacteria and fungus.

For more information about the Extracel Hydrogel Kit visit:

www.glycosan.com

Glycosan BioSystems Inc.
1301 Harbor Bay Parkway
Alameda, CA 94502
1-877-636-4978
www.glycosan.com

Page 2 of 2
Form 003-051: Rev E
Modified Last: Sept. 20, 2011

Appendix C: Matlab Code

Below is the MatLab code that can be used to generate an Iterated Function System fractal from a defined base shape.

```
% define the seed shape of the fractal
vertices = [...]
faces = [...]




% choose the level of recursion
recursionLevel = 3

figure
genFract(vertices,faces,recursionLevel)
axis equal off

% fractal generation algorithm
function genFract(vertices,faces,level)
if n > 0
newVert = vertices;
for k = 1:length(vertices)
newVert(:,1) = vertices(:,1)+vertices(k,1);
newVert(:,2) = vertices(:,2)+vertices(k,2);
newVert(:,3) = vertices(:,3)+vertices(k,3);
if n == 1
patch('vertices',newVert,'faces',
      faces,'facecolor','r');
end
genFract(newVert, faces, n-1);
end
end
return
```

Appendix D: Fractal Mold Images

Below are representative images of each printed PVA fractal mold.

Image	Fractal Mold Name
 A square, light-colored PVA mold with a complex, self-similar fractal pattern. The pattern consists of a central square with smaller squares attached to its sides, creating a dense, interconnected structure.	<p style="text-align: center;">Cluster Fractal (Menger Sponge)</p>
 A square, light-colored PVA mold with a fractal pattern resembling a tree. The pattern starts with a central vertical stem that branches out into smaller, similar structures, creating a complex, branching structure.	<p style="text-align: center;">Tree Fractal (Bifurcating Fractal Tree)</p>
 A square, light-colored PVA mold with a fractal pattern resembling a Sierpinski triangle. The pattern consists of a large triangle with smaller triangles attached to its sides, creating a complex, self-similar structure.	<p style="text-align: center;">Sierpinski Triangle Fractal</p>



Fern Fractal

Appendix E: BrdU Protocol

BrdU Protocol

1. Add 1.0 μ L of BrdU stock solution per mL of culture medium to cells being assayed and incubate overnight.
2. Aspirate culture medium and wash cells 2X in DPBS+.
3. Aspirate DPBS+ and add ice cold (-20°C) methanol (1.0 mL/well for a 24-well plate). Incubate for 10 minutes at -20°C .
4. Aspirate methanol and wash with 1.0 mL PBS for 10 minutes.
5. Aspirate PBS and add 750 μ L 1.5 N HCl and incubate at RT for 20 minutes.
6. Wash 3X with PBS, 5 minutes each.
7. If cells were cultured with serum, blocking is not necessary. If cultured in serum-free system, block at RT for at least 15 minutes with 5% FBS in PBS +0.05% Tween-20.
8. Dilute anti-BrdU antibody 1:100 in PBS +0.05% Tween 20.
9. Add 200 μ L antibody solution and incubate at RT for 30 minutes.
10. Aspirate antibody solution and wash 3X with PBS for 5 minutes each.
11. Add 200 μ L fluorescent dye conjugated secondary antibody diluted 1:500 in PBS +0.05% Tween-20 and incubate at RT for 30 minutes.
12. Wash 3X with PBS (without Tween) for 5 minutes each.
13. Add 0.5 $\mu\text{g}/\text{mL}$ Hoechst 33342 to last wash, and incubate at RT for 10 minutes.
14. Aspirate Hoechst solution, wash with PBS and add 1.0 mL of PBS.
15. Observe cells under fluorescence microscopy.

Appendix F: Leica CM3050 Cryostat Microtome SOP

Worcester Polytechnic Institute
60 Prescott Street
Worcester, MA 01605

SOP 3.0 Leica CM3050 Cryostat
11/1/2012
Page 1 of 6

Instrument Operating Procedure

- I. **PURPOSE:** To describe procedures to be followed for the inspection, use, calibration/standardization, testing, maintenance and cleaning of:
 - A. **Instrument:** Leica CM3050 Cryostat Microtome
 - B. **Manufacturer:** Leica Microsystems Nussloch GmbH, Heidelberger Str. 17- 19, D-69226 Nussloch, Germany
 - C. **Model:** CM 3050
 - D. **Serial (fabrication) No:** 2170/02.1999
 - E. **Location:** Gateway Park Room 3237

Note: This SOP is written specifically for use when conducting non-clinical research studies in support of faculty and student projects.

II. **DEFINITIONS:**

- A. The cryostat is a rotary microtome contained in a mechanically refrigerated chamber. Tissue samples are frozen in poly vinyl alcohol eg, OCT Compound, to make it firm enough for sectioning. The Leica CM 3050 operates at temperatures of $-40 - 0^{\circ}\text{C}$ and is able to cut sections 0.5- 60 μm in thickness. Disposable microtome blades are used for sectioning. Microtome blades have an extremely sharp edge and care must be used when handling them. This cryostat is NOT for use with bio-hazardous or infectious materials.
- B. The automated rotary feature of the cryostat prevents injuries associated with repetitive motion. Once the user is comfortable with the use of the cryostat, the automated motor function will be very useful. However, the automated feature can introduce risk to the user if users do not adhere to the operation protocols.

III. **REQUIREMENTS:**

All users of the Leica CM3050 are required to undergo proper training in frozen sectioning. All users must read the operators' manual and familiarize themselves to the parts of the cryostat and their functions. Everyone is required to log in usage time for cost recovery. Equipment and work areas must be cleaned thoroughly after use. Equipment failure must be reported immediately to Hans Snyder. Users are required to bring their own OCT, plus slides, forceps, brushes, gloves and Kimwipes.

*Before using the Leica CM3050, users should familiarize themselves with the location of the first aid kit, telephone and emergency exit.

Written By Hans B Snyder

III. **INSPECTION:**

A. Before use, check to make sure that:

1. 15 minutes before your session, adjust chamber temperature to -20°C (the optimum cutting temperature for most tissues). Trim specimen to desired size. Apply a small amount of OCT to the specimen disc. Place specimen into OCT and then apply more OCT to surround tissue. Do this quickly as the matrix will start to solidify immediately.

IV. **USE:**

Note: Only qualified personnel that have been trained in the use of the Leica CM3050 Cryostat by Hans B Snyder, Vicki Huntress or other designee may use the microtome.

1. **Lock hand wheel** in the upper position. Loosen clamping screw. Insert specimen disc in opening, tighten clamping screw. Insert disposable microtome blade into the blade holder. Unlock hand wheel. Use motorized coarse feed to bring specimen close to knife. Select desired trimming thickness. Move anti-roll plate away from knife and then rotate hand wheel to trim specimen down to desired sectioning plane. Press trim/section button to start sectioning, select desired sectioning thickness, lower anti-roll plate and start sectioning. Rotate the hand wheel evenly and at uniform speed. Discard the first 2-3 sections to ensure that desired thickness is achieved. To remove the specimen disc, **lock hand wheel** in the upper position, loosen clamping screw and remove specimen disc. Use extreme care near disposable microtome blade.
2. For motorized function, center hand wheel grip. Depress foot pedal gently to start the course feed for trimming specimens and to start fine feed in sectioning mode. Emergency stop function is activated by depressing the foot pedal forcefully or pressing the emergency stop button. To deactivate the emergency stop function, release the foot pedal. In the case of the emergency stop button, rotate the button in the direction of the arrow until it unlocks and slips upward to its original position. To continue work, select one of the sectioning modes (1-2- 3) to resume sectioning.

*Always remember lock hand wheel in the upper position when inserting or removing specimen disc into microtome or changing disposable blades.

V. **CONTINGENCY PLAN AND REPORTING:**

Minor cuts, which do not require medical aid should be treated at once. In case of a more serious injury (a deeper cut or greater extent of bleeding), Emergency extension **5555** should be called to get the injured person to immediate medical care. All injuries must be reported to Worcester Polytechnic Institute using the accident reporting form. The Injury/Incident Report must be forwarded to the histology technician within 24 hours. The SOP for cleanup of human blood should be followed.

VI. **WASTE MANAGEMENT:**

No biological materials are to be left in the cryostat. All leftover tissue should be disposed of properly.

All spent blades are to be disposed of properly and should not be left in the cryostat. Please dispose of sharps in an appropriate sharps container.

VII. **MAINTENANCE AND CLEANING:**

A. Routine:

1. Before cleaning
 - a. Lock the rotary hand wheel.
 - b. Remove the microtome blade from the knife holder.
 - c. Remove knife holder base and knife holder for cleaning
2. Disinfection and cleaning
 - Prior to disinfection, switch the instrument off and unplug it from mains.
 - For disinfection, wear protective gear (gloves, mask, lab coat etc.)!
 - a. Removing/reinstalling the microtome
 1. Before removing the microtome
 - Switch instrument off.
 - Unplug from mains.
 - Place hand wheel grip in lowest position and lock.
 2. Removing the microtome

Written By Hans B Snyder

- When removing the microtome, the specimen head must always be locked in the lowest position. Otherwise the upper part of the slot cover might be bent and consequently damaged!
 - Wear gloves when removing the microtome while it is still frozen.
*** Risk of frost bite!**
 - On instruments with specimen cooling do not distort the refrigerating tube! If distorted it might break, causing extremely cold refrigerant to escape.
*** Risk of frost bite!**
3. Disinfection
- For disinfection, only use alcohol-based disinfectants!
 - Do not use solvents (xylene, acetone etc.) for cleaning or disinfection!
 - Do not spray disinfectants into the evaporator!
*** Risk of icing!**
 - Explosion hazard when working with alcohol Make sure the premises are appropriately ventilated!
 - When using disinfectants and detergents, comply with all safety instructions supplied by the manufacturer of the product!
 - Dispose of waste liquids from disinfection/ cleaning as well as of sectioning waste according to applicable regulations on disposal of special category waste!
 - Disinfected accessories must be thoroughly dry when reinserting them into the chamber!
*** Risk of icing!**
4. Before re-installing the microtome
- Make sure the chamber is completely dry before switching the instrument back on.
 - Humidity in the interior of the microtome freezes and causes the microtome malfunctions and/or damage to the microtome.
*** Explosion hazard through alcohol vapors!**

Written By Hans B Snyder

*** Risk of icing!**

- All accessories/tools removed from the cryo-chamber must be thoroughly dry before putting them back into the chamber!

*** Risk of icing!**

VIII. MALFUNCTIONS and REPAIR:

- A. In case of a malfunction, notify the histology technician. In case of emergency call Hans at 508-308-7800. Describe the problem and any corrective action taken on the Instrument/Equipment log.

IX. PERSONS RESPONSIBLE FOR EACH OPERATION:

- A. Persons responsible for operating the cryostat will be properly trained in its use.
- B. Training and experience will be reflected in the user's Curriculum Vitae.

X. REFERENCES:

- Leica CM3050 Instruction Manual
- Manual of Histologic Staining Methods of the Armed Forces Institute of Pathology, 3rd ed.

APPROVED BY: _____ DATE _____
Management

APPROVED BY: _____ DATE _____
Professor

Written By Hans B Snyder

Instrument/Equipment Inspection, Testing, and Maintenance Log

Instrument/Equipment: Leica CM3050 Cryostat


Model #: CM3050

Serial #: 2170/02.1999

Initials	Date	Inspection	Calibration	Testing	Maintenance	Follow SOP?	Comments / Number of Blocks

Written By Hans B Snyder

Appendix G: H&E Protocol

 WPI	Gateway Park Core labs Protocol Procedure	GPV-000.1
	<i>H&E Frozen</i>	Approved By: _____ Approval Date: _____

1. Hydrate slides in running water----- 5 minutes
2. Stain slides in Harris Hematoxylin -----10 minutes
3. Rinse slides in running water -----2 minutes
4. Differentiate in acid alcohol -----1 quick dip
5. Rinse in water -----3 dips
6. Dip in ammonia water -----15-30 seconds
7. Wash in running tap water -----10 minutes
8. Place in 95% alcohol----- 2 minutes
9. Stain in eosin -----1 minute
10. Dehydrate in 95% alcohol -----1 minute
11. Dehydrate in 95% alcohol -----1 minute
12. Dehydrate in 100% alcohol -----1 minute
13. Dehydrate in 100% alcohol----- 2 minutes
14. Dehydrate in 100% alcohol----- 2 minutes
15. Clear in xylene I----- 2 minutes
16. Clear in xylene II-----5 minutes

Results:

Nuclei – Blue

Cytoplasm – Pink

Blood -- Red

Note: Slides can stay in the last xylene for days without effect.

No Control.

Revision History

Revision	Approval Date	Changes	Purpose

Appendix H: Sigma Aldrich HyStem-C Protocol

SIGMA-ALDRICH®

sigma-aldrich.com
 3050 Spruce Street, St. Louis, MO 63103 USA
 Tel: (800) 521-8956 (314) 771-5765 Fax: (800) 325-5052 (314) 771-5757
 email: techservice@sigma-aldrich.com

Product Information

HyStem®-C Cell Culture Scaffold Kit
for 7.5 ml of hydrogel scaffold

Catalog Number **HYSC020**
Storage Temperature **-20 °C**

TECHNICAL BULLETIN

Product Description

The HyStem®-C Cell Culture Scaffold Kit provides an excellent starting point for optimizing the matrix for stem cell culture. It is recommended for cultures, which require a minimal number of cell attachment sites or the addition of other extracellular matrix (ECM) proteins. Unlike animal-derived ECM products, this kit contains three fully chemically defined components, which are nonimmunogenic:

HyStem – a thiol-modified hyaluronan (a major constituent of native ECM), carboxymethyl hyaluronic acid-thiopropionyl hydrazide (CMHA-S, CMHA-DTPH, carboxymethyl hyaluronic acid-DTPH)

Gelin-S® – a thiol-modified gelatin (denatured collagen), carboxymethyl gelatin-thiopropionyl hydrazide (GTN-DTPH, carboxymethyl gelatin-DTPH)

Extralink® – a thiol-reactive crosslinker, polyethylene glycol diacrylate ($M_w = 3,400$ g/mole, PEGDA)

Hydrogels prepared from these kit components can be customized to fit the growth requirements of the stem cell culture of interest.

The Gelin-S provides basic cell attachment sites for cell lines and primary cells.^{1,2} Several cell types require specific components of the natural ECM, laminin, collagen, fibronectin, and vitronectin, to grow and differentiate. Any of these can easily be incorporated noncovalently into the hydrogel prior to gel formation.

The stem cell culture can be plated on top of the hydrogel for pseudo three dimensional (3D) growth.¹ The hydrogel matrix also provides a basic scaffold for 3D stem cell growth. The stem cells can be encapsulated during crosslinking,³ where they attach and grow within the hydrogel. The hydrogel rigidity may be varied to match the stiffness of native tissues.

Components

HyStem	3 × 1 ml
Each bottle contains 10 mg of HyStem and 9.6 mg of phosphate buffered saline (PBS) salts (Catalog Number H2416)	
Gelin-S	3 × 1 ml
Each bottle contains 10 mg of Gelin-S and 9.6 mg of PBS salts (Catalog Number G3673)	
Extralink 2	3 × 0.5 ml
Each bottle contains 10 mg of Extralink and 4.8 mg of PBS salts (Catalog Number E6659)	
Water, degassed	1 × 10 ml
Ready-to-use bottle contains 10 ml of deionized water with 9.6 mg of PBS salts (Catalog Number W3894)	

Precautions and Disclaimer

This product is for R&D use only, not for drug, household, or other uses. Please consult the Material Safety Data Sheet for information regarding hazards and safe handling practices.

Preparation Instructions

Note: Do not uncup the HyStem and Gelin-S bottles since both materials will crosslink in the presence of oxygen. Use a syringe and needle to add degassed water. Prepare 1× Stock Solutions:

HyStem – reconstitute a bottle with 1 ml of degassed water (Catalog Number W3894)
 Gelin-S – reconstitute a bottle with 1 ml of degassed water (Catalog Number W3894)
 Extralink 2 – reconstitute a bottle with 0.5 ml of degassed water (Catalog Number W3894)

The 1× Stock Solutions will contain 1× phosphate buffered saline (PBS), pH ~7.4.

Storage/Stability

The lyophilized powders are blanketed with argon and under a slight vacuum. They may be stored unopened in the original bottles at -20 °C for up to one year. Do not uncap the HyStem and Gelin-S bottles since both materials will crosslink in the presence of oxygen.

The 1× Extralink 2 Stock Solution may be stored at -20 °C for ~1 month.

Procedure

The 1× Stock Solutions remain liquid at 15–37 °C. The hydrogel is formed when the crosslinking agent, Extralink, is added to a mixture of HyStem (thiol-modified hyaluronan) and Gelin-S (thiol-modified gelatin). Gelation occurs in ~20 minutes after all three solutions are mixed. No steps depend on low temperature or low pH.

The rigidity of the hydrogel can be varied either by changing the volume of 1× Extralink 2 Stock Solution used for crosslinking⁴ or by diluting the 1× HyStem and Gelin-S Stock Solutions using PBS or cell culture medium. Diluting these Stock Solutions with PBS or cell culture medium can increase the gelation time.

The following is a procedure to prepare a 2.5 ml batch of hydrogel scaffold. Sufficient reagents are provided to prepare 3 batches (7.5 ml).

1. Allow the HyStem, Gelin-S, Extralink 2, and degassed water bottles to come to room temperature.
2. Under aseptic conditions, using a syringe and needle, add 1.0 ml of degassed water (Catalog Number W3894) to the HyStem bottle. Repeat for the Gelin-S bottle (see Preparation Instructions).
3. Place both bottles horizontally on a rocker or shaker. It will take <30 minutes for the solids to fully dissolve. Warming to ≤37 °C and/or gently vortexing will speed dissolution. 1× Stock Solutions will be clear and slightly viscous.

4. Under aseptic conditions, using a syringe and needle, add 0.5 ml of degassed water (Catalog Number W3894) to the Extralink 2 bottle. Invert several times to dissolve.
5. As soon as possible, but within 2 hours of making the solutions, aseptically mix the HyStem and Gelin-S 1× Stock Solutions together. To mix, pipette back and forth slowly to avoid trapping air bubbles.
6. If adding other ECM proteins, add sterile ECM protein solution to the 1:1 mixture of HyStem and Gelin-S 1× Stock Solutions. Pipette back and forth to mix.
7. If encapsulating cells, resuspend the cell pellet in the 1:1 mixture of HyStem and Gelin-S 1× Stock Solutions. Pipette back and forth to mix.
8. To form the hydrogel, combine the following and mix by pipette:
 - 0.5 ml of 1× Extralink 2 Stock Solution
 - 2.0 ml of HyStem/Gelin-S 1:1 mixture
9. Gelation will occur within ~20 minutes.

References

1. Shu, X.Z. et al., Synthesis and Evaluation of Injectable, *In Situ* Crosslinkable Synthetic Extracellular Matrices (sECMs) for Tissue Engineering. *J. Biomed Mater. Res. A*, **79A**(4), 901-912 (2006).
2. Shu, X.Z. et al., Disulfide-crosslinked Hyaluronan-Gelatin Hydrogel Films: A Covalent Mimic of the Extracellular Matrix for *In Vitro* Cell Growth. *Biomaterials*, **24**, 3825-3834 (2003).
3. Prestwich, G.D. et al., 3-D Culture in Synthetic Extracellular Matrices: New Tissue Models for Drug Toxicology and Cancer Drug Discovery. *Adv. Enz. Reg.*, **47**, 196-207 (2007).
4. Vanderhooft, J. et al., Rheological Properties of CrossLinked Hyaluronan-Gelatin Hydrogels for Tissue Engineering. *Macromol. Biosci.*, **9**, 20-28 (2009).
5. Shu, X.Z. et al., *In Situ* Crosslinkable Hyaluronan Hydrogels for Tissue Engineering. *Biomaterials*, **25**, 1339-1348 (2004).

HyStem, Gelin-S, and Extralink are registered trademarks of Glycosan BioSystems, Inc.

JW.MAM 11/11-1

©2011 Sigma-Aldrich Co. LLC. All rights reserved. SIGMA-ALDRICH is a trademark of Sigma-Aldrich Co. LLC, registered in the US and other countries. Sigma brand products are sold through Sigma-Aldrich, Inc. Purchaser must determine the suitability of the product(s) for their particular use. Additional terms and conditions may apply. Please see product information on the Sigma-Aldrich website at www.sigmaaldrich.com and/or on the reverse side of the invoice or packing slip.

Appendix I: Sigma Aldrich HyStem-HP Protocol



3050 Spruce Street
 Saint Louis, Missouri 63103 USA
 Telephone 800-325-5832 • (314) 771-5765
 Fax (314) 286-7828
 email: techserv@sigma.com
 sigma-aldrich.com

Product Information

HyStem™-HP Cell Culture Scaffold Kit for 7.5 ml of hydrogel scaffold

Catalog Number HYSHP020
 Storage Temperature -20 °C

TECHNICAL BULLETIN

Product Description

The HyStem™-HP Cell Culture Scaffold Kit provides an excellent starting point for optimizing the matrix for stem cell culture, where slowly released growth factors are crucial in re-creating a stem cell niche. To affect specific cell performance, growth factors or ECM proteins may be added to the HyStem-HP hydrogel. Unlike animal-derived ECM products, this kit contains three fully chemically defined components, which are nonimmunogenic:

HyStem-HP – a thiol-modified hyaluronan (a major constituent of native ECM), carboxymethyl hyaluronic acid-thiopropionyl hydrazide (CMHA-S, CMHA-DTPH, carboxymethyl hyaluronic acid-DTPH) with heparin-thiopropionyl hydrazide (HP-DTPH). HyStem-HP (CMHA-DTPH with HP-DTPH) contains 99.7 wt% CMHA-DTPH and 0.3 wt% HP-DTPH.

Gelin-S™ – a thiol-modified gelatin (denatured collagen), carboxymethyl gelatin-thiopropionyl hydrazide (GTN-DTPH, carboxymethyl gelatin-DTPH)

Extralink™ – a thiol-reactive crosslinker, polyethylene glycol diacrylate ($M_w = 3,400$ g/mole, PEGDA)

HyStem-HP hydrogels contain thiol-modified heparin, which allows the slow release of growth factors (GF) within an easily customizable environment. Several stem cell types depend on specific ECM components to grow and differentiate. ECM proteins and growth factors are easily incorporated noncovalently into the hydrogel prior to gel formation.

The Gelin-S provides basic cell attachment sites for cell lines and primary cells.¹ Several cell types require specific components of the natural ECM, laminin, collagen, fibronectin, and vitronectin, to grow and differentiate.

The immobilized heparin in the hydrogel mimics the heparan sulfate proteoglycans normally present in the extracellular matrix (ECM). The thiolated heparin ionically binds a wide variety of growth factors and slowly releases them over time. It also helps protect GF from proteolysis.² This reduces the amount of GF required to achieve stimulation of cell growth or differentiation when compared to the use of free GF in media. All GF tested (bFGF, VEGF, Ang-1, PDGF, TGFβ1, and KGF) are released at different rates, but over a period of several weeks.^{2,3}

The stem cell culture can be plated on top of the hydrogel for pseudo three dimensional (3D) growth.¹ The hydrogel matrix also provides a basic scaffold for 3D stem cell growth. The stem cells can be encapsulated during crosslinking,⁴ where they attach and grow within the hydrogel. The hydrogel rigidity may be varied to match the stiffness of native tissues.

Components

HyStem-HP	3 × 1 ml
Each bottle contains 10 mg of HyStem-HP and 9.6 mg of phosphate buffered saline (PBS) salts (Catalog Number H2541)	
Gelin-S	3 × 1 ml
Each bottle contains 10 mg of Gelin-S and 9.6 mg of PBS salts (Catalog Number G3673)	
Extralink 2	3 × 0.5 ml
Each bottle contains 10 mg of Extralink and 4.8 mg of PBS salts (Catalog Number E6659)	
Water, degassed	1 × 10 ml
Ready-to-use bottle contains 10 ml of deionized water with 9.6 mg of PBS salts (Catalog Number W3894)	

Precautions and Disclaimer

This product is for R&D use only, not for drug, household, or other uses. Please consult the Material Safety Data Sheet for information regarding hazards and safe handling practices.

Preparation Instructions

Note: Do not uncap the HyStem-HP and Gelin-S bottles since both materials will crosslink in the presence of oxygen. Use a syringe and needle to add degassed water. Prepare 1× Stock Solutions:

HyStem-HP – reconstitute a bottle with 1 ml of degassed water (Catalog Number W3894)

Gelin-S – reconstitute a bottle with 1 ml of degassed water (Catalog Number W3894)

Extralink 2 – reconstitute a bottle with 0.5 ml of degassed water (Catalog Number W3894)

The 1× Stock Solutions will contain 1× phosphate buffered saline (PBS), pH ~7.4.

Storage/Stability

The lyophilized powders are blanketed with argon and under a slight vacuum. They may be stored unopened in the original bottles at -20 °C for up to one year. Do not uncap the HyStem-HP and Gelin-S bottles since both materials will crosslink in the presence of oxygen.

The 1× Extralink 2 Stock Solution may be stored at -20 °C for ~1 month.

Procedure

The 1× Stock Solutions remain liquid at 15–37 °C. The hydrogel is formed when the crosslinking agent, Extralink, is added to a mixture of HyStem-HP and Gelin-S. Gelation occurs in ~20 minutes after all three solutions are mixed. No steps depend on low temperature or low pH.

The rigidity of the hydrogel can be varied either by changing the volume of 1× Extralink 2 Stock Solution used for crosslinking⁴ or by diluting the 1× HyStem-HP and Gelin-S Stock Solutions using PBS or cell culture medium. Diluting these Stock Solutions with PBS or cell culture medium can increase the gelation time.

The following is a procedure to prepare a 2.5 ml batch of hydrogel scaffold. Sufficient reagents are provided to prepare 3 batches (7.5 ml).

1. Allow the HyStem-HP, Gelin-S, Extralink 2, and degassed water bottles to come to room temperature.
2. Under aseptic conditions, using a syringe and needle, add 1.0 ml of degassed water (Catalog Number W3894) to the HyStem-HP bottle. Repeat for the Gelin-S bottle (see Preparation Instructions).
3. Place both bottles horizontally on a rocker or shaker. It will take <30 minutes for the solids to fully dissolve. Warming to ≤37 °C and/or gently vortexing will speed dissolution. 1× Stock Solutions will be clear and slightly viscous.
4. Under aseptic conditions, using a syringe and needle, add 0.5 ml of degassed water (Catalog Number W3894) to the Extralink 2 bottle. Invert several times to dissolve.
5. As soon as possible, but within 2 hours of making the solutions, aseptically mix the HyStem and Gelin-S 1× Stock Solutions together. To mix, pipette back and forth slowly to avoid trapping air bubbles.
6. If adding growth factors/ECM proteins, add sterile growth factors/ECM protein solution to the 1:1 mixture of HyStem and Gelin-S 1× Stock Solutions. Pipette back and forth to mix.
7. If encapsulating cells, resuspend the cell pellet in the 1:1 mixture of HyStem and Gelin-S 1× Stock Solutions. Pipette back and forth to mix.
8. To form the hydrogel, combine the following and mix by pipette:
 - 0.5 ml of 1× Extralink 2 Stock Solution
 - 2.0 ml of HyStem/Gelin-S 1:1 mixture
9. Gelation will occur within ~20 minutes.

References

1. Shu, X.Z. et al., Synthesis and Evaluation of Injectable, *In Situ* Crosslinkable Synthetic Extracellular Matrices (sECMs) for Tissue Engineering. *J. Biomed Mater. Res. A*, **79A**(4), 901-912 (2006).
2. Cai, S., et al., Injectable glycosaminoglycan hydrogels for controlled release of human basic fibroblast growth factor. *Biomaterials*, **26**, 6054-6067 (2005).
3. Pike, D.B. et al., Heparin-regulated release of growth factors in vitro and angiogenic response in vivo to implanted hyaluronan hydrogels containing VEGF and bFGF. *Biomaterials*, **27**, 5242-5251 (2006).
4. Prestwich, G.D. et al., 3-D Culture in Synthetic Extracellular Matrices: New Tissue Models for Drug Toxicology and Cancer Drug Discovery. *Adv. Enz. Reg.*, **47**, 196-207 (2007).
5. Shu, X.Z. et al., *In situ* crosslinkable hyaluronan hydrogels for tissue engineering. *Biomaterials*, **25**, 1339-1348 (2004).

HyStem, Gelin-S, and Extralink are trademarks of Glycosan BioSystems, Inc.

JW/MAM 07/09-1

Sigma brand products are sold through Sigma-Aldrich, Inc.
Sigma-Aldrich, Inc. warrants that its products conform to the information contained in this and other Sigma-Aldrich publications. Purchaser must determine the suitability of the product(s) for their particular use. Additional terms and conditions may apply. Please see reverse side of the invoice or packing slip.

Appendix J: Final Experiment Protocol

Procedure

1. Print 3 of each PVA mold using a nitrogen purge using short bursts of nitrogen after initially purging for 5 minutes.
2. After printing, bring the mold inside a cell culture hood, dip in sterile 70% ethanol, shake off excess ethanol and then place in a weigh boat
3. Turn on the hood UV light and sterilize the molds for 20 minutes
4. While the molds are being sterilized:
 - a. Extract the necessary amounts of Extralink, Gelin-S, and Glycosil
 - b. Place the corresponding amount of Gelin-S and Glycosil into microcentrifuge tubes labeled for each mold
 - c. Spin down NIH3T3 cells and resuspend so there are 2.28×10^6 cells per 0.5mL
5. When the molds are done being sterilized and the gel components are ready to be plated, mix in the corresponding amount of Extralink for 1 mold into its microcentrifuge tube
6. Wait 8 minutes to allow gelation to start
7. At 8 minutes, add the calculated amount of cell suspension and top off with media bringing the total volume to 0.5mL
8. Mix via pipetting and inject into the mold
9. Set the mold aside to allow gelation to complete
10. Plate the other molds
11. When gelation is complete, place molds in a labeled 100mm TCP and cover with media
12. Place the TCP in an incubator on a shaker
13. Monitor PVA degradation and change media when the media becomes opaque with PVA
14. Keeping monitoring and changing the media until the PVA mold is dissolved
15. When all the PVA is dissolved, transfer the gel to a 30mm TCP using a sterile plastic spatula
16. Cover the gel with media and incubate on the shaker
17. Image the gels and change out half the media daily

Appendix K: Glycosan Hydrogel Digestion Protocol

Enzyme Digestion of Extracel™ Hydrogels for Recovery of Encapsulated Cells

For research use only

Material Supplier

- 10x collagenase/hyaluronidase (Cat # 07912) StemCell Technologies

This protocol is for recovering cells that have been encapsulated in Extracel™, Extracel-HP™ and Extracel-X™ hydrogels and grown in tissue-culture inserts.

Key Points

- Be cautious about mechanically breaking up the hydrogel prior to digestion because this can lower cell viability significantly.
- If the 1:10 dilution of 1x collagenase/hyaluronidase is not satisfactory, try a 1:5 dilution with digestion overnight.

Steps

1. Dilute the 10X collagenase/hyaluronidase solution 1:10 in the cell culture media (with no FBS) used to cultivate your cells. *Note:* Do not use undiluted enzyme since this results in low cell viability.
2. If you are using media that contains FBS, make sure to wash the hydrogels with FBS-free media before starting the digestion process. At a minimum, wash hydrogels two times for one hour to clear FBS.
3. Remove the tissue culture insert from the 24-well culture plate. Place upside down in a Petri dish.
4. Run a 200 μ L pipette tip around the edge of the membrane, cutting it loose from the insert. The membrane will stay attached to the insert, but usually flips up out of the way.
5. Turn the insert right side up and, using the back of a 10 μ L pipette tip, punch the hydrogel out of the insert into the Petri dish.
6. Place the hydrogel in a 15 mL conical.
7. Add 5 mL of the dilute collagenase/hyaluronidase solution to the hydrogel for each 100 μ L of hydrogel.
8. Incubate by shaking gently overnight at 37 °C.
9. At the end of the incubation, there will still be some hydrogel left in the tube.
10. Centrifuge the conical at 1500 rpm for five minutes. Aspirate off enzymes in media.
11. Wash cells in 5 mL PBS.
12. Centrifuge at 1500 rpm for five minutes. Aspirate off PBS.
13. Resuspend the cell pellet and remove all the PBS and cells. *Note:* In the PBS you can see any remaining hydrogel.
14. When you remove the cells, leave behind any remaining hydrogel.
15. Wash the cells in media and centrifuge at 1500 rpm for five minutes. Aspirate off all media but ~0.5 mL.
16. Resuspend the 0.5 mL of remaining media and cells in media.

*Put PBS
501 in media
(equal amount)*



Glycosan BioSystems Inc.
675 Arapahoe Drive, Suite 302
Salt Lake City, Utah 84108
801-583-8212

Page 1 of 1

Appendix L: MatLab Code Usage License

Below is the code license provided for the script used to compute Fractal Dimension and Lacunarity.

```
Copyright (c) 2010, Omar Al-Kadi  
All rights reserved.
```

```
Redistribution and use in source and binary forms, with or  
without  
modification, are permitted provided that the following  
conditions are met:
```

```
* Redistributions of source code must retain the above  
copyright notice, this list of conditions and the following  
disclaimer.
```

```
* Redistributions in binary form must reproduce the above  
copyright notice, this list of conditions and the following  
disclaimer in the documentation and/or other materials  
provided with the distribution
```

```
THIS SOFTWARE IS PROVIDED BY THE COPYRIGHT HOLDERS AND  
CONTRIBUTORS "AS IS" AND ANY EXPRESS OR IMPLIED WARRANTIES,  
INCLUDING, BUT NOT LIMITED TO, THE IMPLIED WARRANTIES OF  
MERCHANTABILITY AND FITNESS FOR A PARTICULAR PURPOSE ARE  
DISCLAIMED. IN NO EVENT SHALL THE COPYRIGHT OWNER OR  
CONTRIBUTORS BE LIABLE FOR ANY DIRECT, INDIRECT, INCIDENTAL,  
SPECIAL, EXEMPLARY, OR CONSEQUENTIAL DAMAGES (INCLUDING, BUT  
NOT LIMITED TO, PROCUREMENT OF SUBSTITUTE GOODS OR SERVICES;  
LOSS OF USE, DATA, OR PROFITS; OR BUSINESS INTERRUPTION)  
HOWEVER CAUSED AND ON ANY THEORY OF LIABILITY, WHETHER IN  
CONTRACT, STRICT LIABILITY, OR TORT (INCLUDING NEGLIGENCE OR  
OTHERWISE) ARISING IN ANY WAY OUT OF THE USE OF THIS SOFTWARE,  
EVEN IF ADVISED OF THE POSSIBILITY OF SUCH DAMAGE.
```